

Hysteresis, avalanches, and disorder-induced critical scaling: A renormalization-group approach

Karin Dahmen* and James P. Sethna

Laboratory of Atomic and Solid State Physics, Cornell University, Ithaca, New York 14853-2501

(Received 23 June 1995; revised manuscript received 21 December 1995)

Hysteresis loops are often seen in experiments at first-order phase transformations, when the system goes out of equilibrium. They may have a macroscopic jump (roughly as in the supercooling of liquids) or they may be smoothly varying (as seen in most magnets). We have studied the nonequilibrium zero-temperature random-field Ising-model as a model for hysteretic behavior at first-order phase transformations. As disorder is added, one finds a transition where the jump in the magnetization (corresponding to an infinite avalanche) decreases to zero. At this transition we find a diverging length scale, power-law distributions of noise (avalanches), and universal behavior. We expand the critical exponents about mean-field theory in $6-\epsilon$ dimensions. Using a mapping to the pure Ising model, we Borel sum the $6-\epsilon$ expansion to $O(\epsilon^5)$ for the correlation length exponent. We have developed a method for directly calculating avalanche distribution exponents, which we perform to $O(\epsilon)$. Our analytical predictions agree with numerical exponents in two, three, four, and five dimensions [Perković *et al.*, Phys. Rev. Lett. **75**, 4528 (1995)]. [S0163-1829(96)05118-1]

I. INTRODUCTION

The modern field of disordered systems has its roots in dirt. An important effect of disorder is the slow relaxation to equilibrium seen in many experimental systems.³ This paper is an attempt to unearth *universal, nonequilibrium* collective behavior buried in the muddy details of real materials and inherently due to their tendency to remain far from equilibrium on experimental time scales. In particular, we focus on two distinctly nonequilibrium effects: (a) the avalanche response to an external driving force and (b) the internal history dependence of the system (hysteresis).

Systems far from equilibrium often show interesting memory effects not present in equilibrium systems. Far from equilibrium, the system will usually occupy some metastable state that has been selected according to the history of the system. Jumps over large free-energy barriers to reach a more favorable state are unlikely. The system will move through the most easily accessible local minima in the free-energy landscape as an external driving field is ramped, because it cannot sample other, probably lower-lying minima, from which its current state is separated by large (free-energy) barriers. The complexity of the free-energy landscape is usually greatly enhanced by the presence of disorder. It is well known³⁻⁷ that disorder can lead to diverging barriers to relaxation and consequent nonequilibrium behavior and glassiness.

(a) Avalanches. In some systems, collective behavior in the form of avalanches is found when the system is pushed by the driving field into a region of descending slope in the free-energy surface. In experiments avalanches are often associated with crackling noises as in acoustic emission and Barkhausen noise.⁸⁻¹¹ There are other nonequilibrium systems where no such collective behavior is seen. Bending a copper bar, for example, causes a sluggish, creeping response due to the entanglement of dislocation lines. In contrast, wood snaps and crackles under stress due to “avalanches” of fiber breakings.¹²

Although avalanches are collective events of processes

happening on microscales, in many systems they can become monstrously large so that we—in spite of being large, slow creatures—can actually perceive them directly without technical devices. This reminds one of the behavior observed near continuous phase transitions, where critical fluctuations do attain human length and time scales if a tunable parameter is close enough to its critical value. Correspondingly one might expect to find universal features when the sizes and times of the avalanches get large compared to microscopic scales. Interesting questions concerning the *distribution* of avalanche sizes arise. Many experiments show power-law distributions over several decades. For example, experiments measuring Barkhausen pulses in an amorphous alloy, in iron, and in alumel revealed several decades of power-law scaling for the distribution of pulse areas, pulse durations, and pulse energies.¹³⁻²¹ Similarly, Field, Witt, and Nori²² recorded superconductor vortex avalanches in Nb_{47%}Ti_{53%} in the Bean state as the system was driven to the threshold of instability by the slow ramping of the external magnetic field. The avalanche sizes ranged from 50 to 10⁷ collectively moving vortices. The corresponding distribution of avalanche sizes revealed about three decades of power-law scaling. Numerous other hysteretic systems show similar power-law scaling behavior.²³⁻²⁸

Why should there be avalanches of many sizes? In this paper we propose that the large range of observed avalanche sizes in these systems might be a manifestation of a nearby critical point with both disorder and external magnetic field as tunable parameters. We have modeled the long-wavelength, low-frequency behavior of these systems using the nonequilibrium zero-temperature random-field Ising model (RFIM). Some of our results have been published previously.^{1,29,30} In contrast to some other hysteresis models, like the Preisach model³¹ and the Stoner-Wohlfarth model,⁹ where interactions between the individual hysteretic units (grains) are not included and collective behavior is not an issue, in the RFIM the intergrain coupling is the essential ingredient and cause for hysteresis and avalanche effects. Tuning the amount of disorder in the system we find a

second-order critical point with an associated diverging length scale, measuring the spatial extent of the avalanches of spin flips. A power-law distribution with avalanches of *all* sizes is seen only at the critical value of the disorder. However, our numerical simulations^{1,2} indicate that the critical region is remarkably large: almost three decades of power-law scaling in the avalanche size distribution remain when measured 40% away from the critical point. At 2% away, we extrapolate seven decades of scaling. (The size of the critical region is nonuniversal and will therefore vary with the physical system.) One reason for this large critical range is trivial: avalanche sizes are expressed in terms of volumes rather than lengths, one decade of length scales translates to three decades of size (or less if the avalanches are not compact, i.e., if the Hausdorff dimension is less than three). Some experiments that revealed three decades of power-law scaling have been interpreted as being spontaneously self-similar (“self-organized critical”).^{13,22,32} Our model suggests that many of the samples might just have disorders within 40% of the critical value. Tuning the amount of disorder in these systems might reveal a plain old critical point rather than self-organized criticality.

(b) Hysteresis. At the critical disorder we also find a transition in the shape of the associated hysteresis loops: Systems with low disorder relative to the coupling strength, have rectangle-shaped hysteresis loops and a big (Barkhausen) discontinuity, while systems with large disorder relative to the coupling show smooth hysteresis loops without macroscopic jumps. At the critical disorder R_c separating these two regimes, the size of the jump seen in the low disorder hysteresis loops shrinks to a point at a critical magnetic field $H_c(R_c)$, where the magnetization curve $M(H)$ has infinite slope. The power law with which it approaches this point is universal. Initial experimental results in thin magnetic films seem to show the same kind of crossover.^{33,34} The disorder in these systems was changed by annealing the samples at various temperatures. Detailed discussions of Barkhausen experiments,^{14–21} and related experiments in nonmagnetic avalanching systems (in shape memory alloys,^{23,35} superconductors,^{22,36} liquid helium in Nuclepore,²⁴ and others), and a quantitative comparison with our theory is given in forthcoming publications.^{1,37,38}

(c) Results. The main point of this paper is to report a history-dependent renormalization-group (RG) description for the nonequilibrium zero-temperature random-field Ising model. One of the triumphs of the RG is to show from first principles that near the critical point the interesting long-wavelength properties are given by *homogeneous functions* with respect to a change of length scale in the system. This observation leads to Widom scaling forms for the various macroscopic quantities. The main motivation of the work presented here is then to provide a formal justification of the scaling ansatz used in the data analysis and an explanation for the broad universality of the observed critical exponents. We would like it to be viewed as the ultimate justification for the attempt to extract useful predictions about real complex materials from an extremely simple caricature of the microscopic physics.

In particular, we have used the RG description to derive an expansion for the critical exponents around their mean-field values in powers of the dimensional parameter $\epsilon = d_c$

– d , where d is the dimension of the system and $d_c = 6$ is the upper critical dimension of the transition. Note that the ϵ expansion is an asymptotic expansion in terms of a quite unphysical parameter. Nevertheless it has proven very successful for mathematical extrapolations. In this paper we shall apply its basic ideas to our problem and refer the reader for further details to excellent reviews in the existing literature.^{39–47}

The calculation turns out to be interesting in its own right. In contrast to RG treatments of equilibrium critical phenomena, a calculation for our hysteresis problem has to take into account the entire history of the system. It reveals formal similarities to related *single interface* depinning transitions.^{48–55} Although our problem deals with the seemingly more complex case of *many* interacting advancing interfaces or domain walls,^{56–59} the calculation turns out to be rather simple, much simpler in fact than in the single interface depinning problem. The simplicity of the RG calculation in fact allowed us to develop a method to calculate the avalanche exponents directly in the ϵ expansion, which, to our knowledge, so far has not been possible in depinning transitions. The method involves replicas of the system in a very physical way. We have used it to calculate the avalanche exponents to first order in ϵ . The techniques employed here are likely to be applicable to other nonequilibrium systems as well.

This paper is organized as follows: The model is introduced in Sec. II and a summary of our results is given in Sec. III. In Sec. IV the RG description is set up using the Martin-Siggia-Rose formalism, and a description of the perturbative expansion of the critical exponents is given in Sec. V. Section VI contains a formal discussion of the mapping of our $6 - \epsilon$ expansion to the corresponding $6 - \epsilon$ expansion for the equilibrium or thermal RFIM. We extract corrections to $O(\epsilon^5)$ for most of the exponents and show a comparison between the Borel resummation of the ϵ expansion and numerical results. The mapping does not, however, render the exponents governing the avalanche size distribution. In Sec. VII a new method to calculate avalanche exponents directly in an ϵ expansion is described and performed to $O(\epsilon)$. Finally, in Sec. VIII we compare the results to extensive numerical simulations in two, three, four, and five dimensions.²

Some of the details of the mean-field calculation are given in Appendix A. Details on the implementation of the history in the RG calculation are given in Appendix B. The behavior near the infinite avalanche line in systems with less than critical randomness is discussed in Appendix C. Appendix D renders details on the calculation of the avalanche exponents by the use of replicas. Some related problems and the stability of the universality class against changes in the model are discussed in Appendix E.

II. THE MODEL

As is well known from equilibrium phenomena, behavior on long length scales can often be well described by simple microscopic models that only need describe a few basic properties correctly, such as symmetries, interaction range, and effective dimensions. This notion has been successfully applied in particular to equilibrium magnetic systems: the scaling behavior found in some pure anisotropic ferromag-

nets near the Curie temperature is mimicked reliably by the regular Ising model.^{39,60} At each site i in a simple cubic lattice there is a (spin) variable $s_i = \pm 1$,⁶¹ which interacts with its nearest neighbors s_j on the lattice through a “ferromagnetic” exchange interaction, $J_{ij} \equiv J/z$. z is the coordination number of the lattice and J is a positive constant. The Hamiltonian of the system is

$$\mathcal{H} = - \sum_{ij} J_{ij} s_i s_j - H \sum_i s_i, \quad (1)$$

where it is understood that the sum runs over nearest-neighbor pairs of spins on sites i and j and H is a homogeneous external magnetic field. To model nonequilibrium effects we now impose a straightforward local dynamics, assuming that each spin s_i will always be aligned with the total effective field at its site

$$h_i^{\text{eff}} = - \sum_j J_{ij} s_j - H. \quad (2)$$

We find that the resulting magnetization curve at zero temperature becomes history dependent. The system will typically be in some metastable state rather than the ground state. The upper branch of the rectangular shaped hysteresis curve corresponds to the case where the external magnetic field is lowered monotonically and adiabatically, starting from $H = +\infty$, where all spins were pointing up. At the negative coercive field $H_c^l = -2dJ_{ij} \equiv -J$ all spins flip down in a single system spanning event or “avalanche.” Similarly, for increasing external magnetic field, they all flip up at the positive coercive field $H_c^u = 2dJ_{ij} \equiv +J$. It becomes clear that the underlying cause for hysteresis in this model is the interaction between the spins.

In real materials there will usually also be inhomogeneities and disorder (defects, grain boundaries, impurities) leading to random crystal anisotropies and varying interaction strengths in the system. Consequently not all spins will flip at the same value of the external magnetic field. Instead, they will flip in avalanches of various sizes that can be broken up or stopped by strongly “pinned” spins or clusters of previously flipped spins.

A simple way to implement a certain kind of uncorrelated, quenched disorder is by introducing uncorrelated random fields into the model. In magnets the random fields might model frozen-in magnetic clusters with net magnetic moments that remain fixed even if the surrounding spins change their orientation. In contrast to random anisotropies they break time-reversal invariance by coupling to the order parameter (rather than its square). In shape memory alloys, ramping temperature, the random fields can be thought of as concentration fluctuations that prefer martensite over the austenite phase.⁶² In the martensitic phase, ramping stress, they model strain fields that prefer one martensitic variant over another.⁶² (Other kinds of disorder are discussed in Appendix E.) Including the random fields, the energy function becomes

$$\mathcal{H} = - \sum_{ij} J_{ij} s_i s_j - \sum_i (H + f_i) s_i. \quad (3)$$

The total effective field becomes

$$h_i^{\text{eff}} = - \sum_j J_{ij} s_j - H - f_i, \quad (4)$$

and the local dynamics remains otherwise unchanged. We assume a Gaussian distribution $\rho(f_i)$ of standard deviation R for the fields f_i , which is centered at $f_i = 0$:

$$\rho(f_i) = \frac{1}{\sqrt{2\pi}R} \exp\left(-\frac{f_i^2}{2R^2}\right). \quad (5)$$

As we will show, the critical exponents do not depend on the exact shape of the distribution of random fields. To pick a Gaussian is a standard choice, which [due to the central limit theorem (Ref. 63)] is also more likely to be found in some real experiments than, for example, rectangular distributions.⁶⁴

III. RESULTS

The nonequilibrium model of Eq. (3) can be solved in the mean-field approximation where every spin interacts equally strongly with every other spin in the system. The coupling is of size $J_{ij} = J/N$, where N is the total number of spins (i.e., all spins act as nearest neighbors). The Hamiltonian then takes the form

$$\mathcal{H} = - \sum_i (JM + H + f_i) s_i, \quad (6)$$

i.e., just as in the Curie-Weiss mean-field theory for the Ising model, the interaction of a spin with its neighbors is replaced by its interaction with the magnetization of the system.

It turns out that the mean-field theory already reflects most of the essential qualitative features of the long-length scale behavior of the system in finite dimensions: Sweeping the external field through zero, the model exhibits hysteresis. As disorder is added, one finds a continuous transition where the jump in the magnetization (corresponding to an infinite avalanche) decreases to zero. At this transition power-law distributions of noise (avalanches) and universal behavior are observed. As we will show later in a RG description of the model, the critical exponents describing the scaling behavior near the critical point are correctly given by mean-field theory for systems in six and higher spatial dimensions. The RG allows us to calculate their values in $(6 - \epsilon)$ dimensions in a power-series expansion in $\epsilon > 0$ around their mean-field values at $\epsilon = 0$. In the following we briefly present the results from mean-field theory, from the ϵ expansion and from numerical simulations in three dimensions. More details will be given in later sections.

A. Results on the magnetization curve

Figure 1 shows the hysteresis curve in mean-field theory at various values of the disorder $R < R_c = \sqrt{(2/\pi)}J$, $R = R_c$, and $R > R_c$. For $R < R_c$, where the coupling is important relative to the amount of disorder in the system, the hysteresis curve displays a jump due to an infinite avalanche of spin flips, which spans the system. Close to R_c the size of the jump scales as $\Delta M \sim r^3$, with $r = (R_c - R)/R$, and $\beta = 1/2$ in mean-field theory. Using a mapping to the pure Ising model, we find in $6 - \epsilon$ dimensions⁶⁵

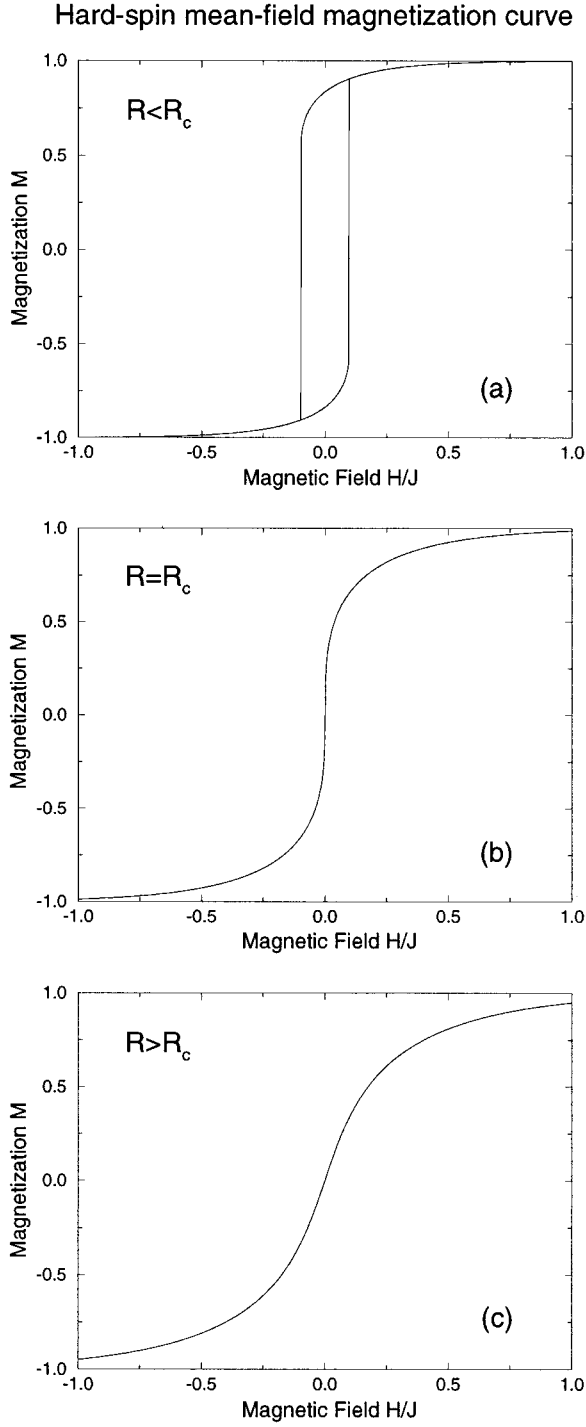


FIG. 1. Mean-field magnetization curves for the nonequilibrium zero-temperature random-field Ising model at various values of the disorder $R=0.6J < R_c$ (a), $R=R_c=\sqrt{(2/\pi)}J=0.798J$ (b), and $R=J > R_c$ (c).

$$\beta = 1/2 - \epsilon/6 + 0.00617685\epsilon^2 - 0.035198\epsilon^3 + 0.0795387\epsilon^4 - 0.246111\epsilon^5 + O(\epsilon^6). \quad (7)$$

At $R=R_c$ the magnetization curve scales as $M - M(H_c(R_c)) \sim h^{(1/\delta)}$, where $h = H - H_c(R_c)$ and $H_c(R_c)$ is the (nonuniversal) magnetic field value at which the magnetization curve has infinite slope. In mean-field theory $H_c(R_c)=0$, and $M(H_c(R_c))=0$, and $\beta\delta=3/2$. In $6-\epsilon$ dimensions⁶⁵

$$\beta\delta = 3/2 + 0.0833454\epsilon^2 - 0.0841566\epsilon^3 + 0.223194\epsilon^4 - 0.69259\epsilon^5 + O(\epsilon^6). \quad (8)$$

Numerical simulations in three dimensions yield $\beta=0.036 \pm 0.036$ and $\beta\delta=1.81 \pm 0.36$.²

For $R > R_c$ the disorder can be considered more important than the coupling. Consequently there are no system spanning avalanches (for infinite systems size) and the magnetization curve is smooth.

Note that the hard-spin mean-field theory does not show any hysteresis for $R \geq R_c$. This is only an artifact of its particularly simple structure and not a universal feature. In finite dimensions the model does show hysteresis for all values of R . Also, an analogous soft-spin model, which is introduced for the RG description in Sec. IV, has the same critical exponents and shows hysteresis at all disorders R , even in mean-field theory as seen in Fig. 2.

Close to R_c and $H_c(R_c)$ the magnetization curve is described by a scaling form:

$$M - M(H_c(R_c)) \equiv m(r, h) \sim r^\beta \mathcal{M}_\pm(h/r^{\beta\delta}), \quad (9)$$

where \mathcal{M}_\pm is a universal scaling function (\pm refers to the sign of r). It is computed in mean-field theory in Appendix A.⁶⁶ Perturbative corrections to the mean-field equation of state in $6-\epsilon$ dimensions are given to $O(\epsilon^2)$ in Sec. VI.

B. Results on the mean-field phase diagram

Figure 3 shows the phase diagram for the lower branch of the hysteresis curve as obtained from the simple hard-spin mean-field theory, defined through Eq. (6). The bold line with the critical endpoint $(R_c, H_c(R_c))$ indicates the function $H_c^u(R)$ for the onset of the infinite avalanche for the history of an *increasing* external magnetic field. The dashed line describes $H_c^l(R)$ for a *decreasing* external magnetic field. The three dotted vertical lines marked (a), (b), and (c) describe the paths in parameter space which lead to the corresponding hysteresis loops shown in Fig. 1. Figures 2 and 4 show the corresponding results for the soft-spin model.

C. Results on scaling near the onset $H_c(R)$ of the infinite avalanche line ($R < R_c$)

The mean-field magnetization curve scales near the onset of the infinite avalanche as

$$[M - M_c(H_c(R))] \sim [H - H_c(R)]^\zeta \quad (10)$$

with $\zeta=1/2$. [$H_c(R)$ stands, respectively, for $H_c^u(R)$ or $H_c^l(R)$ for the history of an increasing or decreasing external magnetic field.] Curiously we do not observe this scaling behavior in numerical simulations with short-range interactions in two, three, four, and five dimensions. Indeed, the RG description suggests that the onset of the infinite avalanche would be an abrupt (“first-order” type) transition for all dimensions $d < 8$ (see Appendix C), and a continuous transition for $d > 8$. Our initial numerical simulations in seven and nine dimensions for system sizes 7^7 and 5^9 at less than critical disorders do in fact seem to confirm the RG prediction.² In the following we will mostly focus on the critical endpoint at $(R_c, H_c(R_c))$, where the mean-field scaling behavior is ex-

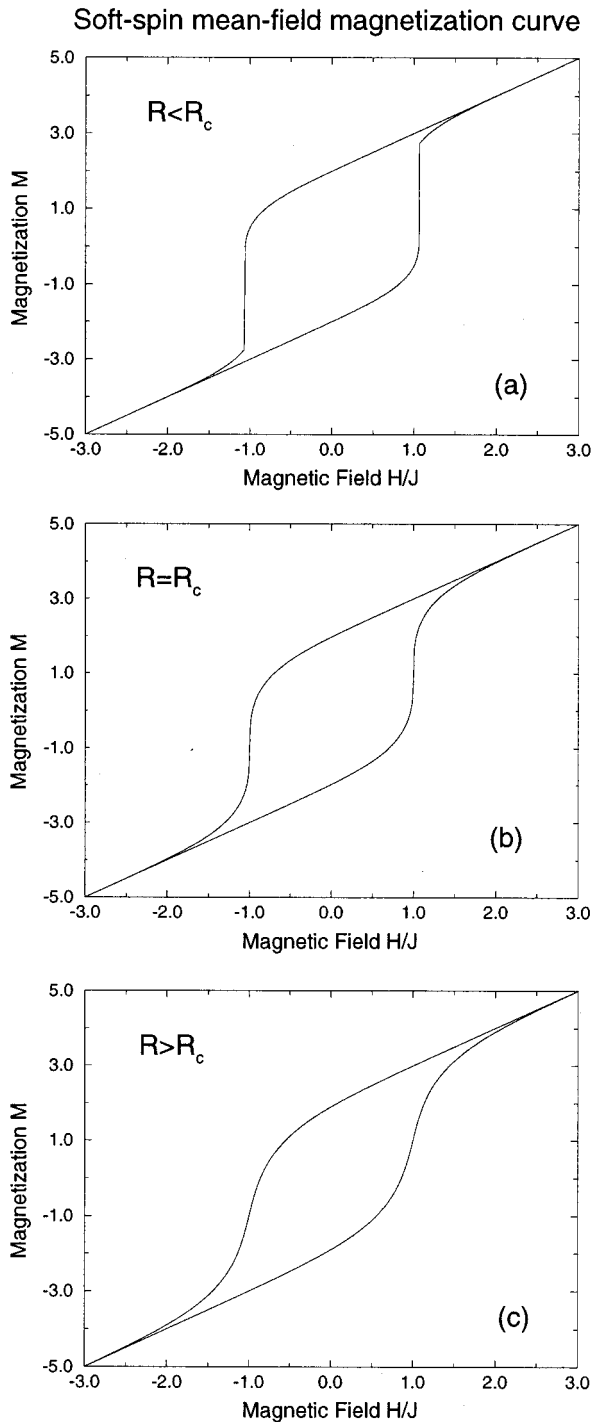


FIG. 2. Mean-field magnetization curves for the soft-spin version of the zero-temperature random-field Ising model at various values of the disorder $R = 1.3J < R_c$ (a), $R = R_c = 2kJ / [(k - J)\sqrt{2\pi}] = 1.6J$ (see Appendix A 6) (b), and $R = 2J > R_c$ (c).

pected to persist in finite (more than two) spatial dimensions with slightly changed critical exponents.

D. Results on avalanches

Magnetization curves from simulations of finite-size systems are not smooth. They display steps of various sizes. Each step in the magnetization curve corresponds to an avalanche of spin flips during which the external magnetic field

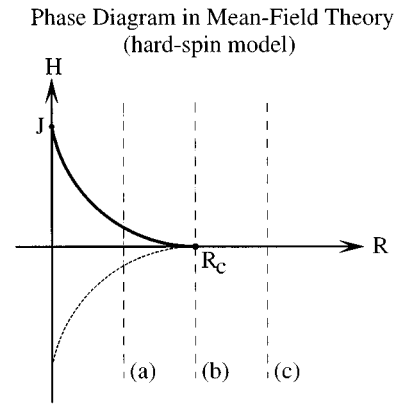


FIG. 3. Mean-field phase diagram for the nonequilibrium zero-temperature random-field Ising model. The critical point studied in this paper is at $R = R_c$, $H = H_c(R_c)$, with $H_c(R_c) = 0$ in the hard-spin mean-field theory. There are two relevant directions $r = (R_c - R)/R$ and $h = H - H_c(R_c)$ near this critical point. The bold line indicates the threshold field $H_c^u(R)$ for the onset of the infinite avalanche upon monotonically increasing the external magnetic field. The dashed line describes $H_c^l(R)$ for a decreasing external magnetic field. The three dotted vertical lines marked (a), (b), and (c) describe the paths in parameter space which lead to the corresponding hysteresis loops shown in Fig. 1.

is kept constant. Figure 5 shows histograms $D(S, r)$ of all avalanche sizes S observed in mean-field systems at various disorders r when sweeping through the entire hysteresis loop. For small r the distribution roughly follows a power law $D(S, r) \sim S^{-(\tau + \sigma\beta\delta)}$ up to a certain cutoff size $S_{\max} \sim |r|^{-1/\sigma}$ which scales to infinity as r is taken to zero.

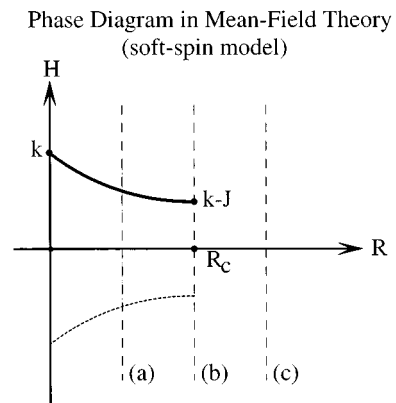


FIG. 4. Mean-field phase diagram for the soft-spin version of the nonequilibrium zero-temperature random-field Ising model. The diagram is plotted analogously to Fig. 3. Magnetic field sweeps along the lines (a), (b), and (c) lead to the corresponding soft-spin hysteresis curves shown in Fig. 2. Note that here, in contrast to the hard-spin model, the value of the critical field $H_c(R_c) = H_c^u(R_c) = k - J$, and for monotonically decreasing external magnetic field $H_c(R_c) = H_c^l(R_c) = -(k - J)$ (see Appendix A 6). This implies that in contrast to the hard-spin mean-field theory of Fig. 3, the soft-spin mean-field theory displays hysteresis for *all* finite disorder values, i.e., even at $R \geq R_c$.

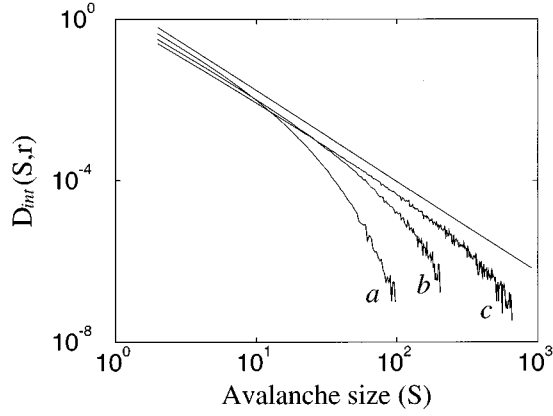


FIG. 5. Mean-field avalanche size distribution integrated over the hysteresis loop for systems with 1 000 000 spins at various disorder values $R > R_c = 0.798J$: (a) $R = 1.46J$ (averaged over ten different configurations of random fields), (b) $R = 1.069J$ (averaged over five different configuration of random fields), and (c) $R = 0.912J$ (averaged over ten different configurations of random fields). Each curve is a histogram of all avalanche sizes found as the magnetic field is raised from $-\infty$ to $+\infty$, normalized by the number of spins in the system. For small $|r| = |R_c - R|/R$ the distribution roughly follows a power law $D(S,r) \sim S^{-(\tau + \sigma\beta\delta)}$ up to a certain cutoff size $S_{\max} \sim |r|^{-1/\sigma}$ which scales to infinity as r is taken to zero. The straight line above the three data curves in the figure represents an extrapolation to the critical point $R = R_c$ in an infinite system, where one expects to see a pure power-law distribution on all length scales $D(S,r) \sim S^{-(\tau + \sigma\beta\delta)}$ with the mean-field values of the corresponding exponents $\tau + \sigma\beta\delta = 2.25$.

In Appendix A we derive a scaling form for the avalanche size distribution for systems near the critical point: Let $D(S,r,h)$ denote the probability of finding an avalanche of size S in a system with disorder r at external magnetic field h upon increasing h by an infinitesimal amount δh . For large S one finds

$$D(S,r,h) \sim 1/S^\tau \mathcal{D}_\pm(Sr^{1/\sigma}, h/r^{\beta\delta}). \quad (11)$$

The scaling form for $D(S,r)$ of the histograms in Fig. 5 is obtained by integrating $D(S,r,h)$ over the entire range of the external magnetic field $-\infty < h < +\infty$.

In mean-field theory we find $\sigma = 1/2$ and $\tau = 3/2$. In $6 - \epsilon$ dimensions we obtain from the RG calculation $\sigma = 1/2 - \epsilon/12 + O(\epsilon^2)$. Numerical simulations in three dimensions render $\sigma = 0.238 \pm 0.017$ and $\tau = 1.60 \pm 0.08$.²

E. Results on correlations near $(R_c, H_c(R_c))$

With the mean-field approximation we have lost all information about length scales in the system. The RG description, which involves a coarse-graining transformation to long length scales, provides a natural means to extract scaling forms for various correlation functions of the system.

1. Avalanche correlations

The avalanche correlation function $G(x,r,h)$ measures the probability for the configuration of random fields in the system to be such that a flipping spin will trigger another at

relative distance x through an avalanche of spin flips. Close to the critical point and for large x the function $G(x,r,h)$ scales as

$$G(x,r,h) \sim 1/x^{d-2+\eta} \mathcal{G}_\pm(x/\xi(r,h)), \quad (12)$$

where η is called ‘‘anomalous dimension’’ and \mathcal{G}_\pm is a universal scaling function. The correlation length $\xi(r,h)$ is the important (macroscopic) length scale of the system. At the critical point, where it diverges, the correlation function $G(x,0,0)$ decays algebraically—there will be avalanches on all length scales. Close to the critical point the correlation length scales as

$$\xi(r,h) \sim r^{-\nu} \mathcal{Y}_\pm(h/r^{\beta\delta}), \quad (13)$$

where \mathcal{Y}_\pm is the corresponding scaling function. From the ϵ expansion one obtains⁶⁵

$$\begin{aligned} 1/\nu = & 2 - \epsilon/3 - 0.1173\epsilon^2 + 0.1245\epsilon^3 - 0.307\epsilon^4 + 0.951\epsilon^5 \\ & + O(\epsilon^6), \end{aligned} \quad (14)$$

and

$$\begin{aligned} \eta = & 0.0185185\epsilon^2 + 0.01869\epsilon^3 - 0.00832876\epsilon^4 \\ & + 0.02566\epsilon^5 + O(\epsilon^6). \end{aligned} \quad (15)$$

The numerical values in three dimensions are $1/\nu = 0.704 \pm 0.085$ and $\eta = 0.79 \pm 0.29$.²

2. Spin-spin (‘‘cluster’’) correlations

Another correlation function measures correlations in the fluctuations of the spin orientation at different sites. It is related to the probability that two spins s_i and s_j at two different sites i and j , that are distanced by x , have the same value.³⁹ It is defined as

$$C(x,r,h) = \langle (s_i - \langle s_i \rangle_f)(s_j - \langle s_j \rangle_f) \rangle_f, \quad (16)$$

where $\langle \rangle_f$ indicates the average over the random fields. From the RG description we find that for large x it has the scaling form

$$C(x,r,h) \sim x^{-(d-4+\bar{\eta})} \mathcal{C}_\pm(x/\xi(r,h)), \quad (17)$$

where $\xi(r,h)$ scales as given in Eq. (13) and \mathcal{C}_\pm is a universal scaling function. At the critical point $C(x,0,0)$ decays algebraically—there will be clusters of equally oriented spins on all length scales. The ϵ expansion renders⁶⁵

$$\begin{aligned} \bar{\eta} = & 0.0185185\epsilon^2 + 0.01869\epsilon^3 - 0.00832876\epsilon^4 \\ & + 0.02566\epsilon^5 + O(\epsilon^6), \end{aligned} \quad (18)$$

which is in fact the same perturbation expansion as for η to all orders in ϵ . (The two exponents however do not have to be equal beyond perturbation theory, see also, Refs. 37 and 38).

F. Results on avalanche durations

Avalanches take a certain amount of time to spread, because the spins are flipping sequentially. The further the avalanche spreads, the longer it takes till its completion. The RG

treatment suggests that there is a scaling relation between the duration T of an avalanche and its linear extent l

$$T(l) \sim l^z \quad (19)$$

with $z = 2 + 2\eta$ to $O(\epsilon^3)$,⁶⁷ i.e.,

$$z = 2 + 0.037037\epsilon^2 + 0.03738\epsilon^3 + O(\epsilon^4). \quad (20)$$

Our numerical result in three dimensions is $z = 1.7 \pm 0.3^2$ (While we expect the $6 - \epsilon$ results for the static exponents β , δ , ν , η , $\bar{\eta}$, τ , σ , etc. to agree with our hard-spin simulation results close to six dimensions, this is not necessarily so for the dynamical exponent z . There are precedences for the dynamics being sensitive to the exact shape of the potential, sometimes only in mean-field theory^{48,49,68} and sometimes even in the ϵ expansion.^{49,69}) The fractal dimension for the biggest avalanches $S_{\max} \sim r^{-1/\sigma} \sim \xi^{1/(\sigma\nu)}$ is

$$d_{\text{fractal}} = 1/(\sigma\nu), \quad (21)$$

so that the time T for the biggest finite avalanches S_{\max} scales as $T(S_{\max}) \sim S_{\max}^{\sigma\nu z}$.

G. Results on the area of the hysteresis loop

In some analogy to the free-energy density in equilibrium systems, one can extract the scaling of the area of the hysteresis loop for this system near the critical endpoint. (This is the energy dissipated in the loop per unit volume.) From the fact that the singular part of the magnetization curve scales as $m(h, r) \sim r^\beta \mathcal{M}_\pm(h/r^{\beta\delta})$ [Eq. (9)] we conjecture that the singular part of the area scales as $A_{\text{sing}} \sim \int m(h, r) dh \sim r^{2-\alpha}$ with $2 - \alpha = \beta + \beta\delta$. (The scaling form for the total area A_{tot} will also have an analytical piece: $A_{\text{tot}} = c_0 + c_1 r + \dots + c_n r^n + \dots + A_{\text{sing}}$; near critical point the terms with $n \leq 2 - \alpha$ are dominant.) In mean-field theory $\alpha = 0$. Numerical and analytical results can be derived from the results for β and $\beta\delta$ quoted earlier.

H. Results on the number of system-spanning avalanches at the critical disorder $R = R_c$

In percolation in less than six dimensions, there is at most one infinite cluster present at any value of the concentration parameter p , in particular also at its critical value p_c .⁷⁰ In contrast, in our system at the critical point $R = R_c$ the number N_∞ of ‘‘infinite avalanches’’ found during one sweep through the hysteresis loop, diverges with system size as $N_\infty \sim L^\theta$ in all dimensions $d > 2$.^{37,38}

The ϵ expansion for our system yields

$$\theta\nu = 1/2 - \epsilon/6 + O(\epsilon^2). \quad (22)$$

Numerical simulations show clearly that $\theta > 0$ in four and five dimensions. In three dimensions one finds $\theta\nu = 0.021 \pm 0.021$ and $\theta = 0.015 \pm 0.015$.²

I. List of exponent relations

In the following sections we list various exponent relations, for which we give detailed arguments in Refs. 37 and 38.

1. Exponent equalities

The exponents introduced above are related by the following exponent equalities:

$$\beta - \beta\delta = (\tau - 2)/\sigma \quad \text{if } \tau < 2, \quad (23)$$

$$(2 - \eta)\nu = \beta\delta - \beta, \quad (24)$$

$$\beta = \frac{\nu}{2}(d - 4 + \bar{\eta}), \quad (25)$$

and

$$\delta = (d - 2\eta + \bar{\eta})/(d - 4 + \bar{\eta}). \quad (26)$$

(The latter three equations are not independent and are also valid in the equilibrium random-field Ising model.^{71–73})

2. Incorrect exponent equalities

In our system there are two different violations of hyperscaling.

(1) In Refs. 37 and 38, we show that the connectivity hyperscaling relation $1/\sigma = d\nu - \beta$ from percolation is violated in our system. There is a new exponent θ defined by

$$1/\sigma = (d - \theta)\nu - \beta, \quad (27)$$

with $\theta\nu = 1/2 - \epsilon/6 + O(\epsilon^2)$ and $\theta\nu = 0.021 \pm 0.021$ in three dimensions.² θ is related to the number of system spanning avalanches observed during a sweep through the hysteresis loop (see above).

(2) As we will discuss in Sec. VI there is a mapping of the perturbation theory for our problem to that of the equilibrium random-field Ising model to all orders in ϵ . From that mapping we deduce the breakdown of an infamous (‘‘energy’’)-hyperscaling relation

$$\beta + \beta\delta = (d - \tilde{\theta})\nu, \quad (28)$$

with a new exponent $\tilde{\theta}$, which has caused much controversy in the case of the *equilibrium* random-field Ising model.⁷¹

In Refs. 37 and 38 we discuss the relation of the exponent $\tilde{\theta}$ to the energy output of the avalanches. The ϵ expansion yields $\tilde{\theta} = 2$ to all orders in ϵ . Nonperturbative corrections are expected to lead to deviations of $\tilde{\theta}$ from 2 as the dimension is lowered. The same is true in the case of the equilibrium RFIM.^{37,38} The numerical result in three dimensions is $\tilde{\theta} = 1.5 \pm 0.5$.² (In the three-dimensional equilibrium RFIM it is $\tilde{\theta}_{\text{eq}} = 1.5 \pm 0.4$.^{71,74})

Another strictly perturbative exponent equality, which is also obtained from the perturbative mapping to the random-field Ising-model^{37,38} is given by

$$\bar{\eta} = \eta. \quad (29)$$

It, too, is expected to be violated by nonperturbative corrections below six dimensions.

3. Exponent inequalities

In Refs. 37 and 38 we give arguments⁷⁵ for the following two exponent-inequalities [from the normalization of the avalanche size distribution $D(s,r,h)$, see Eq. (11), follows that $\tau > 1$]:

$$\nu/\beta\delta \geq 2/d, \quad (30)$$

which is formally equivalent to the ‘‘Schwartz-Soffer’’ inequality, $\bar{\eta} \leq 2\eta$, first derived for the equilibrium random-field Ising model,⁷⁶ and

$$\nu \geq 2/d, \quad (31)$$

which is a weaker bound than Eq. (30) so long as $\beta\delta \geq 1$, as appears to be the case both theoretically and numerically at least for $d \geq 3$.

J. Results on the upper critical dimension of the critical endpoint $(R_c, H_c(R_c))$

The consistency of the mean-field theory exponents for $d \geq 6$ can be shown by a Harris-criterion-type argument,³⁹ which also leads to Eq. (30).³⁸ Approaching the critical point along the $r' = 0$ line, one finds a well-defined transition point only if the fluctuations $\delta h'$ in the critical field H_c due to fluctuations in the random fields are always small compared to the distance h' from the critical point, i.e., $\delta h'/h' \ll 1$ as $h' \rightarrow 0$. With $\delta h' \sim \xi^{-d/2}$ and $\xi \sim (r')^{-\nu} f_{\pm}(h'/(r')^{\beta\delta}) \sim (h')^{-\nu/(\beta\delta)}$ at $r' = 0$, one obtains $\delta h'/h' \sim \xi^{-d/2}/\xi^{-\beta\delta/\nu} \ll 1$, or $\nu/\beta\delta \geq 2/d$. This inequality is fulfilled by the mean-field exponents $\nu = 1/2$ and $\beta\delta = 3/2$ only if $d \geq 6$, i.e., $d = 6$ is the upper critical dimension.

IV. ANALYTICAL DESCRIPTION

Our system is at zero temperature and far from equilibrium. For a given configuration of random fields, the system will follow a deterministic path through the space of spin microstates as the external magnetic field is raised adiabatically. Systems with different configurations of random fields will follow different paths. It seems plausible to introduce time t into the otherwise adiabatic problem and to apply RG methods developed for dynamical systems. We write $H(t) = H_0 + \Omega t$, where H_0 is the magnetic field at time $t = 0$, and $\Omega > 0$ is the sweeping rate for a monotonically increasing external magnetic field. We write down an equation of motion for each spin such that the resulting set of coupled differential equations has a unique solution which corresponds to the correct path which the system takes for a given history. The sweeping frequency Ω is taken to zero in the end. For convenience we introduce soft spins that can take values ranging from $-\infty$ to $+\infty$. This will allow us later to replace traces over all possible spin configurations by path integrals. We assume that each spin is moving in a double-well poten-

tial $V(s_i)$ with minima at the ‘‘discrete’’ spin values $s_i = \pm 1 :=$

$$V(s_i) = \begin{cases} k/2(s_i+1)^2 & \text{for } s < 0 \\ k/2(s_i-1)^2 & \text{for } s > 0. \end{cases} \quad (32)$$

To guarantee that the system takes a finite magnetization at any magnetic field, one needs $k > 0$ and $k/J > 1$. The Hamiltonian of the soft-spin model is then given by

$$\mathcal{H} = - \sum_{ij} J_{ij} s_i s_j - \sum_i [f_i s_i + H s_i - V(s_i)]. \quad (33)$$

A spin flip in this model corresponds to a spin moving from the ‘‘down’’ ($s < 0$) to the ‘‘up’’ ($s > 0$) potential well, after which point the spin slides to the bottom of the new potential well ($\delta s \geq 2$). We impose purely relaxational dynamics

$$(1/\Gamma_0) \partial_t s_i(t) = - \delta \mathcal{H} / \delta s_i(t), \quad (34)$$

where Γ_0 is a ‘‘friction constant.’’

This model shows qualitatively similar behavior to real magnets: As the external magnetic field is ramped, we observe spin flips, which correspond to irreversible domain-wall motions. The linear relaxation between the spin flips corresponds to the reversible domain-wall motion.

The soft-spin mean-field theory, where every spin interacts equally with every other spin yields the same static critical exponents as we have obtained earlier for the hard-spin model. We have also checked that replacing the linear cusp potential by the more common, smooth s^4 double-well potential does not change the static mean-field exponents.⁷⁷

A. Formalism

In equilibrium systems one usually calculates the ensemble averaged correlation functions from a partition function which is the sum over the thermal weights or probabilities of all possible spin states of the system. Here we use the formalism introduced by Martin, Siggia, and Rose⁷⁸ (which is similar to the Bausch-Janssen-Wagner method⁷⁹) to define an analogous quantity for a dynamical system. The partition function for the disorder-averaged dynamical system is the sum over the probabilities of all possible *paths* (i.e., spin states as functions of time as the external magnetic field is slowly increased) which the system follows for different configurations of the disorder. To calculate the path probability distribution one first assigns a δ -function weight to the (deterministic) path for a given, fixed configuration of random fields and then averages this weight-function over all possible configurations of random fields. The emerging expression is the analog of the probability distribution for the possible states in equilibrium systems. The analog of ensemble averaging for equilibrium systems is random-field averaging in our system. The sum over all possible paths weighted by their corresponding probability then plays the role of a partition function Z for our nonequilibrium system from which we can derive the various response and correlation functions.

We start by calculating Z before random-field averaging: it is given by integral over a product of δ functions (one for each spin), each of which imposes the equation of motion at all times on its particular spin:⁴⁸

$$1 \equiv Z = \int [ds] \mathcal{A}[s] \prod_i \delta(\partial_t s_i / \Gamma_0 + \delta \mathcal{H} / \delta s_i). \quad (35)$$

$[ds]$ denotes the path integral over all spins in the lattice at all times, and $\mathcal{A}[s]$ is the necessary Jacobian, which fixes the measures of the integrations over the s_i such that the integral over each δ function yields one.⁴⁸ One can show that $\mathcal{A}[s]$ merely cancels the equal time response functions.^{48,80,81}

In order to write Z in an exponential form in analogy to the partition function in equilibrium problems, we express the δ functions in their Fourier representation, introducing an unphysical auxiliary field $\hat{s}_j(t)$:

$$\begin{aligned} \delta(\partial_t / \Gamma_0 s_i(t) + \delta \mathcal{H} / \delta s_i(t)) \sim 1/2\pi \int d\hat{s} \exp\left(i \sum_j \hat{s}_j(t) \right. \\ \left. \times [\partial_t s_j(t) / \Gamma_0 + \delta \mathcal{H} / \delta s_j(t)] \right). \end{aligned} \quad (36)$$

Absorbing any constants into $\mathcal{A}[s]$, this yields for the (not yet random-field averaged) generating functional (in continuous time):

$$1 = Z = \int \int [ds][d\hat{s}] \mathcal{A}[s] \exp(W), \quad (37)$$

with the action

$$\begin{aligned} W_\epsilon = i \sum_{j \neq k} \int dt \hat{s}_j(t) \left(\partial_t s_j(t) / \Gamma_0 - \sum_l J_{jl} s_l - H - f_j + \delta V / \delta s_j \right) \\ + i \int dt \hat{s}_k(t) \left(\partial_t s_k(t) / \Gamma_0 - \sum_l J_{kl} s_l - H - f_k + \delta V / \delta s_k - J \epsilon_k(t, t'') \right). \end{aligned} \quad (41)$$

Taking the derivative with respect to $J \epsilon_k$ and the limit $\epsilon_k \rightarrow 0$ afterwards one obtains

$$\begin{aligned} \delta s_j(t') / \delta \epsilon_k(t'') = (-i) Z^{-1} \int \int [ds][d\hat{s}] \\ \times \mathcal{A}[s] s_j(t') \hat{s}_k(t'') \exp(W), \end{aligned} \quad (42)$$

so \hat{s} acts as a ‘‘response field.’’ Henceforth we shall suppress $\mathcal{A}[s]$, keeping in mind that its only effect is to cancel equal time response functions.⁸⁰

Since $Z=1$, independent of the random fields, we could have left out the Z^{-1} factors in Eqs. (39), (40), and (42). This greatly facilitates averaging over the random fields: The average response and correlation functions are generated by averaging Z directly over the random fields. Unlike in equilibrium problems with quenched disorder it is not necessary

$$\begin{aligned} W = i \sum_j \int dt \hat{s}_j(t) [\partial_t s_j(t) / \Gamma_0 + \delta \mathcal{H} / \delta s_j(t)] \\ = i \sum_j \int dt \hat{s}_j(t) \left(\partial_t s_j(t) / \Gamma_0 - \sum_l J_{jl} s_l - H - f_j \right. \\ \left. + \delta V / \delta s_j \right). \end{aligned} \quad (38)$$

We can express correlation and response functions of $s_j(t)$ as path integrals in terms of W , because solely the unique deterministic path of the system for the given configuration of random fields makes a nonzero contribution to the path integral over $[ds]$ in Eq. (37). For example the value of spin s_j at time t' is given by

$$s_j(t') = Z^{-1} \int \int [ds'] [d\hat{s}'] \mathcal{A}[s'] s'_j(t') \exp(W), \quad (39)$$

and the correlation function is given by

$$\begin{aligned} s_j(t') s_k(t'') = Z^{-1} \int \int [ds'] \\ \times [d\hat{s}'] \mathcal{A}[s'] s'_j(t') s'_k(t'') \exp(W). \end{aligned} \quad (40)$$

To calculate the response of s_j at time t' to a perturbative field $J \epsilon_k(t', t'')$ switched on at site k at time t'' , we add the perturbation to the magnetic field at site k , such that the action becomes

to calculate the (more complicated) average of $\ln Z$. One obtains for the random-field-averaged correlation functions

$$\langle s_j(t') s_k(t'') \rangle_f = \int \int [ds][d\hat{s}] s_j(t') s_k(t'') \langle \exp(W) \rangle_f, \quad (43)$$

and similarly

$$\begin{aligned} \langle s_j(t') / \delta \epsilon_k(t'') \rangle_f = \langle s_j(t') \hat{s}_k(t'') \rangle_f = \int \int [ds][d\hat{s}] \\ \times s_j(t') \hat{s}_k(t'') \langle \exp(W) \rangle_f, \end{aligned} \quad (44)$$

It is not obvious how to calculate $\langle \exp(W) \rangle_f$ directly, since W involves terms like $J_{ij} s_i \hat{s}_j$ which couple different sites. Following Sompolinsky and Zippelius,⁸² and Narayan and

Fisher,⁴⁸ we can circumvent this problem by performing a change of variables from the spins s_j to local fields $J\tilde{\eta}_i = \sum_j J_{ij}s_j$. (We introduce the coefficient J on the left-hand side to keep the dimensions right.) At the saddle point of the associated action the new variables $\tilde{\eta}_j$ (for all j) are given by

the mean-field magnetization and the different sites become decoupled. A saddle-point expansion becomes possible, because the coefficients in the expansion can be calculated in mean-field theory—they are also the same for all sites j . Formally we insert into Z the expression

$$1 = 1/2\pi \int \int [d\hat{\eta}][d\tilde{\eta}] \mathcal{A}[\tilde{\eta}] \exp \left[i \sum_j \int dt \hat{\eta}(t) \left(s_j(t) - \sum_i J_{ij}^{-1} J \tilde{\eta}_i(t) \right) \right], \quad (45)$$

where $\mathcal{A}[\tilde{\eta}]$ stands for the suitable Jacobian, which is simply a constant and will be suppressed henceforth. Integrating out the auxiliary fields $\hat{\eta}_j$, one recovers that the expression in Eq. (45) is the integral over a product of δ functions which impose the definitions $J\tilde{\eta}_i(t) = \sum_j J_{ij}s_j(t)$ at all times for all i .

After some reshuffling of terms and introducing some redefinitions that are motivated by the attempt to separate the nonlocal from the local terms, one obtains

$$Z = \int \int [d\hat{\eta}][d\tilde{\eta}] \prod_j \bar{Z}_j[\tilde{\eta}_j, \hat{\eta}_j] \exp \left[- \int dt \hat{\eta}_j(t) \left(\sum_l J_{jl}^{-1} J \tilde{\eta}_l(t) \right) \right], \quad (46)$$

where $\bar{Z}_j[\tilde{\eta}_j, \hat{\eta}_j]$ is a *local* functional

$$\bar{Z}_j[\tilde{\eta}_j, \hat{\eta}_j] = \int \int [ds_j][d\hat{s}_j] \left\langle \exp \left[J^{-1} \int dt [J\hat{\eta}_j(t)s_j(t) + i\hat{s}_j(t)(\partial_t s_j(t)/\Gamma_0 - J\tilde{\eta}_j(t) - H - f_j + \delta V/\delta s_j)] \right] \right\rangle_f \quad (47)$$

(we have absorbed a factor i in the definition of $\hat{\eta}_j$). In short this can also be written as

$$Z \equiv \int [d\tilde{\eta}][d\hat{\eta}] \exp(\tilde{S}_{\text{eff}}) \quad (48)$$

with the effective action \tilde{S}_{eff} , now expressed in terms of the ‘‘local field’’ variables $\tilde{\eta}$ and $\hat{\eta}$

$$\begin{aligned} \tilde{S}_{\text{eff}} = & - \int dt \sum_j \hat{\eta}_j(t) \sum_l J_{jl}^{-1} J \tilde{\eta}_l(t) \\ & + \sum_j \ln(\bar{Z}_j[\tilde{\eta}_j, \hat{\eta}_j]). \end{aligned} \quad (49)$$

Physically we can interpret the functional

$$\Phi[\eta] \equiv \int [d\tilde{\eta}] \exp(\tilde{S}_{\text{eff}}) \quad (50)$$

as the random-field-averaged probability distribution for the possible paths the system can take through the ‘‘local field’’ ($J\tilde{\eta}_j$) configuration space as the external magnetic field is slowly increased. Z is the integral of this (normalized) probability distribution over all possible paths of the system and is therefore equal to 1.

The stationary point $[\tilde{\eta}_j^0, \hat{\eta}_j^0]$ of the effective action is given by

$$[\delta \tilde{S}_{\text{eff}} / \delta \tilde{\eta}_j]_{\tilde{\eta}_j^0, \hat{\eta}_j^0} = 0 \quad (51)$$

and

$$[\delta \tilde{S}_{\text{eff}} / \delta \hat{\eta}_j]_{\tilde{\eta}_j^0, \hat{\eta}_j^0} = 0. \quad (52)$$

With Eqs. (47) and (49) we find the saddle-point equations:

$$(-i) \langle \hat{s}_i \rangle_{l, \tilde{\eta}^0, \tilde{\eta}^0} - \sum_j J J_{ij}^{-1} \tilde{\eta}_j^0 = 0, \quad (53)$$

and

$$\langle s_i \rangle_{l, \tilde{\eta}^0, \tilde{\eta}^0} - \sum_j J J_{ij}^{-1} \tilde{\eta}_j^0 = 0. \quad (54)$$

The notation $\langle \rangle_{l, \tilde{\eta}^0, \tilde{\eta}^0}$ here denotes a *local* average, obtained from the *local* partition function \bar{Z}_i , after having fixed $\hat{\eta}_i$ and $\tilde{\eta}_i$ to their stationary-point solutions $\hat{\eta}_i^0$ and $\tilde{\eta}_i^0$. Equation (53) and (54) have the self-consistent solution

$$\hat{\eta}_i^0(t) = 0, \quad (55)$$

and

$$\tilde{\eta}_i^0(t) = M(t) = \langle s_i(t) \rangle_{l, \tilde{\eta}^0, \tilde{\eta}^0}, \quad (56)$$

where $M(t)$ is the random-field average of the solution of the mean-field equation of motion⁸³

$$\partial_t s_j(t)/\Gamma_0 = J\tilde{\eta}_j^0(t) + H + f_j - \delta V/\delta s_j. \quad (57)$$

We can now expand the effective action \tilde{S}_{eff} in the variables $\hat{\eta}_j \equiv (\tilde{\eta}_j - \tilde{\eta}_j^0)$ and $\eta_j \equiv (\tilde{\eta}_j - \tilde{\eta}_j^0)$, which corresponds to an expansion around mean-field theory:

$$Z = \int \int [d\eta][d\hat{\eta}] \exp(S_{\text{eff}}) \quad (58)$$

with an effective action (expressed in the new variables η and $\hat{\eta}$):

$$S_{\text{eff}} = - \sum_{j,l} \int dt J_{jl}^{-1} J \tilde{\eta}_j(t) \eta_l(t) + \sum_j \sum_{m,n=0}^{\infty} \frac{1}{m!n!} \int dt_1 \cdots dt_{m+n} u_{m,n}(t_1, \dots, t_{m+n}) \hat{\eta}_j(t_1) \cdots \hat{\eta}_j(t_m) \eta_j(t_{m+1}) \cdots \eta_j(t_{m+n}). \quad (59)$$

Here, as seen by inspection from Eqs. (49) and (47)

$$\begin{aligned} u_{m,n} &= \frac{\partial}{\partial \eta_j(t_{m+1})} \cdots \frac{\partial}{\partial \eta_j(t_{m+n})} \left[\frac{\delta^m [\ln \bar{Z}_j - \hat{\eta}_j(t) \tilde{\eta}_j^0(t)]}{\delta \hat{\eta}_j(t_1) \cdots \delta \hat{\eta}_j(t_m)} \right]_{\hat{\eta}=0, \eta=0} \\ &= \frac{\partial}{\partial \epsilon(t_{m+1})} \cdots \frac{\partial}{\partial \epsilon(t_{m+n})} \langle [s(t_1) - \eta^0(t_1)] \cdots [s(t_m) - \eta^0(t_m)] \rangle_{l, \hat{\eta}^0, \eta^0}, \end{aligned} \quad (60)$$

i.e., the coefficients u_{mn} are equal to the local (l), connected responses and correlations in mean-field theory. Again, *local* (l) means⁴⁸ that we do not vary the local field η_j^0 in the mean-field equation

$$\frac{1}{\Gamma_0} \partial_t s_j(t) = J \eta_j^0(t) + H + f_j - \frac{\delta V}{\delta s_j(t)} + J \epsilon(t) \quad (61)$$

when we perturb with the infinitesimal force $J \epsilon(t)$.

B. Source terms

Correlations of s and \hat{s} can be related to correlations of η and $\hat{\eta}$.⁴⁸ If we introduce the source terms

$$\int dt [s_j(t) \hat{l}_j(t) - i \hat{s}_j(t) l_j(t)] \quad (62)$$

into the action, we can write the correlations of s and \hat{s} as functional derivatives with respect to \hat{l} and l at $l = \hat{l} = 0$. A shift in the variables η and $\hat{\eta}$ by l and \hat{l} , respectively, leads to a source term for the fields η and $\hat{\eta}$ from

$$J J_{ij}^{-1} [\hat{\eta}_i(t) - \hat{l}_i(t)] [\eta_j(t) - l_j(t)], \quad (63)$$

so that derivatives with respect to l and \hat{l} give correlation functions of $\hat{\eta}$ and η . For low momentum behavior the factor $J J_{ij}^{-1}$ can be replaced by one since $\sum_j J_{ij}^{-1} = J^{-1}$.

C. Implementing the history

Up to here the effective action S_{eff} manifestly involves the entire magnetic-field range $-\infty < H < +\infty$. As we discuss in Appendix B it turns out, however, that in the adiabatic limit a separation of time scales emerges. The relaxation rate $k\Gamma_0$ in response to a perturbation is fast compared to the driving rate Ω/k of the external magnetic field. The static critical exponents can then be extracted self-consistently from a RG calculation performed at a single, fixed value H of the external magnetic field. The analysis is much simpler

than one might have expected. Instead of dealing with the entire effective action which involves *all* field values H , it suffices in the adiabatic limit to calculate all coefficients u_{mn} in Eq. (59) at one single fixed magnetic field H , and then to coarse grain the resulting action $S_{\text{eff}}(H) \equiv S_H$.

Physically this corresponds to the statement that increasing the magnetic field within an infinite ranged model (mean-field theory) and then tuning the elastic coupling to a short-ranged form (RG) would be equivalent to the physical relevant critical behavior, which actually corresponds to *first* tuning the elastic coupling to a short-ranged form and *then* increasing the force within a short-range model.⁴⁹ In their related calculation for charge-density waves (CDW's) below the depinning threshold,⁴⁹ Narayan and Middleton give an argument that this approach is self-consistent for their problem. In the Appendix B we first show that their argument applies to our system as well, and then discuss the consistency of the magnetic field decoupling within the RG treatment of the entire history for separated time scales.

Note that the values of the coefficients u_{mn} at field H are still history dependent (in the way the mean-field solution is). Also, causality must be observed by the coarse-graining transformation, so that even in the adiabatic limit the intrinsic history dependence of the problem does not get lost.

D. Calculating some of the u_{mn} coefficients at field H

In Appendix B we show that u_{mn} basically assume their static values in the adiabatic limit. In this section we will briefly outline their derivation and quote the relevant results.

We have to be consistent with the history of an increasing external magnetic field, when expanding around the ‘‘mean-field path’’ $\tilde{\eta}^0(t)$. This implies that for calculating responses from Eq. (60) we must only allow a perturbing force $J \epsilon(t)$ that *increases* with time in Eq. (61). For example, for $u_{1,1}$ we add a force $J \epsilon(t) \equiv J \epsilon \Theta(t - t')$ in Eq. (61), where $\Theta(t - t')$ is the step function, and solve for $\langle s(t) |_{H+J \epsilon(t)} \rangle_f$. The local response function is then given by the derivative of

$\lim_{\epsilon \rightarrow 0} \{ [\langle s(t) |_{H+J\epsilon(t)} \rangle_f - \langle s(t) |_H \rangle_f] / \epsilon \}$ with respect to $(-t')$. The higher response functions are calculated correspondingly. (See also Appendix B.) One obtains in the low-frequency approximation for the first few terms of the effective action of Eq. (59) at field H

$$S_H = - \sum_{j,l} \int dt J_{jl}^{-1} J \hat{\eta}_j(t) \eta_l(t) - \sum_j \int dt \hat{\eta}_j(t) [a \partial_t / \Gamma_0 - u_{11}^{\text{stat}}] \eta_j(t) + \sum_j \int dt \frac{1}{6} u \hat{\eta}_j(t) (\eta_j(t))^3 + \sum_j \int dt_1 \int dt_2 \frac{1}{2} u_{2,0} \hat{\eta}_j(t_1) \hat{\eta}_j(t_2), \quad (64)$$

with

$$a = [J/k + 4\rho(-J\eta^0 - H + k)]/k, \quad (65)$$

$$u_{11}^{\text{stat}} = 2J\rho(-J\eta^0 - H + k) + J/k, \quad (66)$$

$$w = -2J^2\rho'(-J\eta^0 - H + k), \quad (67)$$

$$u = 2J^3\rho''(-J\eta^0 - H + k), \quad (68)$$

and

$$u_{2,0} = R^2/k^2 + 4 \left(\int_{-\infty}^{-H-\eta^0+k} \rho(h) dh \right) - 4 \left(\int_{-\infty}^{-H-\eta^0+k} \rho(h) dh \right)^2 - 4 \left(\int_{-\infty}^{-H-\eta^0+k} (h/k) \rho(h) dh \right). \quad (69)$$

Equation (69) implies that $u_{2,0} \geq 0$ for any normalized distribution $\rho(f)$.

V. PERTURBATIVE EXPANSION

A. The Gaussian theory for $d > d_c$: Response and correlation functions

One can show^{39,42} that for systems with dimension d above the upper critical dimension d_c , the nonquadratic

terms in the action become less important on longer length (and time) scales. Near the critical point, where the behavior is dominated by fluctuations on long-length scales, the system is then well described by the quadratic parts of the action, and the calculation of correlation and response functions amounts to the relatively simple task of solving Gaussian integrals. It should come as no surprise that the mean-field exponents are recovered, since the quadratic parts of the action represent the lowest-order terms in the saddle-point expansion around mean-field theory.

In our problem the action S_H of Eq. (64) has the quadratic part

$$Q(\eta, \hat{\eta}) = - \sum_{j,l} \int dt J_{jl}^{-1} J \hat{\eta}_j(t) \eta_l(t) - \sum_j \int dt \hat{\eta}_j(t) \times [a \partial_t / \Gamma_0 - u_{11}^{\text{stat}}] \eta_j(t) + (1/2) \sum_j \int dt_1 \int dt_2 \hat{\eta}_j(t_1) \hat{\eta}_j(t_2) u_{2,0}. \quad (70)$$

In the long-wavelength limit we can write $J^{-1}(q) = 1/J + J_2 q^2$.⁴⁰ Rescaling $\hat{\eta}$, ω , and q we can replace the constants $J_2 J$ and a by 1. The low-frequency part of the $\hat{\eta}\eta$ term in $Q(\eta, \hat{\eta})$ is then given by

$$- \int d^d q \int dt \hat{\eta}(-q, t) (\partial_t / \Gamma_0 + q^2 - \chi^{-1}/J) \eta(q, t), \quad (71)$$

where

$$\chi^{-1} = J(u_{11}^{\text{stat}} - 1) = 2J^2\rho(-JM - H + k) - J(k - J)/k \quad (72)$$

is the negative static response to a monotonically increasing external magnetic field, calculated in mean-field theory.

In frequency space $Q(\eta, \hat{\eta})$ can be written as

$$Q(\eta, \hat{\eta}) = - \int d\omega \int d^d q [\hat{\eta}(-q, -\omega), \eta(-q, -\omega)] \begin{pmatrix} -1/2u_{2,0}\delta(\omega) & (-i\omega/\Gamma_0 + q^2 - \chi^{-1}/J) \\ (i\omega/\Gamma_0 + q^2 - \chi^{-1}/J) & 0 \end{pmatrix} \begin{pmatrix} \hat{\eta}(q, \omega) \\ \eta(q, \omega) \end{pmatrix}. \quad (73)$$

Inverting the matrix⁴⁸ one obtains for the response and correlation function at field H to lowest order

$$G_{\hat{\eta}\eta}(q, \omega) = \langle \hat{\eta}(-q, -\omega) \eta(q, \omega) \rangle \approx 1/(-i\omega/\Gamma_0 + q^2 - \chi^{-1}/J) \quad (74)$$

and

$$G_{\hat{\eta}\hat{\eta}}(q, \omega) = \langle \eta(-q, -\omega) \eta(q, \omega) \rangle \approx u_{2,0}\delta(\omega)/|-i\omega/\Gamma_0 + q^2 - \chi^{-1}/J|^2. \quad (75)$$

The $\delta(\omega)$ in Eq. (75) is a consequence of the underlying

separation of time scales. It will lead to an essentially static character of the RG analysis of the problem. This may have been expected, since the critical phenomena we set out to describe are essentially static in nature. At the critical point

$\chi^{-1}=0$ we have $G_{\hat{\eta}\eta}(q, \omega=0) \sim q^{2-\eta}$ with $\eta=0$ and $G_{\eta\eta}(q, \omega=0) \sim q^{4-\bar{\eta}}$ with $\bar{\eta}=0$ at lowest order in perturbation theory. One can Fourier transform the correlation functions back to time

$$G_{\hat{\eta}\eta}(q, t, t') \equiv \langle \hat{\eta}(q, t) \eta(-q, t') \rangle = \begin{cases} \Gamma_0 \exp\{-\Gamma_0(q^2 - \chi^{-1}/J)(t' - t)\} & \text{for } t' > t \\ 0 & \text{for } t' \leq t \end{cases} \quad (76)$$

and

$$G_{\eta\eta}(q, t, t') = \int dt_1 \int dt_2 G_{\hat{\eta}\eta}[q, -(t' - t) + t_1 + t_2] u_{2,0} G_{\hat{\eta}\eta}(q, t_2) = u_{2,0} / (q^2 - \chi^{-1}/J)^2. \quad (77)$$

B. The RG analysis

In dimension $d < d_c$ the nonquadratic parts of the action become important near the critical point. One obtains corrections to the mean-field behavior. The Wilson-Fisher coarse-graining procedure is an iterative transformation to calculate the effective action for the long-wavelength and low-frequency degrees of freedom of the system. Fixed points under the coarse-graining transformation correspond to critical points where no finite (correlation) length determines the long-wavelength behavior and the system is self-similar on all length scales. In each coarse-graining step^{41,42,48,84} one integrates out high momentum modes of *all* frequencies $\hat{\eta}(q, \omega)$ and $\eta(q, \omega)$, with q in a momentum shell $[\Lambda/b, \Lambda]$, $b > 1$, and afterwards rescales according to $q = b^{-1}q'$, $\omega = b^{-1}\omega'$, $\hat{\eta}(q, \omega) = b^{\hat{c}_p} \hat{\eta}'(q, \omega)$, and $\eta(q, \omega) = b^{c_p} \eta'(q, \omega)$. As usual, the field rescaling \hat{c}_p and c_p are chosen such that the quadratic parts of the action at the critical point ($\chi^{-1}=0$) remain unchanged, so that the rescaling of the response and the cluster correlation function under coarse graining immediately gives their respective power-law dependence on momentum (i.e., this is an appropriate choice of the scaling units). Without loop correlations to the mean-field theory this implies that $z=2$, $\hat{\eta}(x, t) = b^{-d/2-z} \hat{\eta}'(x, t)$ and $\eta(x, t) = b^{-d/2+2} \eta'(x, t)$.

Performing one coarse-graining step for the expansion for S_H of Eq. (64) yields a coarse grained action which can be written in the original form, with ‘renormalized’ vertices $u'_{m,n}$. Without loop corrections, the vertices of the coarse-grained action are simply rescalings of the original vertices, which can be easily read off using the rescaling of q , ω , η , and $\hat{\eta}$. Taking into account that each $\delta/\delta\epsilon(t)$ involves a derivative with respect to time, and therefore another factor b^{-z} under rescaling, we arrive at $(\chi^{-1})' = b^2 \chi^{-1}$ and

$$u'_{m,n} = b^{[-(m+n)+2]d/2+2n} u_{m,n}. \quad (78)$$

This shows that above eight dimensions all vertices that are coefficients of terms of higher than quadratic order in the fields, shrink to zero under coarse graining and are therefore ‘irrelevant’ for the critical behavior on long length scales and at low frequencies.

Below eight dimensions the vertex $u_{1,2} \equiv w = 2J\rho'(-J\eta^0 - H + k)$ is the first coefficient of a nonquadratic term to become relevant. An action with the original

parameters $\chi^{-1}=0$ and $w \neq 0$ corresponds to a system with less than critical randomness $R < R_c$ at the onset field of the infinite avalanche. In Appendix C we show how to extract the mean-field exponents for the infinite avalanche line from the scaling above eight dimensions and that the RG treatment suggests a first-order transition for the same systems in less than eight dimensions.

In systems where the bare value of w is zero at the critical fixed point with $\chi^{-1}=0$, all nonquadratic terms are irrelevant above $d_c=6$ dimensions. As can be seen from Appendix A, this case constitutes the interesting ‘critical endpoint’ at $R=R_c$ and $H=H_c(R_c)$, which we have discussed in the introduction. Also, $w=0$ implies that the bare vertex $\chi^{-1} \sim (R_c - R)/R$. For $d < 6$, the vertex $u_{1,3} = u$ becomes relevant, while all higher vertices remain irrelevant. We are left with the effective action which includes all vertices relevant for an expansion around six dimensions:

$$\begin{aligned} \bar{S} = & - \int d^d q \int dt \hat{\eta}(-q, t) [\partial_t / \Gamma_0 + q^2 - \chi^{-1}/J] \eta(q, t) \\ & + (1/6) \sum_j \int dt \hat{\eta}_j(t) (\eta_j(t))^3 u \\ & + (1/2) \sum_j \int dt_1 \int dt_2 \hat{\eta}_j(t_1) \hat{\eta}_j(t_2) u_{2,0}. \end{aligned} \quad (79)$$

We will perform the coarse-graining transformation in perturbation theory in u . At the fixed point, in $6 - \epsilon$ dimensions, u will be of $O(\epsilon)$. The perturbation series for the parameters in the action and thus also for the critical exponents, becomes a perturbation series in powers of ϵ . From the form of the action one can derive Feynman rules (see Appendix B), which enable us to write down the perturbative corrections in a systematic scheme. Examples of their derivation for the ϕ^4 model are given elsewhere.^{39,40,42}

VI. MAPPING TO THE THERMAL RANDOM-FIELD ISING MODEL

A. Perturbative mapping and dimensional reduction

In this section we will show that the ϵ expansion for our model is the same as the ϵ -expansion for the *equilibrium*

random-field Ising model to all orders in ϵ .⁸⁵ Once this equivalence is established, we can use that the $(6-\epsilon)$ expansion of the *equilibrium* random-field Ising has been mapped to *all* orders in ϵ to the corresponding expansion of the regular Ising model in two lower dimensions.^{86,87}

The easiest way to recognize that the ϵ expansion for our model and for the *equilibrium* RFIM should really be the same is by comparing the corresponding effective actions. In a dynamical description of the *equilibrium* RFIM at zero external magnetic field the following effective Langevin equation of motion for the spin-field $\phi(r,t)$ was used⁶⁷

$$\partial_t \phi(x,t) = -\Gamma_0[-\nabla^2 \phi(x,t) + r_0 \phi(x,t) + 1/6g_0 \phi^3(x,t) - h_R(x) - h_T(x,t)]. \quad (80)$$

$h_R(x)$ represents spatially uncorrelated quenched random fields distributed according to a Gaussian of width Δ and mean zero. $h_T(x,t)$ is the thermal noise field, which is taken to be Gaussian with vanishing mean value and the variance

$$\langle h_T(x,t) h_T(x',t') \rangle = 2kT/\Gamma_0 \delta(x-x') \delta(t-t'). \quad (81)$$

The corresponding Martin-Siggia-Rose generating functional is

$$\begin{aligned} Z_{H_0}^{\text{thermal}} = & \int [d\hat{\phi}] \int [d\phi] \exp \left\{ - \int d^d q \int dt \hat{\phi}(-q,t) (\partial_t/\Gamma_0 + q^2 + r_0) \phi(q,t) + \int d^d x \int dt \hat{\phi}(x,t) (-1/6g_0) \phi(x,t)^3 \right. \\ & \left. + \int d^d x \int dt \hat{\phi}(x,t) [h_R(x) + h_T(x,t)] \right\}. \end{aligned} \quad (82)$$

Since again $Z_{H_0}^{\text{thermal}}=1$, we can average the partition function directly over the random fields h_R and the thermal noise h_T :

$$\bar{Z}_{H_0}^{\text{thermal}} = \langle Z_{H_0}^{\text{thermal}} \rangle_{h_R}. \quad (83)$$

The average over the random fields at each x and over the thermal noise fields at each x and t yields, (after completing the square):

$$\begin{aligned} \bar{Z}_{H_0}^{\text{thermal}} = & \int [d\hat{\phi}] \int [d\phi] \exp \left\{ - \int d^d q \int dt \hat{\phi}(-q,t) (\partial_t/\Gamma_0 + q^2 + r_0) \phi(q,t) + \int d^d x \int dt \hat{\phi}(x,t) (-\frac{1}{6} g_0) \phi^3(x,t) \right. \\ & \left. + \int d^d x \int dt_1 \int dt_2 \hat{\phi}(x,t_1) \hat{\phi}(x,t_2) \Delta^2/2 + \int d^d x \int dt \hat{\phi}^2(x,t) (2kT)/\Gamma_0 \right\}. \end{aligned} \quad (84)$$

With the identifications $r_0 = -\chi^{-1}(H_0)$, $u = -1/6g_0$, $u_{2,0} = \Delta^2$ and $T=0$, we see that the argument of the exponential function is the same action as the effective action for our zero-temperature, nonequilibrium model in Eq. (64). Setting T to zero in the action for the equilibrium RFIM does not change the expansion for the static behavior, since it turns out that corrections involving temperature are negligible compared to those involving the random magnetic field^{67,87,88}—the *temperature* dependence is irrelevant in the *thermal* RFIM and the *time* dependence is irrelevant in our zero-temperature *dynamical* RFIM, leaving us with the same starting point for the calculation. This equivalence implies that in $6-\epsilon$ dimensions we should obtain the same critical exponents to all orders in ϵ for our model, as were calculated for the thermal random-field Ising model, which in turn are the same as those of the pure equilibrium Ising model in $4-\epsilon$ dimensions.^{86,87}

This observation is rather convenient, since it provides us with results from the regular Ising model to $O(\epsilon^5)$ for free. In $6-\epsilon$ dimensions we read off⁶⁵

$$\begin{aligned} 1/\nu = & 2 - \epsilon/3 - 0.1173\epsilon^2 + 0.1245\epsilon^3 - 0.307\epsilon^4 + 0.951\epsilon^5 \\ & + O(\epsilon^6), \end{aligned} \quad (85)$$

$$\begin{aligned} \eta = & 0.0185185\epsilon^2 + 0.01869\epsilon^3 - 0.00832876\epsilon^4 + 0.02566\epsilon^5 \\ & + O(\epsilon^6), \end{aligned} \quad (86)$$

$$\begin{aligned} \beta = & 1/2 - \epsilon/6 + 0.00617685\epsilon^2 - 0.035198\epsilon^3 + 0.0795387\epsilon^4 \\ & - 0.246111\epsilon^5 + O(\epsilon^6), \end{aligned} \quad (87)$$

$$\begin{aligned} \beta\delta = & 3/2 + 0.0833454\epsilon^2 - 0.0841566\epsilon^3 + 0.223194\epsilon^4 \\ & - 0.69259\epsilon^5 + O(\epsilon^6). \end{aligned} \quad (88)$$

β and δ have been calculated from η and ν using the perturbative relations: $\beta = (\nu/2)(d-4+\bar{\eta})$ and $\delta = (d-2\eta + \bar{\eta})/(d-4+\bar{\eta})$ (see Sec. III I 1), with $\eta = \bar{\eta}$ to all orders in ϵ .⁶⁷

B. Perturbative mapping of the equation of state

By the same mapping we obtain the universal scaling function for the magnetization to $O(\epsilon^2)$.^{89,90} Since the corresponding calculation has been explained in great detail for the equation of state of the Ising model in $4-\epsilon$ dimensions in the article by Wallace in Ref. 90, we will only briefly outline the main steps and quote the result for the scaling function in the end.

Following the Wallace article one expands the action around the *true* (note mean-field) magnetization $\bar{\eta}^0 = M_{\text{true}}$ and expands the bare vertices in terms of the deviations $h = H - H_c(R_c)$, $r = (R_c - R)/R$, and $m = M_{\text{true}} - M_c$ of the parameters H , R , and M_{true} from their values at the mean-field critical point $\{H_c(R_c) = k - J, R_c = 2kJ/[\sqrt{(2\pi)(k - J)}], \text{ and } M_c = +1, \text{ as given in Appendix A}\}$. One obtains to lowest order³⁸ $u_{1,0} = h/k + 2J/(\sqrt{2\pi R})rm + (2J^3/3!)\rho''(0)m^3 + \dots$, $\chi^{-1} = -2Jr/(\sqrt{2\pi R}) + 1/2um^2 + \dots$ [see Eq. (72)], $w = um + \dots$ [see Eq. (67)], and $u = 2J^3\rho''(0) + \dots$ [see Eq. (68)], where \dots denotes higher orders in h , m , and r , and $\rho''(f)$ is the second derivative of the distribution of random fields with respect to its argument.

Calculating loop corrections in the ϵ expansion of the equation of state is then completely analogous to the calculation described by Wallace for the Ising model in two lower dimensions. For details on solving the loop integrals, etc. we refer the reader to Ref. 90, especially Eq. (3.35). [In fact, with the following formal identifications, the resulting equations of state in the two systems can be mapped onto each

other: $h/k = -h_w$, $2Jr/(\sqrt{2\pi R}) = -t_w$, $2J^3\rho''(0) = -(u_0)_w$, $m = -m_w$. We have denoted the quantities in Wallace's article by an index "w."]

One obtains the following result:

$$h = m^\delta f(x = r/m^{1/\beta}) \quad (89)$$

in which the renormalizations of x and the universal scaling function f are chosen such that

$$f(0) = 1, \quad f(-1) = 0. \quad (90)$$

The expansion to second order in ϵ is then

$$f(x) = 1 + x + \epsilon f_1(x) + \epsilon^2 f_2(x) \quad (91)$$

with

$$f_1(x) = \frac{1}{6}[(x+3)\ln(x+3) - 3(x+1)\ln 3 + 2x \ln 2] \quad (92)$$

and

$$\begin{aligned} f_2(x) = & \left[\frac{1}{18}\right]^2 \{ [6 \ln 2 - 9 \ln 3][3(x+3)\ln(x+3) + 6x \ln 2 - 9(x+1)\ln 3] + \frac{9}{2}(x+1)[\ln^2(x+3) - \ln^2 3] \\ & + 36[\ln^2(x+3) - (x+1)\ln^2 3 + x \ln^2 2] - 54 \ln 2[\ln(x+3) + x \ln 2 - (x+1)\ln 3] \\ & + 25[(x+3)\ln(x+3) + 2x \ln 2 - 3(x+1)\ln 3] \}. \end{aligned} \quad (93)$$

The scaling function $f(x)$ has actually been calculated up to order ϵ^3 .⁴³ As it stands the expression (91) meets the Griffith analyticity requirements⁹¹ only within the framework of the ϵ expansion, but not explicitly. These subtleties can be avoided by writing it in a parametric form,⁸⁹ which can then be compared directly with our numerical results for the universal scaling function of dM/dH in five, four, three, and two dimensions. We will present the results in a forthcoming paper.²

The dynamic exponent z cannot be extracted from the mapping to the regular Ising model. It was calculated separately to $O(\epsilon^3)$ for the equilibrium RFIM (Ref. 67) and found to be given to this order by [Equation (94) is only a perturbative result for z which does not reveal the presence of diverging barrier heights that lead to the observed slow relaxation towards equilibrium.^{4,5-7,71} Nonperturbative corrections are expected to be important in the equilibrium random-field Ising model.]

$$z = 2 + 2\eta = 2 + 0.037037\epsilon^2 + 0.03738\epsilon^3 + O(\epsilon^4). \quad (94)$$

Because of the perturbative mapping of our model to the equilibrium RFIM, Eq. (94) also gives the result for z in our nonequilibrium hysteretic system.

We have performed a Borel resummation^{38,92} of the corrections to $O(\epsilon^5)$ for η , ν , and the derived exponent $\beta\delta$ (see Sec. III I 1). The exponent β is then given through $\beta = \beta\delta - (2 - \eta)\nu$ [Eq. (24)]. Figure 6 shows a comparison with our numerical results in three, four, and five dimensions.

The agreement is rather good near six dimensions. However the apparent dimensional reduction through the perturbative mapping to the Ising exponents in two dimensions gradually loses its validity at lower dimensions. It is after all only due to the equivalence of two asymptotic series, both of which have radius of convergence zero. Table I shows a comparison between the numerical exponents for our model and for the equilibrium RFIM in three dimensions.

C. Nonperturbative corrections

The mapping of the ϵ expansion for the thermal random-field Ising model to the expansion for the Ising model in two lower dimensions caused much controversy when discovered. The problem was that it had to break down at the lower critical dimension, where the transition disappears. There is no transition in the pure Ising model in $d=1$, but the equilibrium RFIM is known rigorously to have a transition in $d=3$.^{93,94} The same is true for our model: numerical simulations indicate^{1,2} that the lower critical dimension is lower than three—probably equal to 2.

In the case of the equilibrium random-field Ising model it was finally agreed^{71,87} that this breakdown might be due to nonperturbative corrections. The point is that proving a relation to all orders in ϵ does not make it true. In the equilibrium RFIM there are at least two sources of nonperturbative corrections:

(a) *The "embarrassing" correction:* It was found that there was a calculational error in the $(6 - \epsilon)$ expansion for the RFIM. The perturbation series was tracing over many un-

TABLE I. Numerical results for the critical exponents in three dimensions for our hysteresis model (Refs. 1 and 2) and for the equilibrium zero-temperature random-field Ising model (Refs. 71 and 119). The breakdown of hyperscaling exponent $\tilde{\theta}$ is calculated for the hysteresis model from the relation $\beta + \beta\delta = (d - \tilde{\theta})\nu$ (see Sec. III I 2 and Refs. 38 and 37). The values of the critical exponents of the two models remain within each other's error bars; their equality was conjectured by Maritan *et al.* (Ref. 96). This may not be so surprising, if one remembers that the $6 - \epsilon$ expansion is the same for all exponents of the two models. Nevertheless there is always room for nonperturbative corrections, so that the exponents might still be different in three dimensions (see Sec. VI C). Physically the agreement is rather unexpected, since the nature of the two models is very different. While the hysteresis model is far from equilibrium, occupying a history dependent, metastable state, the equilibrium RFIM is always in the lowest free-energy state. One may speculate, however, about a presumably universal crossover from our hysteresis model to the equilibrium random-field Ising model as temperature fluctuations and a finite field-sweeping frequency Ω are introduced (see Appendix E 2).

Exponents	Hysteresis loop (Ref. 2) in three dimensions (courtesy Olga Perković)	Equilibrium RFIM (Ref. 120) in three dimensions
ν	1.42 ± 0.17	0.97, 1.30, 1.05 ± 0.1 (Ref. 119)
β	0.0 ± 0.43	-0.1, 0.05
$\beta\delta$	1.81 ± 0.36	1.6, 1.9 ± 0.4
η	0.79 ± 0.29	0.25, 0.5 ± 0.5
$\tilde{\theta}$	1.5 ± 0.5	1.45, 1.5 ± 0.45
R_c (Gaussian)	2.16 ± 0.03	2.3 ± 0.2 (Ref. 119)
$H_c(R_c)$	1.435 ± 0.004	0 (by symmetry)

physical metastable states of the system, instead of just taking into account the ground state, which the system occupies in equilibrium. There were indications that this error leads to nonperturbative corrections, which would destroy the dimensional reduction outside of perturbation theory.⁸⁷

In our calculation we have avoided the embarrassing source of nonperturbative corrections found in the equilibrium random-field Ising problem. Given the initial conditions and a history $H(t)$, the set of coupled equations of motion for all spins will have only one solution. In the Martin-Siggia-Rose (MSR) formalism, the physical state is selected as the only solution that obeys causality, there are no unphysical metastable states coming in. Therefore we believe our results should also apply to systems below the critical randomness, at least before the onset of the infinite avalanche.

(b) *Instanton corrections:* Even without the embarrassing correction, there is no reason why a perturbative mapping of the expansions about the upper critical dimensions should lead to a mapping of the lower critical dimensions also. The ϵ expansion is only an asymptotic expansion—it has radius of convergence zero. As we discuss in Refs. 38 and 92, there is no known reason to assume that the ϵ expansion uniquely determines an underlying function. It leaves room for functions subdominant to the asymptotic power series: If the series $\sum_0^\infty f_k z^k$ is asymptotic to some function $f(z)$ in the complex plane as $z \rightarrow 0$, then it is also asymptotic to any function which differs from $f(z)$ by a function $g(z)$ that tends to zero more rapidly than all powers of z as $z \rightarrow 0$.⁹⁵ An example of such a subdominant function would be $g(z) = \exp(-1/z)$. While some asymptotic expansions can be proven to uniquely define the underlying function, this has not been shown for the ϵ expansion^{38,92}—not for our problem, nor for the equilibrium pure Ising model, nor for the equilibrium thermal random-field Ising model.

At this point, the ϵ expansion for our model is on no worse formal footing than that for the ordinary Ising model. We believe, the asymptotic expansion is valid for both models, despite the fact that their critical exponents are different: the exponents for the Ising model in $\epsilon = 4 - d$ and the exponents for our model in $\epsilon = 6 - d$ are different analytic functions with the same asymptotic expansion. The ϵ expansion cannot be used to decide whether the lower critical dimension is at $\epsilon = 3$ or at $\epsilon = 4$.

We conclude that because of instanton corrections the dimensional reduction breaks down for the equilibrium RFIM as well as for our nonequilibrium, deterministic zero-temperature RFIM. In addition there is another “embarrassing” source of nonperturbative corrections in the equilibrium RFIM, which we do not have in our problem. There is no reason to expect our exponents to be the same as those of the equilibrium RFIM,⁹⁶ though the perturbation series can be mapped. There might actually be three different underlying functions for the same ϵ expansion for any exponent: one for the pure Ising model, one for the equilibrium random-field Ising model, and one for our model, so that the exponents in all three models would still be different although their ϵ expansions are the same.

VII. ϵ EXPANSION FOR THE AVALANCHE EXPONENTS

The exponents whose ϵ expansion we have calculated so far using the mapping to the equilibrium RFIM are ν , η , $\bar{\eta}$, β , $\beta\delta$, $\tilde{\theta}$, and z . Unfortunately, we cannot extract the avalanche exponents τ , $1/\sigma$, and θ from this mapping. The two exponent relations involving these exponents

$$\tau - 2 = \sigma\beta(1 - \delta) \quad (95)$$

and

$$1/\sigma = (d - \theta)\nu - \beta \quad (96)$$

are not enough to determine all three exponents from the information already obtained.

In the following we will compute τ and σ directly in an ϵ expansion. The method employed makes use of the scaling of the higher moments of the avalanche size distribution. They are being calculated using n replicas of the system for the n th moment.

A. The second moment of the avalanche-size distribution

When calculating η and ν we have already used all information from the scaling behavior of the first moment $\langle S \rangle$ of the avalanche size distribution: It is easy to see³⁸ that $\langle S \rangle$ scales as the spatial integral over the avalanche-response-correlation function, which in turn scales as the ‘‘upward susceptibility’’ dM/dh calculated consistently with the history of the system. In the Martin-Siggia-Rose formalism it is given by⁹⁷

$$\begin{aligned} \langle S \rangle &\sim \int dt_0 \int d^d x \langle \hat{s}(t_0, x_0) s(t, x) \rangle_f \\ &= \int dt_0 \int d^d x \langle \delta s(t, x) / \delta \epsilon(t_0, x_0) \rangle_f. \end{aligned} \quad (97)$$

The second moment $\langle S^2 \rangle$ of the avalanche size distribution is the random-field average of the squared avalanche response. Note that it is not simply the square of the expression in Eq. (97) for the first moment—the product rule for taking derivatives gets in the way: A quantity such as

$$\langle \hat{s}(t_0, x_0) s(t_1, x_1) \hat{s}(t_2, x_2) s(t_3, x_3) \rangle_f \equiv A + B, \quad (98)$$

not only contains the term which we need

$$A = \left\langle \frac{\delta s(t_1, x_1)}{\delta \epsilon(t_0, x_0)} \frac{\delta s(t_3, x_3)}{\delta \epsilon(t_2, x_2)} \right\rangle_f \quad (99)$$

but also the terms

$$\begin{aligned} B &= \left\langle \frac{\delta^2 s(t_1, x_1)}{\delta \epsilon(t_0, x_0) \delta \epsilon(t_2, x_2)} s(t_3, x_3) \right\rangle_f \\ &+ \left\langle s(t_1, x_1) \frac{\delta^2 s(t_3, x_3)}{\delta \epsilon(t_0, x_0) \delta \epsilon(t_2, x_2)} \right\rangle_f, \end{aligned} \quad (100)$$

which are not related to $\langle S^2 \rangle$. To separate A and B we introduce a second replica of the system with the identical configuration of random fields, the same initial conditions, and the same history of the external magnetic field. One can then calculate the response in each of the two replicas separately, multiply the results and afterwards take the average over the random fields. Denoting the quantities in the first replica with superscript α and those in the second replica with superscript β one obtains

$$\begin{aligned} A_2 &\equiv \langle \hat{s}^\alpha(t_0, x_0) s^\alpha(t_1, x_1) \hat{s}^\beta(t_2, x_2) s^\beta(t_3, x_3) \rangle_f \\ &= \left\langle \frac{\delta s^\alpha(t_1, x_1)}{\delta \epsilon^\alpha(t_0, x_0)} \frac{\delta s^\beta(t_3, x_3)}{\delta \epsilon^\beta(t_2, x_2)} \right\rangle_f, \end{aligned} \quad (101)$$

since

$$\frac{\delta s^\alpha}{\delta \epsilon^\beta} = 0, \quad (102)$$

and

$$\frac{\delta s^\beta}{\delta \epsilon^\alpha} = 0. \quad (103)$$

Similarly for the n th moment $\langle S^n \rangle$ of the avalanche-size distribution one would use n replicas of the system. In Appendix D we make this argument more precise and derive the scaling relation between $\langle S^2 \rangle$ and A_2

$$\begin{aligned} \langle S^2 \rangle_f &\sim \int dt_1 \int dt_\alpha dt_\beta d^d x_\alpha d^d x_\beta \langle \hat{s}^\alpha(t_\alpha, x_\alpha) \\ &\times s^\alpha(t_0, x_\alpha) \hat{s}^\beta(t_\beta, x_\beta) s^\beta(t_1, x_\beta) \rangle_f. \end{aligned} \quad (104)$$

In the following we generalize the RG treatment from previous sections to the case of two replicas, and extract the scaling behavior of $\langle S^2 \rangle$ from Eq. (104) near the critical point. We will compare the result to the scaling relation

$$\begin{aligned} \langle S^2 \rangle &= \int S^2 D(S, r, h) dS \sim \int S^2 / S^\tau \mathcal{D}_\pm(S r^{1/\sigma}, h / r^{\beta\delta}) dS \\ &\sim r^{(\tau-3)/\sigma} \mathcal{S}_\pm^{(2)}(h / r^{\beta\delta}), \end{aligned} \quad (105)$$

where $\mathcal{S}_\pm^{(2)}$ is the corresponding scaling function, and obtain the missing information to compute the exponents τ and σ .

B. Formalism for two replicas

The generalization of the MSR generating functional to two replicas is rather straightforward. The equation of motion for each spin is the same in both replicas

$$\partial_t s_i^\alpha / \Gamma_0 - \delta \mathcal{H}(s^\alpha) / \delta s_i^\alpha = 0 \quad (106)$$

and

$$\partial_t s_i^\beta / \Gamma_0 - \delta \mathcal{H}(s^\beta) / \delta s_i^\beta = 0, \quad (107)$$

where the Hamiltonian \mathcal{H} is given by Eq. (33).

The new generating functional is a double path integral over two δ functions which impose the equations of motion for both replicas. Again we can write the δ functions in their ‘‘Fourier’’ representation by introducing two auxiliary fields \hat{s}^α and \hat{s}^β .

One obtains simply the square of the generating functional from Eq. (35), expressed in terms of two replicas:

$$Z^{\alpha\beta} = \int \int [ds^\alpha][d\hat{s}^\alpha] \int \int [ds^\beta][d\hat{s}^\beta] J[s^\alpha] J[s^\beta] \exp\left(i \sum_j \int dt \hat{s}_j^\alpha(t) [\partial_t s_j^\alpha(t) / \Gamma_0 - \delta \mathcal{H}(s^\alpha) / \delta s_j^\alpha(t)]\right) \exp\left(i \sum_j \int dt \hat{s}_j^\beta(t) [\partial_t s_j^\beta(t) / \Gamma_0 - \delta \mathcal{H}(s^\beta) / \delta s_j^\beta(t)]\right). \quad (108)$$

We note that the two replicas do not interact before the average over the random fields is taken. Since $Z=1$ we can again average Z directly over the random fields.

We rewrite the action using the same kinds of transformations to the local fields $\bar{\eta}^\alpha$, $\hat{\eta}^\alpha$, $\bar{\eta}^\beta$, and $\hat{\eta}^\beta$ which we introduced previously [see Eq. (46)], i.e.,

$$Z^{\alpha\beta} = \int [d\bar{\eta}^\alpha][d\hat{\eta}^\alpha][d\bar{\eta}^\beta][d\hat{\eta}^\beta] \prod_j \bar{Z}_j[\bar{\eta}_j^\alpha, \hat{\eta}_j^\alpha, \bar{\eta}_j^\beta, \hat{\eta}_j^\beta] \exp\left\{- \int dt \sum_j \hat{\eta}_j^\alpha(t) \left(\sum_{j'} J_{j'}^{-1} J \bar{\eta}_{j'}^\alpha(t) \right) - \int dt \sum_j \hat{\eta}_j^\beta(t) \left(\sum_{j'} J_{j'}^{-1} J \bar{\eta}_{j'}^\beta(t) \right)\right\}, \quad (109)$$

where $\bar{Z}_j[\bar{\eta}_j^\alpha, \hat{\eta}_j^\alpha, \bar{\eta}_j^\beta, \hat{\eta}_j^\beta]$ is a local functional

$$\bar{Z}_j[\bar{\eta}_j^\alpha, \hat{\eta}_j^\alpha, \bar{\eta}_j^\beta, \hat{\eta}_j^\beta] = \int [ds^\alpha][d\hat{s}^\alpha][ds^\beta][d\hat{s}^\beta] \times \langle \exp \bar{S}_{\text{eff},j}^{\alpha\beta} \rangle_f, \quad (110)$$

and

$$\bar{S}_{\text{eff},j}^{\alpha\beta} = \frac{1}{J} \int dt \left\{ J \hat{\eta}_j^\alpha(t) s_j^\alpha(t) + i \hat{s}_j^\alpha(t) \left(\partial_t s_j^\alpha(t) - J \bar{\eta}_j^\alpha - H - f_j + \frac{\partial V^\alpha}{\delta s_j^\alpha} \right) \right\} + \frac{1}{J} \int dt \left\{ J \hat{\eta}_j^\beta(t) s_j^\beta(t) + i \hat{s}_j^\beta(t) \left(\partial_t s_j^\beta(t) - J \bar{\eta}_j^\beta - H - f_j + \frac{\partial V^\beta}{\delta s_j^\beta} \right) \right\}. \quad (111)$$

Here V^α and V^β are given by the linear cusp potential V defined in Eq. (32), to be understood as a function of s^α and s^β , respectively.

Again, we expand the action around its stationary point. It is specified by four coupled equations, which turn out to be

solved self-consistently by the replica symmetric mean-field solution, which we found earlier when studying just one replica:

$$\bar{\eta}_0^\alpha = 0, \quad (112)$$

$$\bar{\eta}_0^\beta = 0, \quad (113)$$

$$\bar{\eta}_0^\alpha = \langle s^\alpha \rangle_f, \quad (114)$$

$$\bar{\eta}_0^\beta = \langle s^\beta \rangle_f, \quad (115)$$

Analogously to before³⁰ we will now expand around the mean-field solution $\bar{\eta}_0^\alpha$, $\bar{\eta}_0^\beta$ [$J \bar{\eta}_0^\alpha$ and $J \bar{\eta}_0^\beta$ denote the local-field configurations about which the log of the integrand in Eq. (109) is stationary]. Introducing shifted fields $\eta^\alpha \equiv \bar{\eta}^\alpha - \bar{\eta}_0^\alpha$ so that $\langle \eta^\alpha \rangle_f = 0$, and $\hat{\eta}^\alpha \equiv \hat{\eta}^\alpha$ (and correspondingly for η^β , and $\hat{\eta}^\beta$), leaves one with the generating functional

$$\bar{Z} = \int [d\eta^\alpha][d\hat{\eta}^\alpha][d\eta^\beta][d\hat{\eta}^\beta] \exp(S^{\alpha\beta}) \quad (116)$$

with an effective action

$$S^{\alpha\beta} = - \sum_{j,l} \int dt J_{jl}^{-1} J \hat{\eta}_j^\alpha(t) \eta_l^\alpha(t) - \sum_{j,l} \int dt J_{jl}^{-1} J \hat{\eta}_j^\beta(t) \eta_l^\beta(t) + \sum_j \sum_{m,n,p,q=0}^{\infty} \frac{1}{m!n!p!q!} \times \int dt_1 \cdots dt_{m+n+p+q} u_{mnpq}^{\alpha\beta}(t_1, \dots, t_{m+n+p+q}) \hat{\eta}_j^\alpha(t_1) \cdots \hat{\eta}_j^\alpha(t_m) \eta_j^\alpha(t_{m+1}) \cdots \eta_j^\alpha(t_{m+n}) \times \hat{\eta}_j^\beta(t_{m+n+1}) \cdots \hat{\eta}_j^\beta(t_{m+n+p}) \eta_j^\beta(t_{m+n+p+1}) \cdots \eta_j^\beta(t_{m+n+p+q}). \quad (117)$$

Here, the $u_{mnpq}^{\alpha\beta}$ are the derivatives of $\ln \bar{Z}_j^{\alpha\beta}$ with respect to the fields $\hat{\eta}_j^\alpha$, η_j^α , $\hat{\eta}_j^\beta$ and η_j^β and thus are equal to the local, connected responses and correlations in mean-field theory:

$$u_{mnpq}^{\alpha\beta} = \frac{\partial}{\partial \epsilon^\alpha(t_{m+1})} \cdots \frac{\partial}{\partial \epsilon^\alpha(t_{m+n})} \frac{\partial}{\partial \epsilon^\beta(t_{m+n+p+1})} \cdots \frac{\partial}{\partial \epsilon^\beta(t_{m+n+p+q})} \langle s^\alpha(t_1) \cdots s^\alpha(t_m) s^\beta(t_{m+n+1}) \cdots s^\beta(t_{m+n+p+q}) \rangle_{f,l,c}. \quad (118)$$

As before, local⁴⁸ (l) means that we do not vary the local field $(\eta_0^\alpha)_j$ in the mean-field equation

$$\partial_t s_j^\alpha(t) = J(\eta_0^\alpha)_j(t) + H + f_i - \frac{\delta V^\alpha}{\delta s_j^\alpha(t)} + J\epsilon^\alpha(t) \quad (119)$$

when we perturb the replica α with the infinitesimal force $J\epsilon^\alpha(t)$ (and correspondingly for replica β). The index c to the average in Eq. (118) is a reminder that these are *connected* correlation and response functions. In the same way as we discussed in Sec. IV D the force $J\epsilon^\alpha(t)$ is only allowed to *increase* with time consistently with the history we have chosen. From Eq. (118) one sees that $u_{0npq} = 0$ if $n \neq 0$, $u_{mn0q} = 0$ if $q \neq 0$, and $u_{0n0q} = 0$, just as we had $u_{0n} = 0$ in our earlier calculation for just one replica.

C. Coarse-graining transformation

The coarse-graining transformation is defined in the same way as in the single replica case. In Appendix D we give the Feynman rules for loop corrections, and derive the canonical dimensions of the various operators in the action.

D. The scaling of the second moment of the avalanche size distribution

In order to find the scaling dimension of $\langle S^2 \rangle$ from Eq. (104) we need to know how

$$\langle \hat{s}^\alpha(t_\alpha, x_0) s^\alpha(t_0, x_\alpha) \hat{s}^\beta(t_\beta, x_0) s^\beta(t_1, x_\beta) \rangle_f \quad (120)$$

scales under coarse graining. The topology of the diagrams permits no $O(\epsilon)$ loop corrections to the corresponding vertex function. Since the anomalous dimensions of the external legs (i.e., Greens functions) in the two replicas are also zero at $O(\epsilon)$ it is sufficient to use the plain field rescalings to extract the scaling behavior of $\langle \hat{s}^\alpha \hat{s}^\beta s^\alpha s^\beta \rangle$ under coarse graining. As shown in Appendix D one obtains

$$\langle \hat{s}^\alpha \hat{s}^\beta s^\alpha s^\beta \rangle \sim \Lambda^{[2(d+z)-4]}, \quad (121)$$

where Λ is the cutoff in the momentum shell integrals.

Inserting this result into Eq. (104) along with the canonical dimensions of the various times $[t] \sim \Lambda^{-z}$ and coordinates $[x] \sim \Lambda^{-1}$, one obtains

$$\langle S^2 \rangle \sim \Lambda^{-(4+z)}. \quad (122)$$

[Formally including the anomalous dimensions $\eta = \bar{\eta} = 0 + O(\epsilon^2)$, one obtains (to first order in ϵ) $\langle S^2 \rangle \sim \Lambda^{-[z+(2-\eta)2]}$. Similarly, one finds for the higher moments $\langle S^n \rangle \sim \Lambda^{-[(n-1)z+(2-\eta)n]}$.]

On the other hand, from Eq. (105) we know that $\langle S^2 \rangle \sim r^{(\tau-3)/\sigma} \mathcal{J}_\pm^{(2)}(h/r^{\beta\delta})$. If we use that r has scaling units $\Lambda^{1/\nu}$, and that $\tau-2 = \sigma\beta(1-\delta)$ (see Sec. III I, and Refs. 37 and 38), we find by comparison with Eq. (122) that $1/\sigma = z\nu + (2-\eta)\nu$ to first order in ϵ . One gets the same result from comparing the dimensions for the n th moment, which scales as $\langle S^n \rangle \sim r^{(\tau-(n+1))/\sigma} \mathcal{J}_\pm^{(n)}(h/r^{\beta\delta})$.

E. Results

We have seen that

$$1/\sigma = z\nu + (2-\eta)\nu + O(\epsilon^2) = 2 + \epsilon/3 + O(\epsilon^2). \quad (123)$$

If one inserts this into the relation $\tau-2 = \sigma\beta(1-\delta)$, one obtains

$$\tau = 3/2 + O(\epsilon^2). \quad (124)$$

From the violated hyperscaling relation $1/\sigma = (d-\theta)\nu - \beta$ one finds

$$\theta\nu = 1/2 - \epsilon/6 + O(\epsilon^2). \quad (125)$$

This concludes the perturbative approach to the problem.

VIII. COMPARISON WITH NUMERICAL SIMULATIONS IN TWO, THREE, FOUR, AND FIVE DIMENSIONS

Figures 6 and 7 show a comparison between the theoretical predictions for various exponents and their values as obtained from numerical simulations in two, three, four, and five dimensions.¹ A complete list of the numerical exponents that were measured in the simulations, and a detailed description of the algorithm that allowed to simulate systems with up to 1000^3 spins is given in a forthcoming publication.² A quantitative comparison of the results to experiments can be found in Refs. 1, 38, and 37. Some first results and conjectures about the behavior in two dimensions, which is likely the lower critical dimension of our critical point, are presented elsewhere.^{1,2} As is seen in the figure, the agreement between the numerics and the results from the ϵ expansion is surprisingly good, even down to $\epsilon=3$.

The numerical values in three dimensions for β , $\beta\delta$, ν ,

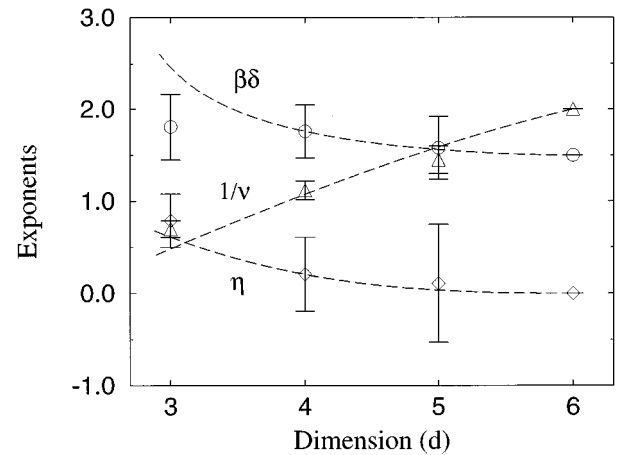


FIG. 6. Borel resummed critical exponents and simulation results. Shown are the numerical values of the exponents $1/\nu$, η , and $\beta\delta = \nu(d-\eta)/2$ (triangles, diamonds, and circles, respectively) in three, four, and five dimensions and in mean-field theory (dimension 6 and higher). The error bars denote systematic error in finding the exponents from collapses of curves at different values of disorder R . Statistical errors are smaller. The dashed lines are the Borel sums to fifth order in ϵ for the same exponents, using the method of Refs. 116 and 117 (see also Ref. 92).

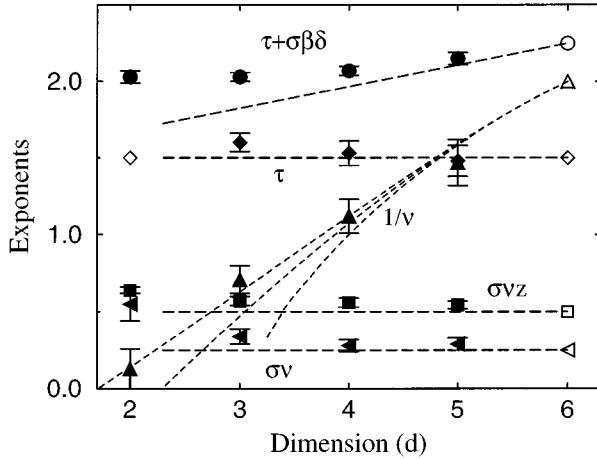


FIG. 7. Comparison to numerical results. Numerical values (filled symbols) of the exponents $\tau + \sigma\beta\delta$, τ , $1/\nu$, $\sigma\nu z$, and $\sigma\nu$ (circles, diamond, triangles up, squares, and triangle left) in two, three, four, and five dimensions. The empty symbols are values for these exponents in mean-field (dimension 6). Note that the value of τ in two dimensions was not measured. The empty diamond represents the expected value (Refs. 1 and 37). The numerical results are courtesy of Olga Perković (Refs. 1 and 2) from simulations of sizes up to 7000^2 , 1000^3 , 80^4 , and 50^5 spins, where for 320^3 , for example, more than 700 different random-field configurations were measured. The long-dashed lines are the ϵ expansions to first order for the exponents $\tau + \sigma\beta\delta = \frac{9}{4} - \epsilon/8$, $\tau = \frac{3}{2} + O(\epsilon^2)$, and $\sigma\nu z = \frac{1}{2} + O(\epsilon^2)$, and $\sigma\nu = \frac{1}{4} + O(\epsilon^2)$ where $\epsilon = 6 - d$ and d is the dimension. The short-dashed lines are the Borel sums (Ref. 22) [92,118] for $1/\nu$ to fifth order in ϵ . The lowest is the variable-pole Borel-sum from LeGuillou *et al.* (Ref. 92), the middle uses the method of Vladimirov *et al.* to fifth order, and the upper uses the method of LeGuillou *et al.* (but without the pole and with the correct fifth-order term). The other exponents can be obtained from exponent equalities (see Sec. III I in the text). The error bars denote systematic errors in finding the exponents from collapses of curves at different values of disorder R . Statistical errors are smaller.

and η seem to have overlapping error bars with the corresponding exponents of the equilibrium RFIM (see Table I). Maritan *et al.*⁹⁶ conjectured that the exponents might be equal in a comment to our first publication²⁹ on this system. Why this should be is by no means obvious. The physical states probed by the two systems are very different. While the equilibrium RFIM will be in the lowest free-energy state, our system will be in a history-dependent metastable state. Nevertheless, as we have seen, the perturbation expansions for the critical exponents can be mapped onto another to all orders in ϵ . In Appendix E 2 we discuss possible connections between the two models that might become clear if temperature fluctuations are introduced in our zero-temperature avalanche model.

ACKNOWLEDGMENTS

We would like to thank Olga Perković very much for providing prior to publication the numerical results in two, three, four, and five dimensions to which the analytical results of this paper compare favorably. Furthermore we thank

Lincoln Chayes, Daniel Fisher, Sivan Kartha, Bill Klein, Eugene Kolomeisky, James A. Krumhansl, Onuttom Narayan, Mark Newman, Mark Robbins, Bruce Roberts, Uwe Tauer, and Jan von Delft for helpful conversations, and NOR-DITA where this project was started. This research was supported by DOE Grant No. DE-FG02-88-ER45364 and NSF Grant No. DMR-9118065 at Cornell University. K.D. also acknowledges support through the Society of Fellows at Harvard University and the National Science Foundation, in part by the MRSEC Program through Grant DMR-9400396 and through Grant DMR-9417047. This research was conducted using the resources of the Cornell Theory Center, which receives major funding from the National Science Foundation (NSF) and New York State with additional funding from the Advanced Research Projects Agency (ARPA), the National Institutes of Health (NIH), IBM Corporation, and other members of the center's Corporate Research Institute. Further pedagogical information is available via World Wide Web: http://www.lassp.cornell.edu/LASSP_Science.html.

APPENDIX A:

HARD-SPIN AND SOFT-SPIN MEAN-FIELD THEORY

1. Hard-spin mean-field theory

In this appendix we derive the scaling forms near the critical point for the magnetization and the avalanche-size distribution in the hard-spin mean-field theory. At the end we briefly discuss changes of nonuniversal quantities for the soft-spin mean-field theory.

We start from the hard-spin mean-field Hamiltonian:

$$\mathcal{H} = - \sum_i (JM + H + f_i)s_i, \quad (\text{A1})$$

where the interaction with the nearest neighbors from the short-range model Eq. (3) has been replaced by an interaction with the average spin value or magnetization $M = (\sum s_i)/N$. This would be the correct Hamiltonian if every spin would interact equally strongly with every other spin in the lattice, i.e., for infinite range interactions.

2. Mean-field magnetization curve

Initially, at $H = -\infty$, all spins are pointing down. The field is slowly increased to some finite value H . Each spin s_i flips, when it gains energy by doing so, i.e., when its local effective field $h_i^{\text{eff}} = JM + H + f_i$ changes sign. At any given field H all spins with $h_i^{\text{eff}} < 0$ will still be pointing down, and all spins with $h_i^{\text{eff}} > 0$ will be pointing up. Self-consistency requires that $M = \int \rho(f)s_i df$. One obtains

$$\begin{aligned} M &= (-1) \int_{-\infty}^{-JM-H} \rho(f)df + \int_{-JM-H}^{\infty} \rho(f)df \\ &= 1 - 2 \int_{-\infty}^{-JM-H} \rho(f)df. \end{aligned} \quad (\text{A2})$$

As in the main text $\rho(f) = \exp(-f^2/2R^2)/(\sqrt{2\pi}R)$ is the distribution of random fields.

For $R > \sqrt{2/\pi}J \equiv R_c$ the solution $M(H)$ of Eq. (A2) is analytic at all values of H . For $R = R_c$ there is a critical magnetic field $H_c(R_c) = 0$ where the magnetization curve

$M(H)$ has diverging slope. For $R < R_c$ and H between the two branching fields $H_c^l(R)$ and $H_c^u(R)$ there are two stable and one unstable solution for $M(H)$. Unlike equilibrium systems, which will always occupy the solution with the lowest overall free energy, our nonequilibrium (zero-temperature) system is forced by the local dynamics to stay in the current local energy minimum until it is destabilized by the external magnetic field. For increasing (decreasing) external magnetic field this implies that the system will always occupy the metastable state with the lowest (highest) possible magnetization. One obtains a hysteresis loop for $M(H)$ with a jump, or “infinite avalanche,” and with diverging slope dM/dH at the upper and lower coercive fields $H_c^u(R)$ and $H_c^l(R)$, respectively (see Fig. 1). From Eq. (A2) follows that $dM/dH = 2\rho(x)/[1 - 2J\rho(x)]$ (with $x = -JM - H$) diverges if $2J\rho(-JM - H) = 1$. Expanding around such a point one obtains

$$dM/dH \equiv \chi = [-\rho(x_c)]/\{J[\rho'(x_c)(x - x_c) + 1/2\rho''(x_c)(x - x_c)^2 + \dots]\} \quad (\text{A3})$$

with $x_c \equiv -JM(H_c(R)) - H_c(R)$. [$H_c(R)$ means $H_c^u(R)$ or $H_c^l(R)$ depending on the history]. For a general analytic distribution of random fields $\rho(x)$ with one maximum with non-vanishing second derivative [$\rho''(x_c) < 0$], this suggests two different scaling behaviors corresponding to the cases $\rho'(x_c) = 0$ and $\rho'(x_c) \neq 0$.

a. The “critical endpoint” $(R_c, H_c(R_c))$

Consider the case $\rho'(x_c) = 0$ first. For a Gaussian distribution of width $R \equiv R_c$ with zero mean this implies that $x_c = -JM(H_c) - H_c = 0$, $\rho(x_c) = 1/(\sqrt{2\pi}R_c) = 1/(2J)$ and consequently $R_c = \sqrt{2/\pi}J$. This is in fact the largest possible value of R for which $M(H)$ has a point of diverging slope. Integrating Eq. (A3) leads to a cubic equation for M and the leading-order scaling behavior

$$M(r, h) \sim |r|^\beta \mathcal{M}_\pm(h/|r|^{\beta\delta}), \quad (\text{A4})$$

for small $h = H - H_c(R_c)$ and $r = (R_c - R)/R$, with the mean-field critical exponents $\beta = 1/2$ and $\delta = 3$. \mathcal{M}_\pm is given by the smallest real root $g_\pm(y)$ of the cubic equation

$$g^3 \mp \frac{12}{\pi} g - \frac{12\sqrt{2}}{\pi^{3/2}R_c} y = 0, \quad (\text{A5})$$

where \pm refers to the sign of r .

b. The “infinite avalanche line” $H_c(R)$ for $R < R_c$

The other case [$\rho(x_c) = 1/(2J)$ and $\rho'(x_c) \neq 0$] is found for distributions with $R < R_c$. Integrating Eq. (A3) with $x_c = -JM(H_c(R)) - H_c(R)$ yields a quadratic equation for the magnetization and the scaling behavior

$$M - M(H_c(R)) \sim [H - H_c(R)]^\zeta \quad (\text{A6})$$

with $\zeta = 1/2$ for H close to $H_c(R)$. From Eq. (A2) and $2J\rho(x_c) - 1 = 0$ one finds $H_c(R_c) = 0$, $H_c(R) \sim \pm r^{\beta\delta}$ for small $r > 0$, and $H_c(R = 0) = \pm J$ (\pm indicates the two monotonic histories). The corresponding phase diagram was shown in Fig. 3. Note that the scaling results for R close to

R_c as given in Eq. (A4) remind us of the scaling results of the Curie-Weiss mean-field theory for the equilibrium Ising model near the Curie temperature ($T = T_c$). For $T < T_c$, however, the equilibrium model has a discontinuity in the magnetization at $H = 0$, while for $R < R_c$ our model displays a jump in the magnetization at a history-dependent nonzero magnetic field $H_c(R)$, where the corresponding metastable solution becomes unstable. Our infinite avalanche line $H_c(R)$ is in fact similar to the spinodal line in spinodal decomposition.³⁹ Note also that this mean-field theory does not show any hysteresis for $R \geq R_c$ (see Fig. 1). As was explained earlier, this is only an artifact of its particularly simple structure and not a universal feature.

3. Mean-field avalanche-size distribution

As we have already discussed in the main text, one finds avalanches of spin flips as the external field is raised adiabatically. Due to the ferromagnetic interaction a flipping spin may cause some of its nearest neighbors to flip also, which may in turn trigger some of their neighbors, and so on. In mean-field theory, where all N spins of the system act as nearest neighbors with coupling J/N , a spin flip changes the effective field of *all* other spins by $2J/N$. For large N , the average number of secondary spins that will be triggered to flip in response to this change in the effective local field is then given by $n_{\text{trig}} = 2J\rho(-JM - H)$. If $n_{\text{trig}} < 1$, any avalanche will eventually peter out, and even in an infinite system all avalanches will only be of finite size. If $n_{\text{trig}} = 1$, the avalanche will be able to sweep the whole system, since each flipping spin triggers on average one other spin. This happens when the magnetic field H takes a value at the infinite avalanche line $H = H_c(R)$, with $R \leq R_c$.

Considering all possible configurations of random fields, there is a probability distribution for the number S of spins that flip in an avalanche. It can be estimated for avalanches in large systems, i.e., for $S \ll N$: For an avalanche of size S to happen, given that the primary spin has random field f_i , it is *necessary* that there are exactly $S - 1$ secondary spins with corresponding random fields in the interval $[f_i, f_i + 2(J/N)S]$. Assuming that the probability density of random fields is approximately constant over this interval, the probability $P(S)$ for a corresponding configuration of random fields is given by the Poisson distribution, with the average value $\lambda = 2JS\rho(-JM - H) = S(t + 1)$, where $t \equiv 2J\rho(-JM - H) - 1$:

$$P(S) = \frac{\lambda^{(S-1)}}{(S-1)!} \exp(-\lambda). \quad (\text{A7})$$

This includes cases in which the random fields of the s spins are arranged in the interval $[f_i, f_i + 2S(J/N)]$ in such a way that they do not flip in one big avalanche, but rather in two separate avalanches triggered at slightly different external magnetic fields. Imposing periodic boundary conditions on the interval $[f_i, f_i + 2S(J/N)]$ one can see that for any arrangement of the random fields in the interval there is exactly one spin which can trigger the rest in one big avalanche. In $1/S$ of the cases, the random field of this particular spin to trigger the avalanche will be the one with the lowest random field, as desired. Therefore we need to multiply

$P(S)$ by $1/S$ to obtain the probability $D(S,t)$ for an avalanche of size S starting with a spin flip at random field $f_i = -JM - H$

$$D(S,t) = S^{(S-2)/(S-1)} (t+1)^{(S-1)} e^{-S(t+1)}. \quad (\text{A8})$$

With Stirling's formula we find for large S the scaling form

$$D(S,t) \sim \frac{1}{\sqrt{2\pi} S^{3/2}} \exp(-St^2/2). \quad (\text{A9})$$

To obtain the scaling behavior near the two different critical points, we will insert into the expression in Eq. (A9) the expansion of $t(x)$ around x_c .

4. Avalanches near the critical endpoint

Near the critical point $(R_c, H_c(R_c))$, where $x_c=0$ and $\rho'(x_c)=0$ we obtain $t=2J\rho(0)-1+J\rho''(0)(-JM-H)^2$, which implies

$$t \sim r[1 \mp 1/4\pi g_{\pm}(h/|r|^{\beta\delta})^2] \quad (\text{A10})$$

[see Eqs. (A4) and ((A5)]. With Eq. (A9) we then obtain the scaling form for the avalanche-size distribution:

$$D(S,r,h) \sim S^{-\tau} \mathcal{D}_{\pm}(S/|r|^{-1/\sigma}, h/|r|^{\beta\delta}), \quad (\text{A11})$$

with the mean-field results $\tau=3/2$, $\sigma=1/2$, $\beta\delta=3/2$, and the mean-field scaling function

$$\mathcal{D}_{\pm}(x,y) = \frac{1}{\sqrt{2\pi}} e^{-x \left[1 \mp \frac{\pi}{4} g_{\pm}(y)^2 \right]^2 / 2}. \quad (\text{A12})$$

5. Mean-field avalanche-size distribution near the ∞ -avalanche line ("spinodal line")

For $R < R_c$ one has $\rho'(x_c) \neq 0$, so that the expansion for t becomes

$$\begin{aligned} t &= 2J\rho'(x_c)(x-x_c) + \dots \\ &= 2J\rho'(x_c)\{-J[M-M(H_c(R))]-[H-H_c(R)]\} + \dots \end{aligned} \quad (\text{A13})$$

Following the steps that led to Eq. (A6) we arrive at

$$\begin{aligned} t &= -2\sqrt{J\rho'(x_c)(H-H_c(R))} \\ &+ \text{higher orders in } [H-H_c(R)], \end{aligned} \quad (\text{A14})$$

so that for H close to the onset to infinite avalanche [with $H \leq H_c^u(R)$ for increasing field H and $H \geq H_c^l(R)$ for decreasing field]

$$\begin{aligned} D\{S, [H-H_c(R)]\} &\sim \frac{1}{\sqrt{2\pi} S^{3/2}} \exp\{-2[\rho'(-JM \\ &-H)J]S[H-H_c(R)]\}. \end{aligned} \quad (\text{A15})$$

or

$$D[S, H-H_c(R)] \sim 1/S^{\tau} \mathcal{F}(S|H-H_c(R)|^{1/\kappa}), \quad (\text{A16})$$

with $\kappa=1$ and $\tau=3/2$ in mean-field theory, and \mathcal{F} is the corresponding mean-field scaling function.

6. Modifications for the soft-spin mean-field theory

a. The static case

In Sec. IV we have, for calculational convenience, switched from the hard-spin model, where each spin s_i could only take the values ± 1 , to a soft-spin model, where s_i can take any value between $-\infty$ and $+\infty$. In realistic systems these soft spins can be considered as coarse-grained versions of the elementary spins. The corresponding Hamiltonian with the newly introduced double-well potential

$$V(s_i) = \begin{cases} k/2(s_i+1)^2 & \text{for } s_i < 0, \\ k/2(s_i-1)^2 & \text{for } s_i > 0, \end{cases} \quad (\text{A17})$$

to mimic the two spin states of the hard-spin model, was given in Eq. (33). In the mean-field approximation, where the coupling term $-J_{ij}s_i s_j$ is replaced by $-\sum_i J M s_i$ with $M = \sum_j s_j / N$, we obtain

$$\mathcal{H} = - \sum_i \{(JM + H + f_i)s_i - V(s_i)\}. \quad (\text{A18})$$

For adiabatically increasing external magnetic field the local dynamics introduced earlier implies that each spin will be negative so long as the "down" well Hamiltonian

$$\mathcal{H}_- \equiv k/2(s_i+1)^2 - (H + JM + f_i)s_i \quad (\text{A19})$$

does have a local minimum with $\delta\mathcal{H}/\delta s_i = 0$ for negative s_i . This implies that $s_i < 0$ if

$$\frac{\delta}{\delta s_i} [k/2(s_i+1)^2 - (H + f_i + JM)s_i]_{s_i=0} \geq 0, \quad (\text{A20})$$

else s_i will be stable only at the bottom of the positive potential well, where

$$\frac{\delta}{\delta s_i} \mathcal{H}_+ = \frac{\delta}{\delta s_i} [k/2(s_i-1)^2 - (H + JM + f_i)s_i] = 0. \quad (\text{A21})$$

We conclude that for the given history

$$\begin{cases} s_i \leq 0 & \text{for } f_i \leq -JM - H + k, \\ s_i > 0 & \text{for } f_i > -JM - H + k. \end{cases} \quad (\text{A22})$$

From the self-consistency condition

$$\langle s_i \rangle \equiv \int \rho(f_i) s_i df_i = M, \quad (\text{A23})$$

we derive for *increasing* external magnetic field:

$$M_u(H) = (k+H)/(k-J) - 2k/(k-J) \int_{-\infty}^{-JM-H+k} \rho(f) df, \quad (\text{A24})$$

and for *decreasing* external magnetic field:

$$M_l(H) = (k+H)/(k-J) - 2k/(k-J) \int_{-\infty}^{-JM-H-k} \rho(f) df. \quad (\text{A25})$$

Figure 2 shows the corresponding hysteresis loops in the three disorder regimes $R < R_c = \sqrt{2/\pi}J[k/(k-J)]$, where the hysteresis loop has a jump, $R = R_c$, where the jump has shrunk to a single point of infinite slope dM/dH , and $R > R_c$, where the hysteresis loop is smooth. In contrast to the hard-spin model, this model displays hysteresis even for $R \geq R_c$.

The critical magnetic fields $H_c^u(R)$ and $H_c^l(R)$ where the slope of the static magnetization curve $dM/dH \sim 1/\tau$ diverges are given by the zeroes of

$$\chi^{-1} = 2J^2\rho(-JM_{\text{stat}} - H + k) - J(k - J)/k. \quad (\text{A26})$$

To find the scaling behavior near the critical point one can expand Eq. (A24) around $H_c^u(R)$, and correspondingly Eq. (A25) around $H_c^l(R)$. For increasing external magnetic field the critical point $R = R_c$, $H = H_c^u(R_c)$, and $M = M_c \equiv M_u(H_c^u(R_c))$ is characterized by $\chi^{-1} = 0$ and $\rho'(-JM_c - H_c + k) = 0$, i.e., $-JM_c - H_c + k = 0$. It follows that $R_c = (1/\sqrt{2\pi})[2kJ/k - J]$. From Eq. (A24) one obtains $M_c^u = 1$ and $H_c^u(R_c) = k - J$. Similarly for a decreasing external magnetic field one finds $H_c^l(R_c) = -(k - J)$ and $M_c^l = M_l(H_c^l(R_c)) = -1$. The corresponding modified phase diagram is depicted in Fig. 4, with $H_c^u(R=0) = +k$ and $H_c^l(R=0) = -k$.

Expanding Eqs. (A24) and (A25) around M_c , H_c , and R_c yield a cubic equation for the magnetization and one obtains the same scaling behavior near the critical point as we derived earlier for the hard-spin model. The same is true for the scaling of the avalanche-size distribution near the critical point. In fact, it turns out that none of the universal scaling features we discussed for the hard-spin model is changed for the soft-spin model. (A ‘‘spin-flip’’ in the hard-spin model corresponds to a spin moving from the ‘‘down’’ to the ‘‘up’’ potential well in the soft-spin model.)

b. The dynamic mean-field theory at finite sweeping frequency Ω

In Sec. IV A, Eq. (61), we have derived the following equation of motion for each spin in the dynamical soft-spin mean-field theory, as the external magnetic field $H(t) = H_0 + \Omega t$ is slowly increased

$$\frac{1}{\Gamma_0} \partial_t s_j(t) = J\eta_j^0(t) + H + f_i - \frac{\delta V}{\delta s_j(t)} + J\epsilon(t). \quad (\text{A27})$$

With the definition of the potential V from Eq. (32) this becomes

$$\begin{aligned} 1/(\Gamma_0 k) \partial_t s_j(t) = & -s_j(t) + J\eta_j^0(t)/k + H(t)/k + f_i/k \\ & + \text{sgn}(s_j) + J\epsilon(t)/k. \end{aligned} \quad (\text{A28})$$

From Eq. (54) we know that $\eta^0(t) = \langle s \rangle \equiv M(t)$ is the time-dependent mean-field magnetization of the system. It can be calculated by taking the random-field average of Eq. (A28) and solving the resulting equation of motion for $\eta^0(t)$. One can show³⁸ that for driving rate Ω/k small compared to the relaxation rate $k\Gamma_0$ of the system, for all values of H_0 the solution $\eta^0(t)$ can be expanded in terms of (Ω/Γ_0) in the form

$$\begin{aligned} \eta^0(t) \equiv M(t) = & M_{\text{stat}}(H_0) + (\Omega/\Gamma_0)^{p_1} f_1(H_0)t \\ & + (\Omega/\Gamma_0)^{p_2} f_2(H_0)t^2 + \dots \end{aligned} \quad (\text{A29})$$

with $0 < p_1 < p_2 < \dots$. The p_i depend on whether $R < R_c$ or $R = R_c$. $M_{\text{stat}}(H_0)$ is the solution of the static mean-field theory equation (A24) for the given history. If the series converges for $\Omega \rightarrow 0$, it follows that $\eta^0(t)$ approaches the constant magnetization $M_{\text{stat}}(H_0)$ in the adiabatic limit. This is certainly expected for H_0 away from the critical field $H_c(R)$, where the static magnetization is non-singular: as Ω tends to zero the time-dependent magnetization $M(t)$ simply lags less and less behind the static value $M_{\text{stat}}(H(t))$. The magnetization $M(t)$ can be expanded as $M(t) = M_{\text{stat}}(H_0) + [dM/dH]_{H_0} \Omega t + \dots$ and converges towards $M_{\text{stat}}(H_0)$ as $\Omega \rightarrow 0$, as long as all derivatives $[d^n M_{\text{stat}}/dH^n]_{H_0}$ are well defined and finite. This argument, however, does not obviously hold at the critical fields $H_0 = H_c(R)$ with $R \leq R_c$, where dM_{stat}/dH and all higher derivatives diverge. Using boundary layer theory one can show³⁸ that even at these singular points $M(t)$ converges toward its static limit $M(H_c(R))$ as $\Omega \rightarrow 0$, though with power laws smaller than one in Ω , as indicated in Eq. (A29). This convergence is reassuring, since we use $M_{\text{stat}}(H_0)$ as the foundation for our ϵ expansion.

APPENDIX B: SOME DETAILS OF THE RG CALCULATION

1. Calculating some u_{mn} coefficients

In Sec. IV A in Eq. (60) we have given an expression for the coefficients u_{mn} in the expansion around mean-field theory:

$$\begin{aligned} u_{m,n} = & \frac{\partial}{\partial \epsilon(t_{m+1})} \dots \frac{\partial}{\partial \epsilon(t_{m+n})} \langle [s(t_1) - \eta^0(t_1)] \dots [s(t_m) \\ & - \eta^0(t_m)] \rangle_{l, \eta^0, \eta^0}, \end{aligned} \quad (\text{B1})$$

where $s_j(t)$ is the solution of the local mean-field equation

$$\begin{aligned} 1/(\Gamma_0 k) \partial_t s_j(t) = & -s_j(t) + J\eta_j^0(t)/k + H(t)/k + f_j/k \\ & + \text{sgn}(s_j) + J\epsilon(t)/k. \end{aligned} \quad (\text{B2})$$

In order to calculate the higher response and correlation functions u_{mn} as given in Eq. (B1) one needs to insert the solution for $\eta^0(t)$ from Appendix A 6 into Eq. (B2). As is explained in Appendix A 6, $\eta^0(t)$ can be expanded in terms of Ω [at least for $R \geq R_c$ and for $R < R_c$ before the jump up to $H_c(R)$]:

$$\eta^0(t) = M(H_0) + \Omega^p t + \dots, \quad (\text{B3})$$

where $M(H_0)$ is the static magnetization, $p > 0$, and \dots implies higher orders in Ω . Inserting this expansion into Eqs. (B2) and (B1) allows us to calculate the coefficients u_{mn} perturbatively in Ω . Only the lowest order remains as $\Omega \rightarrow 0$. The calculation is rather straightforward, some details are given in Ref. 38. One obtains

$$u_{1,0}(t) = \langle s_j(t) \rangle_l - \eta^0(t) = 0 \quad (\text{B4})$$

by construction. The vertex function $u_{11}(t_1, t_2)$ is given by

$$\lim_{\Omega \rightarrow 0} [\partial_{-t_1} (\lim_{\epsilon \rightarrow 0} \langle s(t_2) |_{H(t_2) + J\epsilon\theta(t_2 - t_1)} - s(t_2) |_{H(t_2)} \rangle_f / \epsilon)], \quad (\text{B5})$$

where $\theta(x)$ is the Heavyside step function. In the corresponding term in the action the above expression is multiplied by $\eta(t_2)$ and $\hat{\eta}(t_1)$ and integrated over dt_1 and dt_2 . After some algebra and integration by parts in t_1 one obtains two terms: the boundary term which has a purely static integrand and leaves only one time integral, and a time-dependent transient part with two time integrals. The static term contributing to the action is

$$- \int_{-\infty}^{+\infty} dt_1 \hat{\eta}(t_1) \eta(t_1) [-J/k - 2J\rho(f_i = -J\eta^0 - H + k)]. \quad (\text{B6})$$

The dynamical part can be written as

$$\begin{aligned} & \int_{-\infty}^{+\infty} dt_2 \int_{-\infty}^{+\infty} dt_1 \Theta(t_2 - t_1) \hat{\eta}(t_2) [\partial_{t_1} \eta(t_1)] \\ & \times \exp[-k\Gamma_0(t_2 - t_1)] \{-J/k - 2J[1 + k\Gamma_0(t_2 - t_1)]\} \\ & \times \rho(-J\eta^0 - H + k). \end{aligned} \quad (\text{B7})$$

In the low-frequency approximation this becomes

$$\begin{aligned} & \int_{-\infty}^{\infty} dt_1 \hat{\eta}(t_1) \partial_{t_1} \eta(t_1) [-J/k - 4J\rho(-J\eta^0 - H + k)] / (\Gamma_0 k) \\ & = - \int_{-\infty}^{\infty} dt_1 \hat{\eta}(t_1) \partial_{t_1} \eta(t_1) a / \Gamma_0, \end{aligned} \quad (\text{B8})$$

with

$$a = [J/k + 4J\rho(-J\eta^0 - H + k)] / k. \quad (\text{B9})$$

Equation (B8) contributes to the “ $i\omega$ ” term in the propagator expressed in frequency space.

The above results were computed for the case $H(t_1) = H(t_2)$. If instead one keeps $H(t_2) - H(t_1) = \Delta H \neq 0$ fixed as $\Omega \rightarrow 0$ (i.e., $t_2 - t_1 \rightarrow \infty$), one obtains

$$\begin{aligned} u_{2,0}(t_1, t_2) = & R^2/k^2 + \left(\int_{-\infty}^{-H(t_2) - \eta^0(t_2) + k} \rho(h) dh \right) \left(4 - 4 \int_{-H(t_2) - \eta^0(t_2) + k}^{-H(t_1) - \eta^0(t_1) + k} \rho(h) dh \right) - 4 \left(\int_{-\infty}^{-H(t_2) - \eta^0(t_2) + k} \rho(h) dh \right)^2 \\ & - 4 \left(\int_{-\infty}^{-H(t_2) - \eta^0(t_2) + k} (h/k) \rho(h) dh \right) - 2 \left(\int_{-H(t_2) - \eta^0(t_2) + k}^{-H(t_1) - \eta^0(t_1) + k} (h/k) \rho(h) dh \right), \end{aligned} \quad (\text{B13})$$

which is positive (or zero) for any normalized distribution $\rho(f)$.

2. Feynman rules

In the following discussion we denote with u_{mn} the static part of $u_{mn}(t_1 \dots t_{m+n})$, i.e., the part which, (for $n \neq 0$, after

$$\begin{aligned} & \lim_{\epsilon \rightarrow 0} \langle s_i(t_2) |_{H(t_2 + J\epsilon\theta(t_2 - t_1)} - s_i(t_2) |_{H(t_2)} \rangle_f / \epsilon \\ & = J/k + 2J\rho[-J\eta^0(t_2) - H(t_2) + k] \end{aligned} \quad (\text{B10})$$

up to dynamical corrections of the form $[\exp(-\Delta H\Gamma_0/\Omega)]$, which are negligible as $\Omega \rightarrow 0$. Consequently, the derivative with respect to $(-t_1)$ in Eq. (B5) yields zero in this limit. There is no contribution to the action from these cases and the result converges to the expressions in Eqs. (B6) and (B7) as $\Omega \rightarrow 0$.

The coefficients $u_{1,2}$ and $u_{1,3}$ at field H are calculated similarly. One obtains for the terms in the action corresponding to $u_{1,2}$ in the adiabatic limit:

$$\begin{aligned} & \int d^d x \int_{-\infty}^{+\infty} dt \hat{\eta}(x, t) \left(w[\eta(x, t)]^2 \right. \\ & + \int_{-\infty}^t dt_2 a(t, t_2, t_2) \partial_{t_2} \eta(x, t_2) \\ & \left. + \int_{-\infty}^t dt_2 \int_{-\infty}^{t_2} dt_1 a(t, t_1, t_2) \partial_{t_2} \eta(x, t_2) \partial_{t_1} \eta(x, t_1) \right). \end{aligned} \quad (\text{B11})$$

Here, $w = -2J^2\rho'(f_i = -J\eta^0 - H + k)$, and $a(t, t_1, t_2)$ is a transient function due to the relaxational dynamics of the system. It consists of terms proportional to $\exp\{-\Gamma_0(t - t_1)\}$ or $\exp\{-\Gamma_0(t - t_2)\}$. The transient terms proportional to $a(t, t_1, t_2)$ turn out to be irrelevant for the critical behavior observed on long length scales.

The static and the transient terms in the action contributed by $u_{1,3}$ are calculated similarly. Again, only the static part turns out to be relevant for the calculation of the exponents below the upper critical dimension. It is given by

$$\int d^d x \int_{-\infty}^{+\infty} dt u \hat{\eta}(x, t) [\eta(x, t)]^3, \quad (\text{B12})$$

with $u = 2J^3\rho''(f_i = -J\eta^0 - H + k)$.

Finally, the vertex $u_{2,0}(t_1, t_2) = \langle s_i(t_1) s_i(t_2) \rangle$ is a local correlation function. The times t_1 and t_2 can be infinitely far apart, i.e., even for $H(t_1) \neq H(t_2)$ the vertex $u_{2,0}$ is still non-zero. One obtains

taking the time derivative and integrating by parts) is not multiplied by any time derivative of the fields. This is usually the only part of the vertex which is not irrelevant under coarse graining (except for the propagator term, which also has a contribution proportional to $i\omega$).

In our Feynman diagrams for the perturbation expansion a vertex $u_{1,n}$ is denoted by a dot with m outgoing arrows (one

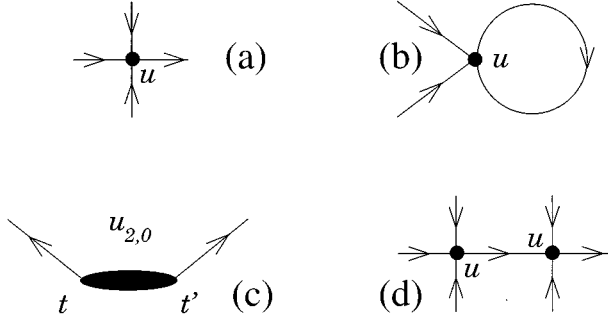


FIG. 8. Feynman diagrams. The perturbative expansion about mean-field theory is presented here by Feynman diagrams. (a) Graph for the vertex u . Incoming arrows denote η fields, outgoing arrows denote $\hat{\eta}$ fields. (b) Example of a diagram which violates causality and is therefore forbidden. (c) Graph for the vertex $u_{2,0}$. (d) Example of a diagram that is zero due to momentum conservation (Ref. 84).

for each $\hat{\eta}$ operator) and n incoming arrows (one for each η operator). Figure 8(a) shows the graph for the vertex u . Figure 8(c) shows the graph for the vertex $u_{2,0}$. The black ellipse connects the two parts of the vertex that are taken at different times. From the integration over the short-wavelength degrees of freedom (of all frequencies) one obtains loop corrections to various vertices. Figures 9(a) and 9(b) show the corrections to χ^{-1} and u which are important for an $O(\epsilon)$ calculation.

We consider the $\hat{\eta}\eta$ term in the action as propagator and all other terms as vertices. An internal line in a diagram corresponds to the contraction

$$\langle \hat{\eta}(q, t) \eta(-q, t') \rangle = \begin{cases} \Gamma_0 \exp\{-\Gamma_0(q^2 - \chi^{-1}/J)(t' - t)\} & \text{for } t' > t, \\ 0 & \text{for } t' \leq t \end{cases} \quad (\text{B14})$$

with q in the infinitesimal momentum shell $\Lambda/b < q < \Lambda$ ($b > 1$) over which is integrated. This expression can be approximated by $\delta(t - t')$ in the low-frequency approximation.⁴⁸ Note, however, that causality must be obeyed, i.e., $t' > t$. Figure 9(c) shows an example of a dia-

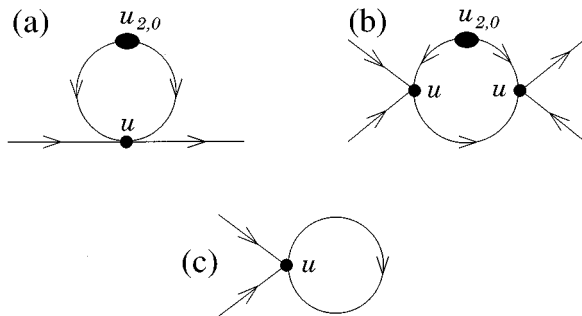


FIG. 9. Feynman diagrams. The relevant corrections to first order in $\epsilon = 6 - d$ for the constant part in χ^{-1}/J in the propagator (a), and for the vertex u (b). (c) shows an example for a diagram forbidden by causality.

gram that violates causality and is therefore forbidden. External (loose) ends in a diagram correspond to operators that are not integrated out, i.e., modes of momentum $q < \Lambda/b$ outside of the momentum shell. Each internal line carrying momentum contributes a factor

$$1/(q^2 - \chi^{-1}/J). \quad (\text{B15})$$

In each diagram, momentum conservation requires that vertices should be connected by loops rather than a single, dead end propagator line. Figure 8(d) shows an example of a diagram that is zero.⁸⁴ The entire loop in diagram 9(a) contributes to the integral

$$I_1 = \int_{\Lambda/b}^{\Lambda} d^d q / (2\pi)^d 1/(q^2 - \chi^{-1}/J)^2 \quad (\text{B16})$$

(integration over time is already performed). Similarly the loop diagram in Fig. 9(b) yields the integral

$$I_2 = \int_{\Lambda/b}^{\Lambda} d^d q / (2\pi)^d 1/(q^2 - \chi^{-1}/J)^3. \quad (\text{B17})$$

After each integration step we also have to rescale momenta, frequencies and fields. The recursion relations for χ^{-1}/J and u including the lowest-order corrections become

$$(\chi^{-1}/J)' = b^2 \left(\chi^{-1}/J + \frac{u_{x,0}}{2!} \frac{u}{3!} 6I_1 \right) \quad (\text{B18})$$

and

$$u' = b^\epsilon \left(\frac{u}{3!} + \frac{u_{2,0}}{2!} \left[\frac{u}{3!} \right]^2 36I_2 \right). \quad (\text{B19})$$

(There are no loop corrections to $u'_{2,0} = u_{2,0}$.) The integrals I_1 and I_2 have to be computed in $6 - \epsilon$ dimensions in the usual way.³⁹

3. Implementation of the history

As we have mentioned in Sec. IV C it turns out that on long length scales different magnetic fields decouple and the static critical exponents can be extracted from a renormalization-group analysis performed at a single, fixed value of the external magnetic field H_0 due to a separation of time scales. In the following paragraph we will show that this statement is self-consistent using an argument by Narayan and Middleton in the context of the CDW depinning transition.⁴⁹

An expansion around mean-field theory in the way performed here corresponds to *first* increasing the magnetic field H within an infinite ranged model and *then* tuning the elastic coupling to a short-ranged form, while the actual physical behavior corresponds to *first* tuning the elastic coupling to a short-ranged form and *then* increasing the force within the short-ranged model. The concern is that in the presence of many metastable states the critical behavior of the two approaches might not be the same. For example, spins might tend to flip backwards upon reduction of the interaction range in the expansion around mean-field theory. Although there will of course always be *some* spins for which this is the case, no such effects are expected on long length scales

since the susceptibility is actually *more* divergent near the critical point for $d < 6$ than in mean-field theory. Near the critical point we have

$$(dm/dh)_{h=0} \sim r^{-\gamma} \quad (\text{B20})$$

and

$$(dm/dh)_{r=0} \sim h^{1/\delta-1}. \quad (\text{B21})$$

Since the numerical and analytical analysis render

$$\gamma(\text{in } d < 6) > \gamma(\text{in mean-field theory}) \quad (\text{B22})$$

and

$$(1 - 1/\delta)(\text{in } d < 6) > (1 - 1/\delta)(\text{in mean-field theory}) \quad (\text{B23})$$

one expects that on long length scales spins tend to flip *forward* rather than backward upon reduction of the coupling range. This is consistent with the corresponding assumptions we have made for our expansion around mean-field theory for a monotonic history of an increasing (decreasing) external magnetic field.

Reassured by this self-consistency argument we now briefly discuss the formal decoupling of the different magnetic fields within the RG description for separated time scales. As discussed in Appendix B 1 the response functions $u_{1,n}(t_1, \dots, t_{n+1})$ with fixed $H(t_1) \neq H(t_j)$ with $j \neq 1$ tend to zero in the adiabatic limit. However, the original action S of Eq. (59) also contains terms of the form $u_{2,0}(H_1, H_2)$ which do couple different fields even as $\Omega \rightarrow 0$. These ‘‘multifield’’ vertices however do not contribute to the renormalization of the vertices evaluated at a *single* value of the external magnetic field, because in the adiabatic limit the propagator does not couple different field values. [It turns out that the multifield vertices are also *irrelevant* on long length scales. For the vertex $u_{2,0}(H_1, H_2)$ this can be seen from a calculation of the corresponding corrections to second order in epsilon for random-field disorder.³⁸ However, even if that would not be the case these terms would not feed into the calculation presented here for the reasons discussed above.] Therefore, if we leave out all the terms in the action that are zero or irrelevant at $d = 6 - \epsilon$, the different magnetic fields are completely decoupled, and the critical exponents (for $R \geq R_c$ at least) can be extracted from coarse graining the following action at fixed magnetic field H_0 :

$$\begin{aligned} \tilde{S}_{H_0} = & - \int d^d q \int dt \hat{\eta}(-q, t) (1/\Gamma_0 \partial_t + q^2 - \chi^{-1}/J) \eta(q, t) \\ & + 1/6 \int d^d x \int dt \hat{\eta}(x, t) \eta(x, t)^3 u \\ & + 1/2 \int d^d x \int dt_1 \int dt_2 u_{2,0} \hat{\eta}(x, t_1) \hat{\eta}(x, t_2) \quad (\text{B24}) \end{aligned}$$

where all vertices are evaluated at field H_0 . The time inte-

grals extend from $-\infty$ to ∞ . The constant coefficients of the ∂_t term and the q^2 term have been rescaled to 1 (see Sec. V A).

APPENDIX C: INFINITE AVALANCHE LINE

In most of this paper we have focused on the critical endpoint $(R_c, H_c(R_c))$, in particular as it is approached from $R \geq R_c$. Our ϵ expansion can be applied to the entire line $H_c(R)$, $R < R_c$ at which the infinite avalanche occurs (with some reservations which we will discuss later). In mean-field theory the approach to this line is continuous with a power-law divergence of the susceptibility $\chi \sim dM/dH$ and precursor avalanches on all scales (see Appendix A). From Eq. (B24) [or equivalently Eq. (64)] and from the rescaling of the vertices given in Eq. (78)

$$u'_{m,n} = b^{[-(m+n)+2]d/2+2n} u_{m,n}, \quad (\text{C1})$$

one sees that on long length scales the effective action is purely quadratic above eight dimensions. This suggests that there is a *continuous* transition [as H approaches $H_c(R)$] with mean-field critical exponents and a diverging correlation length $\xi(\chi^{-1})$ with the scaling behavior $\xi(\chi^{-1}) = b \xi(b^2 \chi^{-1})$, i.e., $\xi \sim (\chi^{-1})^{1/2}$. Since $\chi^{-1} \sim \sqrt{|H - H_c(R)|}$ (see Appendix A) it follows that $\xi \sim |H - H_c(R)|^{-\nu_h}$ with $\nu_h = 1/4$ for $d > 8$.⁹⁸

For $d = 8 - \tilde{\epsilon}$ ($\tilde{\epsilon} > 0$) the vertex w in the action S_H becomes relevant. In contrast to the critical endpoint where $\chi^{-1} = 0$ and $w = 0$, the infinite avalanche line is characterized by the ‘‘bare values’’ $\chi^{-1} = 0$ and $w = -2J\rho'[-JM(H_c(R)) - H_c(R) + k] \neq 0$. With the Feynman rules of Appendix B 2 the recursion relation to the same order becomes

$$\begin{aligned} w'/2 = & b^{(-d/2+4)} \left\{ w/2 + (u_{2,0}/2)(w/2)^3 8/(4\pi)^4 \right. \\ & \left. \times \int_{\Lambda/b}^{\Lambda} d_q 1/(q^2 - \chi^{-1}/J)^4 \right\}. \quad (\text{C2}) \end{aligned}$$

Performing the integral over the momentum shell $\Lambda/b < q < \Lambda$ and writing $b^{(-d/2+4)} = b^{(\tilde{\epsilon}/2)} = 1 + \tilde{\epsilon}/2 \ln b$ we find

$$w'/2 = w/2 + (w/2)(\tilde{\epsilon}/2 + u_{2,0}(w/2)^2 4/(4\pi)^4 \ln b). \quad (\text{C3})$$

Since $u_{2,0} > 0$, this equation has only two fixed points w^* with $w' = w$ for $\tilde{\epsilon} > 0$: either $w^* = 0$ or $w^* = \infty$. Any system with bare value $w \neq 0$ will have effectively larger w on longer length scales. The system flows to the strong-coupling limit. We interpret this as an indication that in perturbation theory the transition is of first-order type below eight dimensions.

There are some questions as to whether in an infinite system the onset of the infinite avalanche would be abrupt in *any* finite dimension due to large rare preexisting clusters of flipped spins which provide a preexisting interface that might be able to advance *before* the perturbatively calculated critical field $H_c(R)$ is reached. These large rare fluctuations might be nonperturbative contributions which are not taken into account by our ϵ expansion. The progression of a pre-

existing interface has been studied previously in the framework of depinning transitions.^{50,51,99} Our numerical simulation, however, does suggest a smooth onset of the infinite avalanche in nine dimensions and an abrupt onset in two, three, four, five, and seven dimensions,² as predicted by the RG calculation.

APPENDIX D: DETAILS FOR THE ϵ EXPANSION OF THE AVALANCHE EXPONENTS

1. The second moment of the avalanche-size distribution

In this section we show that the second moment $\langle S^2 \rangle_f$ of the avalanche-size distribution $D(S, r, h)$ scales in the adiabatic limit as

$$\langle S^2 \rangle_f \sim \int dt_1 \int dt_\alpha dt_\beta d^d x_\alpha d^d x_\beta \times \langle \hat{s}^\alpha(t_\alpha, x_\alpha) s^\alpha(t_0, x_\alpha) \hat{s}^\beta(t_\beta, x_\beta) s^\beta(t_1, x_\beta) \rangle_f, \quad (\text{D1})$$

where α and β specify the corresponding replica that have identical configurations of random fields and are exposed to the same external magnetic field $H(t) = H_0 + \Omega t$, with $\Omega \rightarrow 0$. A heuristic justification of this was given in Sec. VII together with an explanation of why replicas are necessary.

We start by computing the (not yet random-field averaged) expression

$$\begin{aligned} & \int dt_\alpha d^d x_\alpha dt_\beta d^d x_\beta \{ \hat{s}^\alpha(t_\alpha, x_\alpha) s^\alpha(t_0, x_\alpha) \hat{s}^\beta(t_\beta, x_\beta) s^\beta(t_1, x_\beta) \} \\ &= \int dt_\alpha d^d x_\alpha \{ \hat{s}^\alpha(t_\alpha, x_\alpha) s^\alpha(t_0, x_\alpha) \} \int dt_\beta d^d x_\beta \{ \hat{s}^\beta(t_\beta, x_\beta) s^\beta(t_1, x_\beta) \}, \end{aligned} \quad (\text{D2})$$

where $\{ \}$ stands for the path integral over the product with the δ -function weight in Z that singles out the correct path through the space of possible states for the given configuration of random fields and the given history. In Eq. (D2) the two replicas are uncoupled since we have not yet averaged over the random fields. As we have seen in Appendix B

$$\begin{aligned} (\Delta S / \Delta H)_\alpha \equiv & \int dt_\alpha d^d x_\alpha \{ \hat{s}^\alpha(t_\alpha, x_\alpha) s^\alpha(t_0, x_\alpha) \} = \int dt_\alpha d^d x_\alpha \frac{\partial}{\partial t_\alpha} \lim_{\Delta H \rightarrow 0} [s^\alpha(t_0, x_\alpha) |_{H_{x_0}^a(t_0) = H(t_0) + \Delta H \Theta(t_0 - t_\alpha)} \\ & - s^\alpha(t_0, x_\alpha) |_{H_{x_0}^a(t_0) = H(t_0)}] / \Delta H \end{aligned} \quad (\text{D3})$$

is the response of replica α to a perturbing pulse of amplitude ΔH applied at field $H(t_\alpha)$ at site x_0 integrated over the entire system.

If no spin flips in response to the perturbation, the total response will be

$$(\Delta S / \Delta H) = \Delta S_{\text{harmonic}} / \Delta H = C_2, \quad (\text{D4})$$

where C_2 is a constant that depends only on the parameters k , J , and the coordination number z of the lattice.

If, on the other hand, the perturbation triggers an avalanche of spin flips from the “down” to the “up” potential well, $\Delta S = S_{\text{flip}} = S_\alpha$ will be of the order of the number of spins participating in the avalanche¹⁰⁰ (see also Appendix B 1).

The expression in Eq. (D2) is the product of the total response to the same perturbation at site x_0 measured in replica α at time t_0 and in replica β at time t_1 . At finite sweeping rate Ω/k the corresponding values $[(\Delta S)_\alpha / \Delta H]$ and $[(\Delta S)_\beta / \Delta H]$ do not have to be the same, since the responses are measured at potentially different values of the external magnetic field [$H_0 \equiv H(t_0)$ and $H_1 \equiv H(t_1)$, respectively]. (We only consider the adiabatic case, in which the sweeping rate Ω/k is small compared to the relaxation rate $\Gamma_0 k$, so that the magnetic field can be assumed to be constant during the course of an avalanche. We take the adiabatic limit $\Omega \rightarrow 0$ at finite correlation length ξ , before approaching the critical

point of diverging avalanche size and time to avoid triggering a new avalanche before the previous one has come to a halt. This is consistent with our computer simulations at finite system sizes where avalanches occur only sequentially.)

Without loss of generality let us assume that $H(t_1) \geq H(t_0)$. First we discuss the case that there is an avalanche S_α triggered by the perturbation of amplitude ΔH in replica α at field H_0 . We further assume that t_1 is much bigger than t_0 , such that $H_1 \geq H_0 + \Delta H$. In this case the response to the pulse in replica β will be substantially different from the response S_α in replica α . The spins that are pushed over the brink by the *perturbation* at field H_0 in replica α , will in replica β be triggered by the increased external magnetic field *before* it reaches the bigger value H_1 at which the response is measured. For Ω/Γ_0 , ΔH , and $H_1 - H_0$ small enough, the response in replica β at field H_1 will then be just the harmonic response C_2 or a *different* avalanche. If it is the harmonic response, the expression in Eq. (D2) takes the form

$$(\Delta S / \Delta H)_\alpha (\Delta S / \Delta H)_\beta = (S_\alpha / \Delta H) C_2. \quad (\text{D5})$$

Similarly one might imagine scenarios in which there is an avalanche S_β triggered only in replica β , i.e.,

$$(\Delta S / \Delta H)_\alpha (\Delta S / \Delta H)_\beta = (S_\beta / \Delta H) C_2, \quad (\text{D6})$$

or where there is no avalanche happening at either field value

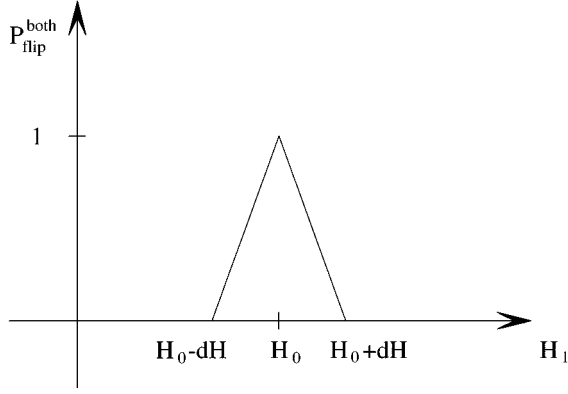


FIG. 10. The function $P_{\text{flip}}^{\text{both}}$ defined in Eq. (D10), plotted as a function of H_1 . In the figure, dH denotes the amplitude which is called ΔH in the text.

$$(\Delta S/\Delta H)_\alpha(\Delta S/\Delta H)_\beta = (C_2)^2. \quad (\text{D7})$$

It is also possible that two *different* avalanches are triggered in the two replicas:

$$(\Delta S/\Delta H)_\alpha(\Delta S/\Delta H)_\beta = (S_\alpha/\Delta H)(S_\beta/\Delta H) \quad (\text{D8})$$

with $S_\alpha \neq S_\beta$.

We are interested however in contributions due to the *same avalanche* response in both replicas

$$(\Delta S/\Delta H)_\alpha(\Delta S/\Delta H)_\beta = (S_\alpha/\Delta H)(S_\beta/\Delta H) \quad (\text{D9})$$

with $S_\alpha = S_\beta$. As we have seen, a necessary condition is that $H_0 - \Delta H \leq H_1 \leq H_0 + \Delta H$. We denote with $P_{\text{flip}} = c_0 \Delta H + o((\Delta H)^2)$ (with c_0 a constant in the critical regime) the fraction of all possible configurations of random fields in which a local perturbation of amplitude ΔH at field H , applied at site x_0 , causes at least one spin to flip. For Ω and ΔH small enough the fraction of all possible configurations of random fields in which the local perturbation will lead to the same initial spin flip triggering the same avalanche S in replica α and replica β , is to leading order in ΔH proportional to the size of the overlap $P_{\text{flip}}^{\text{both}}$ of the two intervals $[H_0, H_0 + \Delta H]$ and $[H_1, H_1 + \Delta H]$, multiplied by P_{flip} , with

$$P_{\text{flip}}^{\text{both}} = [1 - \Theta(|H_1 - H_0| - \Delta H)](\Delta H - |H_1 - H_0|)/\Delta H \quad (\text{D10})$$

(see Fig. 10). We can now compute the random-field average of the expression in Eq. (D2), denoted by $\langle \rangle_f$ to leading order in ΔH

$$\begin{aligned} \left\langle \frac{\Delta S}{\Delta H_\alpha} \frac{\Delta S}{\Delta H_\beta} \right\rangle_f &= \bar{C}_1 \frac{\langle S^2 \rangle_f}{\Delta H^2} P_{\text{flip}}^{\text{both}} P_{\text{flip}} \\ &+ \bar{C}_2 \frac{\langle S \rangle_f}{\Delta H} (1 - P_{\text{flip}}^{\text{both}}) P_{\text{flip}} + (C_2)^2 \\ &+ \langle S_\alpha S_\beta \rangle / (\Delta H)^2 P_{\text{flip}}^2 (1 - P_{\text{flip}}^{\text{both}}), \end{aligned} \quad (\text{D11})$$

where $\langle S^2 \rangle_f$ is the mean-square avalanche size, and $\langle S \rangle_f$ is the mean avalanche size, and \bar{C}_1 and \bar{C}_2 are constants in the critical regime. The last term accounts for cases in which two different avalanches $S_\alpha \neq S_\beta$ are triggered in the two replicas.

The last three terms in Eq. (D11) approach a constants as $\Delta H \rightarrow 0$, since $P_{\text{flip}} \sim \Delta H$. We will now analyze the first term, which is proportional to $\langle S^2 \rangle_f$ in more detail. The function multiplying $\langle S^2 \rangle_f$ is sharply peaked around $H_0 = H_1$ (see Fig. 10). Since $P_{\text{flip}} \sim \Delta H$ it is proportional to $P_{\text{flip}}^{\text{both}}/\Delta H$. From Eq. (D10) we have

$$\int_{H_0 - \Delta H}^{H_0 + \Delta H} dH_1 P_{\text{flip}}^{\text{both}}/\Delta H = 1 \quad (\text{D12})$$

independent of ΔH . The same integral applied to the other terms in Eq. (D11) yields contributions of order $O(\Delta H)$ which are negligible compared to the first term as ΔH is chosen small. With $H_1 = H_0 + \Omega t$ we can express the integral in terms of time

$$\int_{-\Delta H/\Omega}^{\Delta H/\Omega} \Omega dt_1 P_{\text{flip}}^{\text{both}}/\Delta H = 1. \quad (\text{D13})$$

We then obtain

$$\lim_{\Delta H \rightarrow 0} \lim_{\Omega \rightarrow 0} \int_{-\Delta H/\Omega}^{\Delta H/\Omega} \Omega dt_1 \left\langle \frac{\Delta S}{\Delta H_\alpha} \frac{\Delta S}{\Delta H_\beta} \right\rangle_f = \bar{C}_1 \langle S^2 \rangle_f. \quad (\text{D14})$$

With Eq. (D3) this leads to the scaling relation

$$\begin{aligned} \langle S^2 \rangle_f &\sim \int dt_1 \int dt_\alpha dt_\beta d^d x_\alpha d^d x_\beta \langle \hat{s}^\alpha(t_\alpha, x_\alpha) \\ &\times s^\alpha(t_0, x_\alpha) \hat{s}^\beta(t_\beta, x_\beta) s^\beta(t_1, x_\beta) \rangle_f \end{aligned} \quad (\text{D15})$$

which was to be shown. In this notation we have suppressed the factor Ω and the various limits for clarity. The integrals over time extend from $-\infty$ to $+\infty$ with an infinitesimal associated change in magnetic field.

2. Feynman rules for two replicas

We study the behavior of $S^{\alpha\beta}$ of Eq. (117) under coarse graining analogously to the calculation done before for just one replica, with the difference that instead of two, there are now four fields to be considered (two for each replica). In the following section we briefly describe the associated Feynman rules. This section may be skipped by the reader uninterested in the details, since it turns out that there are no loop corrections to $O(\epsilon)$ to $\langle S^2 \rangle$. In Sec. VII B we already derived the appropriate partition function. Here we use the same notation.

In the Feynman graphs for the loop corrections, the fields of the α replica are symbolized by arrows on full lines, whereas those for the β replica are symbolized by arrows on dashed lines. A vertex u_{mnpq} has them m outgoing arrows on full lines, n incoming arrows on full lines, p outgoing arrows on dashed lines, and q incoming arrows on dashed lines. In this notation, the fact that $u_{0npq} = 0$ if $n \neq 0$, $u_{mn0q} = 0$ if $q \neq 0$ and $u_{0n0q} = 0$, which we discussed in Sec. VII B, means that any vertex with incoming arrows of a certain replica must have at least one outgoing arrow of the same type of replica, i.e., there are no ‘‘sinks,’’ with only incoming lines of a certain replica. Furthermore, since the spins from different replica do not interact directly, and since $u_{0,1,1,0} = u_{1,0,0,1} = 0$, there are only two kinds of propagators, one for

each replica. In any diagram, an outgoing line can be connected only to an incoming line of the same replica.

Using the above rules and causality, one finds that corrections to vertices with lines of only one replica, can only receive corrections from vertices of the *same* replica. There are no contributions from diagrams that also involve the other replicas. That means that our results for the magnetization and other quantities that can be calculated using only one replica, are unaffected by the introduction of a second replica.

“Pure” (or one-replica) vertices which depend on more than one time usually have several different contributions. For example the vertex $u_{2,2}(t_1, t_2, t_3, t_4)$ has two main contributions that are obtained by partial integration of the corresponding term in the action as discussed in Appendix B. One contribution is derived from $u_{2,2}(t_1, t_2, t_3, t_4)$ and has $t_1 = t_3^+$ and $t_2 = t_4^+$. The other contribution is derived from $u_{2,2}(t_1, t_2, t_3, t_4)$ and has $t_1 = t_3^+$ and $t_1 = t_4^+$. In the case of two replicas there are corresponding “mixed” vertices (with legs from *different* replicas). With “corresponding” we mean that the times associated with the different legs of the mixed vertex, are assigned in the same way to the legs of the corresponding part of the corresponding pure vertex. The part of the pure vertex $u_{2,2}$ formally corresponding to $u_{1,1,1,1}$, for example, is given by that contribution to $u_{2,2}(t_1, t_2, t_3, t_4)$, which has $t_1 = t_3^+$ and $t_2 = t_4^+$. Conversely the part of the pure vertex $u_{2,2}$ corresponding to $u_{1,2,1,0}$ is given by that contribution to $u_{2,2}(t_1, t_2, t_3, t_4)$, which has $t_1 = t_3^+$ and $t_1 = t_4^+$. (Notice that in any mixed vertex all legs carrying a certain time label (one outgoing and any number of incoming arrows), must belong to the same replica.) Notice that each mixed vertex has the same *bare* value as its pure counterpart, since both are obtained in the same way from mean-field theory.

The loop corrections to mixed vertices formally look the same as those the corresponding parts to the pure vertices. For each loop correction to a mixed vertex there is a matching correction to the corresponding *part* of the pure vertex and vice versa. The combinatoric factors are also the same. This implies in particular that choosing the same spin rescaling for both replicas as we did before in the case of only one replica, renders marginal not only $u_{2,0}^\alpha$ and $u_{2,0}^\beta$, but also $u_{1,0,1,0}$.

3. Scaling of the second moment of the avalanche-size distribution

We need to find the scaling behavior of the “Green’s function”

$$\langle \hat{s}^\alpha(t_\alpha, x_\alpha) s^\alpha(t_0, x_\alpha) \hat{s}^\beta(t_\beta, x_\beta) s^\beta(t_1, x_\beta) \rangle_f \quad (\text{D16})$$

from its behavior under coarse graining. The topology of the diagrams permits no $O(\epsilon)$ loop corrections to the corresponding vertex function.

One finds the canonical dimensions of the field¹⁰¹ (where “dimension of” is denoted by “[]” and Λ is the upper cutoff in momentum): $[\eta(p, w)] = \Lambda^{-d/2-2-z}$, $[\hat{\eta}(p, w)] \sim \Lambda^{-d/2}$.

For calculating Green’s functions one introduces source terms in the action. From the (functional) derivative with respect to the source fields, one obtains the

corresponding average correlation functions. In the end the source fields are taken to zero again, since usually they have no physical significance. In our case the following three source terms are needed: $\int d^d q \int d\omega L(q, \omega) \eta(q, \omega)$, $\int d^d q \int d\omega L(q, \omega) \hat{\eta}(q, \omega)$, and the term needed for the calculation of the (spatially) composite operator in $\langle S^2 \rangle_f$, given by

$$\int d^d q \int d\omega_1 \int d\omega_2 L_2(q, \omega_1, \omega_2) \times \int d^d q \hat{\eta}(q, \omega_1) \hat{\eta}(p-q, \omega_2). \quad (\text{D17})$$

L , \hat{L} , and L_2 are the respective source fields: the corresponding canonical dimensions are $[L(q, \omega)] \sim \Lambda^{-d/2+2}$, and $[\delta/\delta L(q, \omega)] \sim \Lambda^{(d/2-2)} \Lambda^{-(d-z)} \sim \Lambda^{-d/2-2-z}$. Similarly $[\hat{L}(q, \omega)] \sim \Lambda^{-d/2-z}$, and $[\delta/\delta \hat{L}(q, \omega)] \sim \Lambda^{-d/2}$. And also $[L_2(p, \omega_1, \omega_2)] \sim \Lambda^{(d-2z)}$, and $[\delta/\delta L_2(p, \omega_1, \omega_2)] \sim \Lambda^0$. From Eq. (D1) and the fact that Green’s functions in the fields η and $\hat{\eta}$ scale in the same way as those in terms of s and \hat{s} (see Sec. IV B), we then find (without loop corrections) that $\langle S^2 \rangle_f \sim \Lambda^{-(4+z)}$. Below the upper critical dimension, the canonical dimensions of the fields $\eta(q, \omega)$ and $\hat{\eta}(q, \omega)$ are corrected by $\Lambda^{(\eta/2)}$ and $\Lambda^{(\eta-\bar{\eta}/2)}$, respectively. With $\eta = \bar{\eta}$ from the mapping to the pure Ising model,⁶⁷ one obtains $[O(\epsilon)] \langle S^2 \rangle_f \sim \Lambda^{-(z+(2-\eta/2))}$. Similarly, one finds for the higher moments $\langle S^n \rangle_f \sim \Lambda^{-[(n-1)z+(2-\eta)n]}$ to $O(\epsilon)$. In Sec. VII D this result is compared to the scaling behavior of $\langle S^2 \rangle$ as obtained from the scaling form of the avalanche-size distribution

$$\langle S^2 \rangle \sim r^{(\tau-3)/\sigma} S_\pm^{(2)}(h/r^{\beta\delta}) \quad (\text{D18})$$

(with the appropriate scaling function S_\pm) to extract the results for $1/\sigma$ and τ . One obtains

$$1/\sigma = 2 + \epsilon/3 + O(\epsilon^2) \quad (\text{D19})$$

and

$$\tau = 3/2 + O(\epsilon^2). \quad (\text{D20})$$

APPENDIX E: RELATED PROBLEMS

There exist several studies of related hysteresis models and depinning transitions (Refs. 64, 99, 102, 103, 104–109), which we discuss in more detail in Refs. 37 and 38.

1. Conjectures about other models in the same universality class

Recently Vives *et al.* found¹⁰³ that the numerical exponents ν , β , τ , and z in the nonequilibrium zero-temperature RFIM and the random-bond Ising model with positive mean bond strength (RBIM) have very similar values in two and three dimensions. In two dimensions, the exponents for the random-field Blume-Emery-Griffiths model¹¹⁰ seem to be similar also. In this interesting paper the authors suggest that these models might actually be in the same universality class. Admiring their work, we have some concerns however, as to whether their critical exponents will remain unchanged for larger system size: they used systems of linear

size up to $L=100$; we used much larger systems, up to 7000^2 and 800^3 for the RFIM, and found that finite-size effects are actually quite prominent and lead to shifted results for the exponents.¹ Nevertheless, symmetry arguments and preliminary RG calculations which we discuss below, suggest that their conjecture about a shared universality class still applies. There is a precedent: it is known,^{50,51} for example, that the nonequilibrium *single interface depinning* transitions of the RFIM and the RBIM do have the same critical exponents, although the *equilibrium* versions of the same models are not in the same universality class.

In the following section we will discuss some symmetry arguments, that do indeed speak in favor of the conjecture of Vives *et al.* and would even suggest that the universality class of our model extends far beyond just the RFIM and RBIM. A large universality class would also explain the surprisingly good agreement with experiments discussed in Sec. VIII and Ref. 1. Generally one may ask how robust the universality class of our model is against the introduction of other kinds of disorder, other symmetries for the order parameter, long-range interactions, different dimensions, and altered dynamics. (The variation with dimension has already been discussed at the appropriate places in this paper (see, for example, Sec. VIII).) If a new kind of disorder in an otherwise unaltered system changes neither the symmetries, nor the interaction range, nor the dynamics, nor the relevant dimensions, we may be hopeful that it does not lead to a different universality class.

Random fields and random bonds: Uncorrelated fluctuations in the nearest-neighbor coupling strengths (random bonds) in the presence of random field disorder do not break any new symmetries. Our random-field Ising model fulfills two Harris criteria $\nu/\beta\delta \geq 2/d$ and $\nu \geq 2/d$. Adding random-bond disorder cannot destroy the fixed point in the Harris-criterion sense through added statistical fluctuations, because the random-field disorder has already broken the relevant (translational) symmetry. It then seems plausible that systems with random bonds and random fields are in the same universality class as systems with random fields only. The ultimate justification for this conjecture may be drawn from the renormalization-group picture. If the change in the generating functional due to the added new disorder turns out to be irrelevant under coarse graining, it will not affect the critical behavior on long length scales. Some preliminary studies seem to indicate that this would indeed be the case for random bonds in the presence of random fields.

Random bonds only: Similarly one might expect systems with random bonds only to be in the same universality class also. Because the critical magnetization $M_c \equiv M(H_c(R_c))$ is nonzero, the time-reversal invariance will be broken at the critical point, just as it is broken in the case of random fields. The symmetries of the random-field model and the random-bond model would then be the same. Also, in a soft-spin model the same relaxational dynamics could be used. One would then expect to see the same critical behavior on long length scales. In fact, in the random-bond model one may consider the spins that flip outside the critical region to act as random fields for the spins that participate in the large avalanches near the critical point. We have already suggested that random bonds in the presence of random fields do not change the critical behavior. It then seems plausible that the

random-bond problem would be in the same universality class also, as numerical simulations seem to confirm.¹⁰³ In fact, initial analytic calculations for nonzero, positive mean of the distribution of random bonds and $H_c \neq 0$ lead to the same effective action as for the random-field case. One finds the same RG description with the same fixed point and universality class. For zero mean of the distribution of random bonds however, the term corresponding to $u_{2,0}$ appears to be zero, leading to a different RG description. In this case one expects a different behavior on long length scales. This may have been anticipated since in this case there is no relative energy scale present in the system, which qualitatively changes the problem.

Random anisotropies: Realistic models of Barkhausen noise in polycrystalline magnets usually involve random anisotropies rather than random fields. On symmetry grounds it appears plausible that a nonequilibrium $O(n)$ model with random anisotropies^{9,111,112} may be in the same universality class as the nonequilibrium RFIM also. The external magnetic driving field breaks the rotational symmetry and time-reversal invariance. Again, spins that do not flip in the critical region may act as random fields for the spins participating in avalanches near the critical point, so that the essential features are the same as in our model, and one may expect to see the same critical exponents. (It may be that in some strong-coupling limit the system will lose the ability to avalanche and all spins will smoothly rotate from down to up as the external magnetic field is increased. Our discussion here refers to the case where the coupling is weaker and avalanches do occur, as of course they do experimentally.) The $O(n)$ model with random anisotropies is very similar to a continuous scalar spin model with random couplings to the external magnetic field (random “ g factors”). The mean-field theory for the random g -factor model turns out to have the same critical exponents as our random-field Ising model. There are no new terms generated in the RG description of this model either, it is therefore expected to be in the same universality class as our model.

By symmetry we would expect neither any change in the exponents if there was randomness added through a distribution in the soft-spin potential well curvatures k [see our definition of the soft-spin potential $V(s_i)$ in Eq. (32)], nor a change if random bonds are added to the system, as may be the case in real experimental systems.

The RG formalism developed in this paper can be used as a convenient tool to verify these conjectures. One can write down the most general generating functional and see for each of these models whether on long length scales the same terms become important or irrelevant as in our model.

Long-range interactions: The question about the effect of long-range interactions is of equal importance. Depending on the sample shape, dipole-dipole interactions can lead to long-range, antiferromagnetic interaction forces which are the reason for the breakup of the magnetization into Weiss domains in conventional magnets.^{9,111} In the case of martensites there are long-range antiferroelastic strain fields present.^{10,62} In Refs. 37 and 38 we note that a critical exponent in a system with long-range elastic forces (from avalanche duration measurements in martensites²³) appears to be quite different from the corresponding exponents in our model, perhaps due to the long-range elastic forces. On the other hand, measure-

ments of Barkhausen-noise distributions in magnets in the presence of long range demagnetizing fields²¹ seem to yield a critical exponent quite close to the corresponding exponent in our model.

In a recent paper²¹ Urbach, Madison, and Markert study a model for a *single* moving domain wall without overhangs in the presence of infinite range antiferromagnetic interactions and quenched (random-field) disorder. In an infinite system their model self-organizes¹¹³ without necessary parameter tuning to the same critical state seen in the absence of the infinite range interactions right at the interface depinning threshold.⁹⁹ An analysis¹¹⁴ of our ferromagnetic RFIM in the presence of infinite range antiferromagnetic interactions leads to an unchanged critical behavior except for a tilt of the entire magnetization curve in the (M, H) plane: here too it does not change the critical properties. It would be interesting to see how these results would change for more physical long-range interactions. Dipole-dipole interactions decaying with distance as $1/x^3$, for example, might be more appropriate.

2. Thermal fluctuations

a. The equilibrium random-field Ising model

The equilibrium properties of the random-field Ising model, in particular, the phase transition from paramagnetic to ferromagnetic (long-range-ordered) behavior, have been the subject of much controversy since the 1970's.⁷¹ The reason is intriguing: experimental and theoretical studies of the approach to equilibrium show that near the critical temperature there seems to appear a “glassy” regime where relaxation to equilibrium becomes very slow. Activated by thermal fluctuations the system tumbles over free-energy barriers to lower and lower valleys in the free-energy landscape, until it has reached the lowest possible state, the equilibrium or ground state. The higher those barriers are compared to the typical energy of thermal fluctuations, the longer the relaxation process takes. At low temperatures, due to the effect of disorder, some of these barriers are so large (diverging in an infinite system), that the system gets stuck in some metastable state and never reaches true equilibrium on measurement time scales. On long length scales (and experimental time scales) thermal fluctuations become irrelevant and collective behavior emerges. When driven by an external field, the system moves through a local valley in the free-energy landscape, and collective behavior in the form of avalanches is found when the system reaches a descending slope in the free-energy surface. The present state of the system depends on its history—a phenomenon commonly observed as hysteresis.

b. The nonequilibrium random-field Ising model

We have studied this hysteresis in the zero-temperature random-field Ising model, far from equilibrium and in the absence of any thermal fluctuations. We found a critical point, at which the shape of the hysteresis loops (magnetization versus magnetic field) changes continuously from displaying a jump in the magnetization to a smooth curve. The nonequilibrium critical exponents associated with the universal behavior near this point in $d=3$ dimensions seems to match those obtained from three-dimensional simulations of the equilibrium phase-transition point approximately within the error bars⁹⁶ (see Table I). This is surprising, since the physical starting points of the two systems are very different. Furthermore, our perturbations expansion in $\epsilon=6-d$ for nonequilibrium critical exponents can be mapped onto the expansion for the equilibrium problem to all orders in ϵ . Our expansion stems from a dynamical systems description of a deterministic process, which takes into account the history of the system and is designed to single out the correct metastable state, while the calculation for the equilibrium problem involves temperature fluctuations and no history dependence at all.

c. The crossover

It would be interesting to see if there is actually a deeper connection between the nonequilibrium and equilibrium critical points, and whether the calculation for the nonequilibrium model could be used to resolve long-standing difficulties with the perturbation expansion for the equilibrium model. The idea is to introduce temperature fluctuations in the nonequilibrium calculation, and at the same time a finite sweeping frequency for the external driving force. The lower the sweeping frequency Ω at fixed temperature, the more equilibrated the system and the longer the length scale above which nonequilibrium behavior emerges. Tuning Ω would allow one to explore the whole crossover region between the two extreme cases that are found in the literature (far from and close to equilibrium). Contrary to previous treatments of relaxation, the history dependence that is so essential in experimental realizations, emerges naturally from this approach. At fixed temperature, but for progressively lower sweeping frequencies, one expects to see smaller hysteresis loops, asymptotically attaining a universal shape at low enough frequencies. The tails of these hysteresis loops will match the equilibrium magnetization curve. In the limit of zero frequency, the hysteresis loop shrinks to a point, and equilibrium is expected at all values of the external magnetic field. On the other hand, taking temperature to zero first, should yield nonequilibrium behavior as seen in our recent work. The prospect of relating equilibrium and nonequilibrium crossover regime is an exciting challenge.

*Current address: Department of Physics, Harvard University, Cambridge, MA 02138.

¹O. Perković, K. Dahmen, and J. P. Sethna, Phys. Rev. Lett. **75**, 4528 (1995).

²O. Perković, K. A. Dahmen, and J. P. Sethna (unpublished).

³J. P. Sethna, J. D. Shore, and M. Huang, Phys. Rev. B **44**, 4943 (1991), and references therein, J. D. Shore, Ph.D. thesis, Cornell University, 1992, and references therein; *Phase Transitions and Relaxation in Systems with Competing Energy Scales*, Vol. 45 of

NATO Advanced Study Institute, Series C: Mathematical and Physical Sciences, edited by T. Riste and D. Sherrington (Kluwer Academic, Dordrecht, The Netherlands, 1993), and references therein; M. Mézard, G. Parisi, and M. A. Virasoro, *Spin Glass Theory and Beyond* (World Scientific, Singapore, 1987), and references therein; K. H. Fischer and J. A. Hertz, *Spin Glasses* (Cambridge University Press, Cambridge, 1993), and references therein.

⁴J. Villain, Phys. Rev. Lett. **29**, 6389 (1984); M. Mézard and A. P.

- Young, *Europhys. Lett.* **18**, 653 (1992), and references therein.
- ⁵G. Grinstein and J. F. Fernandez, *Phys. Rev. B* **29**, 6389 (1984); J. Villain, *Phys. Rev. Lett.* **52**, 1543 (1984).
- ⁶A. J. Bray and M. A. Moore, *J. Phys. C* **18**, L927 (1985).
- ⁷D. S. Fisher, *Phys. Rev. Lett.* **56**, 416 (1986).
- ⁸J. C. McClure, Jr. and K. Schröder, *CRC Crit. Rev. Solid State Sci.* **6**, 45 (1976).
- ⁹D. Jiles, *Introduction to Magnetism and Magnetic Materials* (Chapman and Hall, London, 1991).
- ¹⁰*Martensite*, edited by G. B. Olson and W. S. Owen (American Society for Metals, Metals Park, OH, 1992); A. D. Bruce and R. A. Cowley, *Structural Phase Transitions* (Taylor and Francis, London, 1981); *Solid State Phase Transformations in Metals and Alloys*, edited by P. F. Gobin and G. Guenin, Aussois Summer School (Les Éditions de Physique, Orsay, 1978).
- ¹¹D. Sornette, *J. Phys. (France) I* **4**, 209 (1994).
- ¹²References 16–25 in D. Sornette, *J. Phys. (France) I* **4**, 209 (1994); R. L. Smith, S. L. Phoenix, M. R. Greenfields, R. B. Hengstenburg, and R. E. Pitt, *Proc. R. Soc. London Ser. A* **388**, 353 (1983), and references therein; P. C. Hemmer and A. Hansen, *Theor. Phys. Seminar Trondheim*, **4** (1991).
- ¹³P. J. Cote and L. V. Meisel, *Phys. Rev. Lett.* **67**, 1334 (1991); L. V. Meisel and P. J. Cote, *Phys. Rev. B* **46**, 10 822 (1992).
- ¹⁴K. Stierstadt and W. Boeckh, *Z. Phys.* **186**, 154 (1965) (in German).
- ¹⁵G. Bertotti, G. Durin, and A. Magni, *J. Appl. Phys.* **75**, 5490 (1994).
- ¹⁶H. Bittel, *IEEE Trans. Magn.* **5**, 359 (1969).
- ¹⁷U. Lieneweg, *IEEE Trans. Magn.* **10**, 118 (1974).
- ¹⁸U. Lieneweg and W. Grosse-Nobis, *Int. J. Magn.* **3**, 11 (1972).
- ¹⁹G. Bertotti, F. Fiorillo, and A. Montorsi, *J. Appl. Phys.* **67**, 5574 (1990).
- ²⁰G. Montalenti, *Z. Angew. Phys.* **28**, 295 (1970).
- ²¹J. S. Urbach, R. C. Madison, and J. T. Markert, *Phys. Rev. Lett.* **75**, 276 (1995).
- ²²S. Field, J. Witt, F. Nori, and X. Ling, *Phys. Rev. Lett.* **74**, 1206 (1995).
- ²³E. Vives, J. Ortín, L. Mañosa, I. Ràfols, R. Pérez-Magrané, and A. Planes, *Phys. Rev. Lett.* **72**, 1694 (1994).
- ²⁴K. M. Godshalk and R. B. Hallock, *Phys. Rev. B* **36**, 8294 (1987); M. P. Lilly, P. T. Finley, and R. B. Hallock, *Phys. Rev. Lett.* **71**, 4186 (1993).
- ²⁵G. L. Vasconcelos, M. de Sousa-Vieira, and S. R. Nagel, *Physica A* **191**, 69 (1992).
- ²⁶R. Burridge and L. Knopoff, *Bull. Seismol. Soc. Am.* **57**, 341 (1967); P. Bak and C. Tang, *J. Geophys. Res.* **94**, 15 635 (1989); Z. Olami, H. J. S. Feder, and K. Christensen, *Phys. Rev. Lett.* **68**, 1244 (1992); K. Christensen and Z. Olami, *Phys. Rev. A* **46**, 1829 (1992); L. Pietronero, P. Tartaglia, and Y. C. Zhang, *Physica (Amsterdam)* **137A**, 22 (1991); E. J. Ding and Y. N. Lu, *Phys. Rev. Lett.* **70**, 3627 (1993).
- ²⁷J. M. Carlson and J. S. Langer, *Phys. Rev. Lett.* **62**, 2632 (1989).
- ²⁸C. F. Richter, *Ann. Geophys.* **9**, 1 (1956).
- ²⁹J. P. Sethna, K. Dahmen, S. Kartha, J. A. Krumhansl, B. W. Roberts, and J. D. Shore, *Phys. Rev. Lett.* **70**, 3347 (1993); K. Dahmen, S. Kartha, J. A. Krumhansl, B. W. Roberts, J. P. Sethna, and J. D. Shore, *J. Appl. Phys.* **75**, 5946 (1994).
- ³⁰K. Dahmen and J. P. Sethna, *Phys. Rev. Lett.* **71**, 3222 (1993).
- ³¹F. Preisach, *Z. Phys.* **94**, 277 (1935); M. Krasnoselskii and A. Pokrovskii, *Systems With Hysteresis* (Nauka, Moscow, 1983); I. D. Mayergoyz, *J. Appl. Phys.* **57**, 3803 (1985); *Mathematical Models of Hysteresis* (Springer-Verlag, Berlin, 1991); P. C. Clapp, *Mater. Sci. Eng.* **A127**, 189 (1990).
- ³²K. P. O'Brien and M. B. Weissman, *Phys. Rev. E* **50**, 3446 (1994), and references therein; K. P. O'Brien and M. B. Weissman, *Phys. Rev. A* **46**, R4475 (1992).
- ³³A. Berger (unpublished).
- ³⁴Details about the experimental setup used by Berger are given in A. W. Pang, A. Berger, and H. Hopster, *Phys. Rev. B* **50**, 6457 (1994); A. Berger, A. W. Pang, and H. Hopster, *J. Magn. Magn. Mater.* **137**, L1 (1994); A. Berger, A. W. Pang, and H. Hopster, *Phys. Rev. B* **52**, 1078 (1995).
- ³⁵V. Raghavan, in *Martensite* (Ref. 10), p. 197.
- ³⁶W. Wu and P. W. Adams, *Phys. Rev. Lett.* **74**, 610 (1995).
- ³⁷K. A. Dahmen, O. Perković, and J. P. Sethna (unpublished).
- ³⁸K. A. Dahmen, Ph.D. thesis, Cornell University, 1995.
- ³⁹N. Goldenfeld, *Lectures on Phase Transitions and the Renormalization Group* (Addison-Wesley, Reading, MA, 1992).
- ⁴⁰J. J. Binney, N. J. Dowrick, A. J. Fisher, and M. E. J. Newman, *The Theory of Critical Phenomena* (Clarendon, Oxford, 1992).
- ⁴¹S. K. Ma, *Modern Theory of Critical Phenomena* (Benjamin-Cummings, Reading, MA, 1976).
- ⁴²M. Fisher, *Critical Phenomena, Proceedings of Stellenbosch, South Africa, 1982* (Springer-Verlag, Berlin, 1982).
- ⁴³J. Zinn-Justin, *Quantum Field Theory and Critical Phenomena*, 2nd ed. (Clarendon, Oxford, 1993).
- ⁴⁴D. J. Amit, *Field Theory, the Renormalization Group, and Critical Phenomena* (World Scientific, Singapore, 1984).
- ⁴⁵P. C. Hohenberg and B. I. Halperin, *Rev. Mod. Phys.* **49**, 435 (1977).
- ⁴⁶For a review of the real-space renormalization group, which we do not employ here, see also R. J. Creswick, H. A. Farach, and C. P. Poole, Jr., *Introduction to Renormalization-Group Methods in Physics* (Wiley, New York, 1992).
- ⁴⁷P. Ramond, *Field Theory: A Modern Primer* (Addison-Wesley, Reading, MA, 1990).
- ⁴⁸O. Narayan and D. S. Fisher, *Phys. Rev. Lett.* **68**, 3615 (1992); *Phys. Rev. B* **46**, 11 520 (1992).
- ⁴⁹O. Narayan and A. A. Middleton, *Phys. Rev. B* **49**, 244 (1994).
- ⁵⁰O. Narayan and D. S. Fisher, *Phys. Rev. B* **48**, 7030 (1993).
- ⁵¹T. Nattermann, S. Stepanow, L. H. Tang, and H. Leschhorn, *J. Phys. (France) II* **2**, 1483 (1992).
- ⁵²D. Ertaş and M. Kardar, *Phys. Rev. E* **49**, R2532 (1994); *Dynamics in Small Confining Systems II*, edited by J. M. Drake, S. M. Troian, J. Klafter, and R. Kapelman, MRS Symposium Proceedings Series No. 366 (Materials Research Society, Pittsburgh, 1994); J. F. Joanny and M. O. Robbins, *J. Chem. Phys.* **92**, 3206 (1990).
- ⁵³D. Ertaş and M. Kardar, *Phys. Rev. Lett.* **73**, 1703 (1994).
- ⁵⁴C. Myers and J. P. Sethna, *Phys. Rev. B* **47**, 11 171 (1993); **47**, 11 194 (1993).
- ⁵⁵A. A. Middleton and D. S. Fisher, *Phys. Rev. Lett.* **66**, 92 (1991), and references therein; *Phys. Rev. B* **47**, 3530 (1993).
- ⁵⁶S. N. Coppersmith, *Phys. Rev. Lett.* **65**, 1044 (1990), has shown that on sufficiently large length scales the elastic theory always breaks down.
- ⁵⁷A. Brass, H. J. Jensen, and A. J. Berlinsky, *Phys. Rev. B* **39**, 102 (1989).
- ⁵⁸R. Lenormand and C. Zargone, *Phys. Rev. Lett.* **54**, 2226 (1985).
- ⁵⁹O. Narayan and D. S. Fisher, *Phys. Rev. B* **49**, 9469 (1994), and references therein.

- ⁶⁰J. M. Yeomans, *Statistical Mechanics of Phase Transformations* (Clarendon, Oxford, 1992).
- ⁶¹In this paper we consider a lattice of *classical* spins. For an illustrative *quantum mechanical* description of magnetic moments in an external field see also S. Brandt and H. D. Dahmen, *The Picture Book of Quantum Mechanics*, 2nd ed. (Springer Verlag, New York, 1995).
- ⁶²S. Kartha, Ph.D. thesis, Cornell University, 1994.
- ⁶³N. G. van Kampen, *Stochastic Processes in Physics and Chemistry* (North-Holland, Amsterdam, 1990).
- ⁶⁴S. Maslov and Z. Olami (unpublished).
- ⁶⁵H. Kleinert, J. Neu, V. Schulte-Frohlinde, and K. G. Chetyrkin, *Phys. Lett. B* **272**, 39 (1991).
- ⁶⁶In the Appendix on mean-field theory we derived scaling forms for the magnetization and the avalanche size distribution, which depended on the (mean-field) scaling fields $r=(R-R_c)/R$ and $h=H-H_c$. In finite dimensions, however, the corresponding scaling forms may depend not on r and h , but on rotated variables $r'=r+ah$ and $h'=h+br$. The amount by which the scaling axes $r'=0$ and $h'=0$ are tilted relative to the $(r,0)$ and $(0,h)$ direction in the (r,h) plane is a nonuniversal quantity and has no effect on the critical exponents. Nevertheless it can be important in the data analysis as discussed in Refs. 38 and 2. [The numerical results in three, four, and five dimensions do indeed seem to indicate a slight tilting (Ref. 2).]
- ⁶⁷U. Krey, *J. Phys. C* **17**, L545 (1984); **18**, 1455 (1985); U. Krey and H. Ostermeier, *Z. Phys. B* **66**, 219 (1987).
- ⁶⁸D. S. Fisher, *Phys. Rev. B* **31**, 1396 (1985).
- ⁶⁹G. Parisi and L. Pietronero, *Europhys. Lett.* **16**, 321 (1991).
- ⁷⁰D. Stauffer and A. Aharony, *Introduction to Percolation Theory* (Taylor and Francis, London, 1992).
- ⁷¹T. Nattermann and J. Villain, *Phase Transitions* **11**, 5 (1988), and references therein; T. Nattermann and P. Rujan, *Int. J. Mod. Phys. B* **3**, 1597 (1989); D. P. Belanger and A. P. Young, *J. Magn. Magn. Mater.* **100**, 272 (1991); E. B. Kolomeisky, in *JETP Lett.* **52**, 538 (1990).
- ⁷²H. Rieger and A. P. Young, *J. Phys. A* **26**, 5279 (1993).
- ⁷³M. E. J. Newman, B. W. Roberts, G. T. Barkema, and J. P. Sethna, *Phys. Rev. B* **48**, 16 533 (1993), and references therein.
- ⁷⁴B. W. Roberts, Ph.D. thesis, Cornell University, 1995, and references therein.
- ⁷⁵J. T. Chayes, L. Chayes, D. S. Fisher, and T. Spencer, *Phys. Rev. Lett.* **57**, 2999 (1986).
- ⁷⁶M. Schwartz and A. Soffer, *Phys. Rev. Lett.* **55**, 2499 (1985).
- ⁷⁷In the CDW depinning transition the form of the potential does change the (dynamical) mean-field exponents (Ref. 48) and some properties that are associated with the thermal rounding of the CDW transition in finite dimensions (Ref. 115).
- ⁷⁸P. C. Martin, E. Siggia, and H. Rose, *Phys. Rev. A* **8**, 423 (1973); C. De Dominicis, *Phys. Rev. B* **18**, 4913 (1978); H. Sompolinsky and A. Zippelius, *ibid.* **25**, 6860 (1982); A. Zippelius, *ibid.* **29**, 2717 (1984).
- ⁷⁹R. Bausch, H. K. Janssen, and H. Wagner, *Z. Phys. B* **24**, 113 (1976); U. C. Täuber and F. Schwabl, *Phys. Rev. B* **46**, 3337 (1992), and references therein.
- ⁸⁰To that end, one chooses the following regularization (when discretizing in time): Let $t=n\epsilon$ with ϵ a small number taken to zero later when n is taken to infinity, such that their product remains fixed. Then $\partial_t s_i(t)$ becomes $[s_i(n\epsilon) - s_i((n-1)\epsilon)]/\epsilon$ and we integrate over $ds_i(n\epsilon)$. Because of the analyticity we are free to take the rest of the argument of the δ function at the lower value $s_i((n-1)\epsilon)$, or the average value $[s_i(n\epsilon) + s_i((n-1)\epsilon)]/2$, or the upper value $s_i(n\epsilon)$. If we choose the first possibility, one finds that Jacobian will be only a constant, since each argument only depends on $s_i(n\epsilon)$, and is independent of any other $s_j(n\epsilon)$ with $i \neq j$. This corresponds to allowing a force at time $(n-1)\epsilon$ to have an effect only *after* some time ϵ , i.e., equal times response functions are manifestly zero.
- ⁸¹C. De Dominicis, *Phys. Rev. B* **18**, 4913 (1978).
- ⁸²H. Sompolinsky and A. Zippelius, *Phys. Rev. B* **25**, 6860 (1982); A. Zippelius, *ibid.* **29**, 2717 (1984).
- ⁸³This can be seen by setting $\hat{\eta}^0 = 0$ in
- $$\langle s_i(t) \rangle_{l, \hat{\eta}, \tilde{\eta}} = [(\delta' \delta \hat{\eta}_i) \Sigma_j \ln(\bar{Z}_j[\tilde{\eta}_j, \hat{\eta}_j])]_{\hat{\eta}, \tilde{\eta}}$$
- $$= (1/\bar{Z}_i) \int \int [ds] [d\hat{s}] s_i(t) \langle \exp\{J^{-1} \int dt [\Sigma_j J \hat{\eta}_j^0(t) s_j(t) + i \hat{s}_j(t) (\partial_t s_j(t)/\Gamma_0 - J \hat{\eta}_j^0(t) - H - f_i + \delta V / \delta s_j)]\} \rangle_f,$$
- which is obtained from Eqs. (47), (49), (52), and (54). Integrating out the \hat{s} fields we see that \bar{Z}_j is the random field average over a product of δ functions which impose Eq. (57) by their argument. Equation (56) is the self-consistency condition for this mean-field equation of motion.
- ⁸⁴K. G. Wilson and J. Kogut, *Phys. Rep.* **12C**, 76 (1974).
- ⁸⁵The $O(\epsilon^2)$ diagram which we constructed in Ref. 30 and had argued to lead to different results in $O(\epsilon^2)$ for the two models, turned actually out to be irrelevant, as all other diagrams which are different from the equilibrium model.
- ⁸⁶A. Aharony, Y. Imry, and S. K. Ma, *Phys. Rev. Lett.* **37**, 1364 (1976); A. P. Young, *J. Phys. A* **10**, L257 (1977); G. Parisi and N. Sourlas, *Phys. Rev. Lett.* **43**, 744 (1979).
- ⁸⁷G. Parisi, in *Recent Advances in Field Theory and Statistical Mechanics*, 1982 Les Houches Lectures, edited by J. B. Zuber and R. Stora (North-Holland, Amsterdam, 1984), and references therein.
- ⁸⁸B. Tadic, *Z. Phys.* **41**, 13 (1981).
- ⁸⁹E. Brézin, D. J. Wallace, and K. G. Wilson, *Phys. Rev. Lett.* **29**, 591 (1972); *Phys. Rev. B* **7**, 232 (1973); D. J. Wallace and R. P. K. Zia, *J. Phys. C* **7**, 3480 (1974).
- ⁹⁰C. Domb and M. S. Green, *Phase Transitions and Critical Phenomena* (Academic, New York, 1976), Vol. 6.
- ⁹¹R. B. Griffiths, *Phys. Rev.* **158**, 176 (1967).
- ⁹²H. Kleinert, J. Neu, V. Schulte-Frohlinde, K. G. Chetyrkin, and S. A. Larin [*Phys. Lett. B* **272**, 39 (1991) and **319**, 545 (1993)] provide the expansion for the pure, equilibrium Ising exponents to fifth order in $\epsilon=4-d$. A. A. Vladimirov, D. I. Kazakov, and O. V. Tarasov [*Sov. Phys. JETP* **50**, 521 (1979), and references therein] introduce a Borel resummation method with one parameter, which is varied to accelerate convergence. J. C. LeGuillou and J. Zinn-Justin [*Phys. Rev. B* **21**, 3976 (1980)] do a coordinate transformation with a pole at $\epsilon=3$, and later [*J. Phys. Lett.* **46**, L137 (1985) and *J. Phys.* **48**, 19 (1987)] make the placement of the pole a variable parameter (leading to a total of four real acceleration parameters for a fifth order expansion). Unfortunately, LeGuillou *et al.* used a form for the fifth-order term which turned out to be incorrect (Kleinert, above). The ϵ expansion is an asymptotic series, which need not determine a unique underlying function [J. Zinn-Justin, *Quantum Field Theory and Critical Phenomena*, 2nd ed. (Clarendon, Oxford, 1993)]. Our model likely has nonperturbative corrections [as did the equilibrium, thermal random-field Ising model: G. Parisi, in *Recent Advances in Field Theory and Statistical Mechanics* (Ref. 87).]
- ⁹³J. Z. Imbrie, *Phys. Rev. Lett.* **53**, 1747 (1984); *Commun. Math.*

- Phys. **98**, 145 (1985); Physica A **140**, 291 (1986).
- ⁹⁴J. Bricmont and A. Kupiainen, Phys. Rev. Lett. **59**, 1829 (1987); Commun. Math. Phys. **116**, 539 (1988).
- ⁹⁵C. Bender and S. A. Orszag, *Advanced Mathematical Methods for Scientists and Engineers* (McGraw-Hill, New York, 1978).
- ⁹⁶A. Maritan, M. Cieplak, M. R. Swift, and J. Banavar, Phys. Rev. Lett. **72**, 946 (1994); J. P. Sethna, K. Dahmen, S. Kartha, J. A. Krumhansl, O. Perković, B. W. Roberts, and J. D. Shore, *ibid.* **72**, 947 (1994).
- ⁹⁷As explained in Sec. IV A and in Ref. 38 the expression $\int dt_0 \langle \hat{s}(t_0, x_0) s(t, x) \rangle_f$ gives the random-field-averaged static response of the system at time t and position x to a positive θ -function pulse applied at position x_0 an infinitely long time before t (so that all transients have died away). The integral over all space will then give the *total* static random-field averaged response of the system to a θ -function pulse applied at site x_0 . This should scale in the same way as the first moment of the avalanche size distribution, i.e., as the average avalanche size.
- ⁹⁸The same result can be obtained from the Harris criterion: If the Harris-criterion is not violated through the presence of large rare nonperturbative fluctuations in an infinite system, such as a pre-existing interface (for a discussion, see Appendix E), i.e., if $\nu_h \geq 2/d$ is a valid exponent inequality, then the mean-field critical exponents with $\nu_h = 1/4$ are correct only for $d \geq 8$, which is consistent with our result from perturbation theory.
- ⁹⁹M. Cieplak and M. O. Robbins, Phys. Rev. Lett. **60**, 2042 (1988); Phys. Rev. B **41**, 11 508 (1990); N. Martys, M. Cieplak, and M. O. Robbins, Phys. Rev. Lett. **66**, 1058 (1991); N. Martys, M. O. Robbins, and M. Cieplak, Phys. Rev. B **44**, 12 294 (1991); B. Koiller, H. Ji, and M. O. Robbins, *ibid.* **45**, 7762 (1992); H. Ji and M. O. Robbins, *ibid.* **46**, 14 519 (1992); B. Koiller, H. Ji, and M. O. Robbins, Phys. Rev. B **46**, 5258 (1992).
- ¹⁰⁰ S_α is not exactly equal to the number of spins flipping in the avalanche. It contains also the harmonic response that each spin flip causes through the coupling to the neighboring spins. This harmonic response couples back to the original spin and propagates to the next-nearest neighbors with an amplitude damped by the factor J_{ij}/k and so on. Occasionally it may cause an avalanche to continue which would otherwise (in the hard spin model) have come to a halt. However since this is a short-ranged effect, we do not expect it to be of any relevance to the scaling behavior on long length scales. In mean-field theory the harmonic response only amounts to a constant factor relating S_α to the number of spins participating in the avalanche.
- ¹⁰¹L. H. Ryder, *Quantum Field Theory* (Cambridge University Press, Cambridge, 1985).
- ¹⁰²V. M. Rudyak, Bull. Acad. Sci. USSR Phys. Ser. **57**, 955 (1993), and references therein; **45**, 1 (1981).
- ¹⁰³E. Vives and A. Planes, Phys. Rev. B **50**, 3839 (1994); E. Vives, J. Goicoechea, J. Ortín, and A. Planes, Phys. Rev. E **52**, R5 (1995).
- ¹⁰⁴C. M. Coram, A. Jacobs, N. Heinig, and K. B. Winterbon, Phys. Rev. B **40**, 6992 (1989).
- ¹⁰⁵G. Bertotti and M. Pasquale, J. Appl. Phys. **60**, 5066 (1991).
- ¹⁰⁶G. Bertotti and M. Pasquale, J. Appl. Phys. **67**, 5255 (1990).
- ¹⁰⁷D. Dhar and P. B. Thomas, J. Phys. A **25**, 4967 (1992); P. B. Thomas and D. Dhar, J. Phys. **26**, 3973 (1993); S. Gupta (unpublished); J. Zemmouri, B. Ségard, W. Sergent, and B. Macke, Phys. Rev. Lett. **70**, 1135 (1993).
- ¹⁰⁸M. Rao, H. R. Krishnamurthy, and R. Pandit, Phys. Rev. B **42**, 856 (1990), and references therein.
- ¹⁰⁹K. K. Babcock and R. M. Westervelt, Phys. Rev. A **40**, 2022 (1989); K. L. Babcock, R. Seshadri, and R. M. Westervelt, *ibid.* **41**, 1952 (1990); K. L. Babcock and R. M. Westervelt, Phys. Rev. Lett. **64**, 2168 (1990); P. Bak and H. Flyvbjerg, Phys. Rev. A **45**, 2192 (1992).
- ¹¹⁰M. Blume, V. J. Emery, and R. B. Griffiths, Phys. Rev. A **4**, 1071 (1971).
- ¹¹¹S. Chikazumi, *Physics of Magnetism* (Wiley, New York, 1964).
- ¹¹²N. W. Ashcroft and N. D. Mermin, *Solid State Physics* (Saunders, Philadelphia, 1976).
- ¹¹³This self-organization to the critical point is similar to the trivial self-organization expected in an experiment in the presence of a gradient field, which is discussed in Refs. 38 and 37.
- ¹¹⁴B. W. Roberts and J. P. Sethna (unpublished).
- ¹¹⁵A. A. Middleton, Phys. Rev. B **45**, 9465 (1992).
- ¹¹⁶A. A. Vladimirov, D. I. Kazakov, and O. V. Tarasov, Sov. Phys. JETP **50**, 521 (1979), and references therein.
- ¹¹⁷D. I. Kazakov, O. V. Tarasov, and D. V. Shirkov, Teor. Mat. Fiz. **38**, 15 (1979).
- ¹¹⁸J. C. Le Guillou and J. Zinn-Justin, *Large-Order Behavior of Perturbation Theory* (North-Holland, Amsterdam, 1990).
- ¹¹⁹M. E. J. Newman and G. T. Barkema, Phys. Rev. E **53**, 393 (1996).
- ¹²⁰A. P. Young and M. Nauenberg, Phys. Rev. Lett. **54**, 2429 (1985); A. T. Ogielski and D. A. Huse, *ibid.* **56**, 1298 (1986).